University of São Paulo
"Luiz de Queiroz" College of Agriculture

Unraveling the impact of genotype by environment interaction complexity and a new proposal to understand the contribution of additive and non-additive effects on genomic prediction in tropical maize single-crosses

Filipe Couto Alves

Thesis presented to obtain the degree of Doctor in Science. Area: Genetics and Plant Breeding

Piracicaba
2018

Filipe Couto Alves
Bachelor in Biological Sciences

Unraveling the impact of genotype by environment interaction complexity and a new proposal to understand the contribution of additive and non-additive effects on genomic prediction in tropical maize single-crosses

versão revisada de acordo com a resolução CoPGr 6018 de 2011

Advisor:
Prof. Dr. **ROBERTO FRITSCHE NETO**

Thesis presented to obtain the degree of Doctor in Science. Area: Genetics and Plant Breeding

Piracicaba
2018

Dados Internacionais de Catalogação na Publicação
DIVISÃO DE BIBLIOTECA – DIBD/ESALQ/USP

Alves, Filipe Couto

Unraveling the impact of genotype by environment interaction complexity and a new proposal to understand the contribution of additive and non-additive effects on genomic prediction in tropical maize single-crosses / Filipe Couto Alves. - - versão revisada de acordo com a resolução CoPGr 6018 de 2011. - - Piracicaba, 2018.

119 p.

Tese (Doutorado) - - USP / Escola Superior de Agricultura “Luiz de Queiroz”.

1. Kernels paramétricos e semi-paramétricos 2. Epistasia 3. Estresse 4. Nitrogênio 5.Interação complexa I. Título

To my family, that have always supported me,
and to my grandfather Odilon (in memorian)

CONTENTS

RESUMO

Desvendando o impacto da complexidade da interação genótipo por ambiente e uma nova proposta para entender a contribuição de efeitos aditivos e não-aditivos na predição genômica em híbridos simples de milho tropical

O uso de marcadores moleculares para a predição do fénotipo de materiais não testados em campo tem sido amplamente utilizado em programas de melhoramento genético de plantas. A predição genômica de hibridos simples é uma ferramenta promissora no melhoramento genético do milho, pois além da redução do tempo necessário para cada ciclo de seleção, ela pode ser utilizada para a identificação de cruzamentos promissores. Dependendo da característica em estudo, a inclusão de efeitos não aditivos em modelos de predição genômica pode aumentar significativamente sua acurácia de predição. Além disso, estes modelos foram inicialmente propostos para a predição de materiais em apenas um único ambiente. Atualmente, foram expandidos para considerarem os efeitos da interação genótipos por ambiente. O uso de tais modelos têm se mostrado vantajoso em vários aspectos, um deles é o considerável aumento da acurácia de predição de novos materiais. Contudo, ainda são escassos estudos envolvendo a inclusão de efeitos não aditivos nesses modelos. Ademais, fatores como a complexidade da interação genótipo por ambiente pode influenciar de maneira significativa a acurácia preditiva de modelos considerando múltiplos ambientes. Portanto, os objetivos foram: *i)* avaliar a contribuição de efeitos aditivos e não aditivos (dominância e epistasia) para a predição de caracteres agronômicos com diferentes arquiteturas genéticas em cruzamentos simples de milho tropical cultivados sob dois níveis de disponibilidade de nitrogênio (ideal e estressado), e *ii)* verificar o impacto da complexidade da interação genótipo por ambiente, e da inclusão de desvios de dominância na acurácia de predição de modelos multi-ambientes para a predição da produtividade grãos de híbridos simples de milho. Para isto, foram utilizados os dados fenótipicos e genotípicos de 906 híbridos simples de milho avaliados durante dois anos, em dois locais, sob dois níveis de adubação nitrogenada, totalizando oito ambientes distintos (combinação ano x local x nivel de adubação nitrogenada). Os caracteres estudados foram produtividade de grãos, altura de espiga, e plantas. Os resultados acerca da inclusão de efeitos aditivos e não aditivos (dominancia e epistasia) sugerem que, efeitos não aditivos são mais importantes sob condições de estresse, contribuem de maneira significativa para produtividade grãos, de modo intermediário para altura de plantas e possuem pouca importância para altura de espiga. A inclusão de desvios de dominância em modelos de predição multi-ambientes aumentou de forma significativa a acurácia de predição. Além disto, observou-se uma relação linear entre complexidade da interação genótipos por ambientes e acurácia preditiva do modelo.

Palavras-chave: Kernels paramétricos e semi-paramétricos; Epistasia; Estresse; Nitrogênio; Interação complexa

ABSTRACT

Unraveling the impact of genotype by environment interaction complexity and a new proposal to understand the contribution of additive and non-additive effects on genomic prediction in tropical maize single-crosses

The use of molecular markers to predict non-tested materials in field trials has been extensively employed in breeding programs. The genomic prediction of single crosses is a promising approach in maize breeding programs as it reduces selection cycle and permits the selection of promising crosses. Accounting for non-additive effects on genomic prediction can increase prediction accuracy of models depending on the traits genetic architecture. Genomic prediction was first developed for single environments and recently extended to exploit the genotype by environment interactions for prediction of non-evaluated individuals. The employment of multi-environment genomic models is advantageous in several aspects and has enabled significant higher prediction accuracies than single environment models. However, only a small number of studies regarding the inclusion of non-additive effects in these models are reported. Moreover, the genotype by environment interaction complexity can largely impact the prediction accuracy of these models. Thus, the objectives were to *i)* evaluate the contribution of additive and non-additive (dominance and epistasis) effects for the prediction of agronomical traits with different genetic architecture in tropical maize single-crosses grown under two nitrogen regimes (ideal and stressing), and *ii)* verify the impact of the genotype by environment interaction complexity, and the inclusion of dominance deviations, on the prediction accuracy of hybrids grain yield using a multi-environment prediction model. For this, we used phenotypic and genotypic data of 906 single-crosses evaluated during two years, at two locations, under two nitrogen regimes, totaling eight contrasting environments (combination of year x locations x nitrogen regimes). The traits considered in the study were grain yield, ear, and plant height. The results regarding the inclusion of additive and non-additive effects (dominance and epistasis) in genomic prediction models suggest that non-additive effects play an important role in stressing conditions, having a high, medium and low contribution for phenotypic expression of grain yield, plant height, and ear height, respectively. The inclusion of dominance deviations in multi-environment prediction model increases the prediction accuracy. Furthermore, a linear relationship between genotype by environment complexity and prediction accuracy was found.

Keywords: Parametric and semi-parametric kernels; Epistasis; Stress; Nitrogen; Crossover interaction

LIST OF FIGURES

LIST OF TABLES

1. INTRODUCTION

Due to the massive number of possible combinations of inbred lines in breeding programs, only a small fraction of all the possible crosses are evaluated on field experiments (Schrag et al. 2010). In this scenario, genomic models can be used to predict the performance of un-tested hybrids; therefore, genomic prediction (GP, e.g., Meuwissen et al. 2001) arises as a powerful approach to overcome this problem. Most commercial maize breeding programs perform selection on inbred lines and then select optimal crosses among elite materials (often from divergent heterotic groups) to produce commercial hybrids.

In the literature, the hybrids genetic value is often decomposed into the general and specific combining ability variance components (GCA and SCA, respectively, Sprague and Tatum, 1942). The GCA variance represents the amount of variance that can be explained by the mean of the parental lines, while the SCA variance quantifies the amount of variance on the genotypic values that cannot be explained by parental means. This component is attributable to deviations from additivity due to dominance and epistasis (Reif et al. 2007). Unfortunately, additive and non-additive contrasts are often not mutually orthogonal. For this reason, the variance parameters entering in genomic models (e.g., the additive and dominance variance) cannot be directly used to decompose the total genetic variance into GCA and SCA components.

Besides the prediction of non-tested materials in single environments, GP can be helpful when a genotype must be evaluated in several environments. In this case, due to the occurrence of the G×E, it is worthwhile to account for the interaction in prediction models, once it can boost the predictive accuracy and the genetic gains (Jarquín et al. 2014; Zhang et al. 2014; Lopez-Cruz et al. 2015; Cuevas et al. 2016; Sousa et al. 2017). Furthermore, use of multi-environment trials enables to target parents for specific environments. The inclusion of parental information in training sets establishment through its progenies in genomic prediction models to single environment analysis has been proven to impact prediction accuracy (Technow et al. 2012, 2014; Zhao et al. 2015; Kadam et al. 2016). Nevertheless, it has been shown that the inclusion of information from at least one parental line leads to intermediate prediction accuracies when compared to situations in which two or none parental are represented in the training set. However, the effect of G×E on the inclusion of parental information in training sets has not been reported yet.

In this context, we conducted two studies. In the first manuscript, we present an overview of genomic models for prediction of agronomic traits in maize hybrids and use the described models to evaluate the contribution of additive and non-additive effects for prediction

of agronomic traits (grain yield, ear, and plant height) in tropical maize. At the second paper, we extended the genomic model proposed by Lopez-Cruz et al. (2015) to regard additive and dominance effects. In this study, we verified the G×E's complexity influence over the prediction accuracy of grain yield in maize hybrids, and the impact of parental information for hybrid prediction in multi-environment situations.

REFERENCES

Bernardo R (2010) Breeding for quantitative traits, 2nd edn. Stemma Press, Woodbury

Cuevas J, Crossa J, Soberanis V, et al (2016) Genomic Prediction of Genotype × Environment Interaction Kernel Regression Models. Plant Genome 9:. doi: 10.3835/plantgenome2016.03.0024

Heslot N, Jannink J, Sorrells ME (2015) Perspectives for genomic selection applications and research in plants. Crop Sci 55:1–30. doi: 10.2135/cropsci2014.03.0249

Jarquín D, Crossa J, Lacaze X, et al (2014) A reaction norm model for genomic selection using high-dimensional genomic and environmental data. Theor Appl Genet 127:595–607. doi: 10.1007/s00122-013-2243-1

Kadam DC, Potts SM, Bohn MO, et al (2016) Genomic prediction of single crosses in the early stages of a maize hybrid breeding pipeline. G3:Genes|Genomes|Genetics 6:3443–3453. doi: 10.1534/g3.116.031286

Lopez-Cruz M, Crossa J, Bonnett D, et al (2015) Increased Prediction Accuracy in Wheat Breeding Trials Using a Marker × Environment Interaction Genomic Selection Model. G3 Genes|Genomes|Genetics 5:569–582. doi: 10.1534/g3.114.016097

Meuwissen TH, Hayes BJ, Goddard ME (2001) Prediction of total genetic value using genome-wide dense marker maps. Genetics 157:1819–1829

Reif JC, Gumpert FM, Fischer S, Melchinger AE (2007) Impact of interpopulation divergence on additive and dominance variance in hybrid populations. Genetics 176:1931–1934. doi: 10.1534/genetics.107.074146

Schrag TA, Möhring J, Melchinger AE, et al (2010) Prediction of hybrid performance in maize using molecular markers and joint analyses of hybrids and parental inbreds. Theor Appl Genet 120:451–461. doi: 10.1007/s00122-009-1208-x

Sousa MB e, Cuevas J, Couto EG de O, et al (2017) Genomic-enabled prediction in maize using kernel models with genotype x environment interaction. G3 Genes|Genomes|Genetics 7:1995–2014. doi: 10.1534/g3.117.042341

Sprague GF, Tatum LA (1942) General vs. specific combining ability in single crosses of corn. J Am Soc Agron 34:923–932

Technow F, Riedelsheimer C, Schrag TA, Melchinger AE (2012) Genomic prediction of hybrid performance in maize with models incorporating dominance and population specific marker effects. Theor Appl Genet 125:1181–1194. doi: 10.1007/s00122-012-1905-8

Technow F, Schrag TA, Schipprack W, et al (2014) Genome properties and prospects of genomic prediction of hybrid performance in a breeding program of maize. Genetics 197:1343–1355. doi: 10.1534/genetics.114.165860

Windhausen VS, Atlin GN, Hickey JM, et al (2012) Effectiveness of Genomic Prediction of Maize Hybrid Performance in Different Breeding Populations and Environments. G3 Genes|Genomes|Genetics 2:1427–1436. doi: 10.1534/g3.112.003699

Zhang X, Pérez-Rodríguez P, Semagn K, et al (2014) Genomic prediction in biparental tropical maize populations in water-stressed and well-watered environments using low-density and GBS SNPs. Heredity (Edinb) 114:291–299. doi: 10.1038/hdy.2014.99

Zhao Y, Li Z, Liu G, et al (2015) Genome-based establishment of a high-yielding heterotic pattern for hybrid wheat breeding. Proc Natl Acad Sci 112:201514547. doi: 10.1073/pnas.1514547112

2. A NEW PROPOSAL TO UNDERSTAND THE CONTRIBUTION OF ADDITIVE AND NON-ADDITIVE EFFECTS TO AGRONOMIC TRAITS IN TROPICAL MAIZE HYBRIDS

ABSTRACT

Background: Hybrid selection is an essential step in maize breeding. Evaluating a large number of hybrids in field trials can be extremely costly and, in some cases, not feasible. This problem can be avoided by predicting the performance of non-tested hybrids through the use of genomic models. Generally, the genotypic value of a hybrid is decomposed into general and specific combining abilities (additive and non-additive effects, respectively). However, due to the lack of orthogonality between the modeled effects, genomically estimated general and specific combining abilities cannot be used to make inferences about the importance of additive and non-additive effects on the genetic control of agronomical traits in maize hybrids. *Results:* In our study, we provide an overview of genomic models for prediction of agronomic traits in maize hybrids and outline a general modeling framework that includes parametric and semi-parametric models for additive and non-additive effects. Furthermore, we discuss how to use these models to orthogonally decompose the genotypic variance into components due to general and specific combining ability, and how to obtain gaussian kernels based on the additive relationship kernels. We applied the proposed methodologies to data from 906 single cross tropical maize hybrids derived from a convergent population. Our results indicate that: *(i)* non-additive effects make a sizable, intermediate, and minimal contribution to the genetic variance of grain yield, plant height, and ear height, respectively; *(ii)* non-additive effects were more important under stress conditions; *(iii)* genomic prediction can achieve relatively high accuracy in predicting phenotypes of un-tested hybrids and in pre-screening. *Conclusions:* The proposed method for partitioning the total genetic variance into general and specific combining ability components in genomic prediction models can be useful tool to study the influence of additive and non-additive effects on the phenotypic expression of complex traits in hybrids. Furthermore, deriving gaussian kernels based on additive relationship matrices is possible, and permits to standardize the bandwidth parameters values for semi-parametric regressions

Keywords: Genomic prediction; Hybrid prediction; Convergent populations; Tropical maize; Bayesian; BGLR; Semi-parametric models; RKHS; Dominance; Epistasis; Specific combining ability; Nitrogen; Stress

First draft submitted for review in the "Plant Methods" journal

2.1. INTRODUCTION

Most commercial maize breeding programs perform selection on inbred lines and then

select optimal crosses among elite materials (often from divergent heterotic groups) to produce commercial hybrids. Single crosses are highly homogeneous, can express heterosis, have greater yield stability in marginal environments, and are a convenient way to stack traits controlled by large-effect dominant genes [1]. Furthermore, hybrids are appealing for seed companies because they can generate sustained demand for seeds. These biological and commercial advantages prompted the adoption of hybrids in many crops, being maize one of the most prominent.

Selecting optimal matings becomes an important aspect of any maize hybrid breeding program. Ideally one would choose crosses based on the observed agronomic performance in field trials. However, evaluating all possible crosses can be extremely expensive, especially in early stages of a breeding program when the number of candidate lines can be large. In this situation, only a small fraction of all the possible crosses are evaluated on field experiments [2]. Genomic models can be used to predict the performance of un-tested hybrids; therefore, genomic prediction (GP, e.g.,[3]), a methodology originally developed for selection and breeding, also arises as a promising approach in hybrid prediction and mate selection.

Most of the theoretical and applied GP studies have focused on prediction of traits and diseases in outbreed materials from either animal [4–7] and plant [8–12] breeding populations. Another field of research has considered genomic models for prediction of agronomic traits in inbred lines [13–17]. More recently, some authors have considered using genomic models for prediction of hybrid performance [18–25]; these studies have shown that genomic models can yield reasonably accurate predictions of the agronomic performance of hybrids. In this manuscript we present *an overview of genomic models for prediction of agronomic traits* in maize hybrids and use the models described to evaluate the contribution of additive and non-additive effects for prediction of agronomic traits in tropical maize.

Most of the literature on the genomic analysis of hybrid performance in maize has focused on the study of materials produced by crossing lines from divergent heterotic groups. Crosses from such groups are expected to express less specific-combining ability [26,27] than the one expected among crosses of lines from showing small degree of divergence among heterotic groups. In this study, we focus *on the evaluation of the contribution of additive and non-additive effects to general and specific combining ability among crosses of inbred lines from a convergent population*.

In the hybrid literature the genetic variance is often decomposed into the general and specific combining ability variance (GCA and SCA, respectively, [28]) components. The GCA variance represents the amount of variance that can be explained by the mean of the parental lines, while the SCA variance quantifies the amount of variance on the genotypic values that cannot be explained by parental means. This component is attributable to deviations from

additivity due to dominance and epistasis [29]. Unfortunately, additive and non-additive contrasts are often not mutually orthogonal. For this reason, the variance parameters entering in genomic models (e.g., the additive and dominance variance) cannot be directly used to decompose the total genetic variance into GCA and SCA components. Here, following ideas presented by Lehemeier et al. [30] *we discuss how GCA and SCA variance components can be estimated in models including additive and several types of non-additive effects*, regardless of the orthogonality of contrasts used to accommodate those effects.

Genomic prediction studies of hybrid performance have pre'dominantly used parametric models for additive and dominance effects modeling [18,23,25,31], and a few studies have considered the inclusion of epistatic interactions in cassava [32], pinus [10], eucalyptus [12], and rice [21]. Nevertheless, in most of them, the additive-by-additive epistatic relationship matrices used (which are often based on Hadamard products of additive relationship matrices) do not allow for a clear distinction of the contribution dominance and epistasis. Thus, in our study, we make this distinction explicit and *described kernels that distinguish these two sources of non-additive variation*. More recently, Gianola *et al.* [33] and de los Campos *et al.* [34] considered using semi-parametric models (e.g., Reproducing Kernel Hilbert Spaces, RKHS) to capture both additive and non-additive genetic effects into genomic analyses. Here, we *consider a range of models including parametric models, accounting for additive and non-additive effects, and semi-parametric RKHS regressions and compare their performance for hybrid prediction.*

What remains of the manuscript is organized as follows: the next section describes a general framework for the hybrid prediction that encompasses parametric and semi-parametric methods in a unified setting. In this section, we also discuss methods to estimate variance due to general and specific combining ability. Subsequently, we applied the described methods to a data set of hybrids from a convergent population and reported both variance components and predictive performance.

2.2. A general framework for the hybrid prediction

2.2.1. Genomic models for analysis of hybrid data

The problem of predicting the hybrid performance of a set of all the possible crosses that can be generated from n lines can be viewed as one of smoothing phenotypic data (e.g., yield observed on hybrids) over a grid of crosses (Figure 1). The left panel represents all possible crosses, and the right plot describes surfaces with different degree of genetic complexity. The

phenotype of the kth replicate of the progeny of lines i and j (y_{ijk}) can be decomposed into a genetic component (g_{ij}) plus an environmental effect (ε_{ijk}), that is $y_{ijk} = g_{ij} + \varepsilon_{ijk}$. Here, g_{ij} represents the expected phenotypic performance (average over replicates) of the progeny of lines i and j that is $g_{ij} = \mathrm{E}(y_{ijk})$. Ideally, we would like to predict g_{ij} for all possible crosses (i.e., all possible (i , j) pairs for i ≠ j). This task can be achieved by smoothing phenotypic data concerning genotypes. The surface smoothness (right pannel of Figure 1) depends on the relationship among the inbred lines and on the types of effects modeled in g_{ij}. The additive model will give the smoothest pattern (a hyper-plane), dominance and epistasis make this surface more irregular (compare the top, and lower right plots of Figure 1).

2.2.2. General and specific combining abilities

The expected hybrid performance (g_{ij}) is often represented as the sum of the general and specific combining abilities (GCA and SCA, respectively,[28]). The GCA-portion of a hybrid's genotypic value is the average of the parental means, $GCA_{ij}=\frac{1}{2}(u_i+u_j)$; here, $u_i = E_{j|i}(g_{ij})$ represent the average genotypic value of the progeny of i^{th} parental line in respect to the second parents (likewise, $u_j = E_{i|j}(g_{ij})$). The SCA portion accounts for deviations of the hybrid mean (g_{ij}) relative to the average of the parental means, that is $\delta_{ij}=g_{ij}-\frac{1}{2}(u_i+u_j)$. From the perspective of Analysis of Variance, the GCA represent main effects of the parental lines and SCA represent interactions between those lines. Therefore, the total genetic variance can be decomposed into two orthogonal components, that is $\sigma_G^2 = \sigma_{GCA}^2 + \sigma_{SCA}^2$ where $\sigma_G^2 = Var(g_{ij})$, $\sigma_{GGA}^2 = Var(GCA_{ij})$ and $\sigma_{SCA}^2 = Var(SCA_{ij})$.

The GCA of a line can be modeled using an **additive model**. In a genomic regression this can be achieved by regressing phenotypes on a linear combination of markers genotypes, that is $u_i = \sum_{k=1}^{p} x_{ik}\alpha_k$ where $x_{ik} \in \{0,2\}$ is the genotype of the i^{th} line at the k^{th} SNP and α_k is the additive effect of the k^{th} SNP. In convergent populations crosses one can assume that additive effects are the same for all lines. Therefore, the additive component of the model can be expressed as $g_{ij} = \frac{1}{2}(u_i + u_j) = \frac{1}{2}\sum_{k=1}^{p}(x_{ik} + x_{jk})\alpha_k$. Here, $x_{ijk} = \frac{1}{2}(x_{ik} + x_{jk})$ is the hybrid genotype at the k^{th} loci which is simply the average of the parental genotypes.

Additive model (A): $g_{ij} = \frac{1}{2}(u_i + u_j) = \sum_{k=1}^{p} x_{ijk}\alpha_k$ [1]

Expression [1] defines a hyperplane with respect to the general combining abilities (Figure 1b).

Deviations from the hyperplane (SCA effects) can be introduced by adding dominance and epistatic interactions. Dominance (i.e, within locus interaction of alleles, β_k) can be accommodated by adding dummy-variables for heterozygous loci that is

Additive+Dominance (A+D): $g_{ij} = \sum_{k=1}^{p} x_{ijk}\alpha_k + \sum_{k=1}^{p} \Delta_{ijk}\beta_k$; [2]

where, $\Delta_{ijk} = 1(x_{ijk} = 1)$ is an indicator variable for the k^{th} loci that takes value 1 for heterozygous loci and 0 for homozygous.

Epistatic interactions can take various forms (additive-by-additive, additive-by-dominance, dominance by dominance, additive-by-additive-by-additive, etc., [29,35]) ; for simplicity, in parametric models, we focus on 1st order interaction of alleles among loci involving additive effects, that is additive-by-additive and additive-by-dominance interactions. With p markers, we can form $\frac{p(p-1)}{2}$ additive-by-additive (*A by A)* interactions; a specification including additive, dominance and additive-by-additive interactions (γ_{kl}) effects takes the form

Additive+Dominance+A-by-A(A+D+AA): $g_{ij} = \sum_{k=1}^{p} x_{ijk}\alpha_k + \sum_{k=1}^{p} \Delta_{ijk}\beta_k + \sum_{k=1}^{p}\sum_{l>k}^{p} x_{ijk}x_{ijl}\gamma_{kl}$ [3]

Likewise, one can have a total of $\frac{p(p-1)}{2}$ additive-by-dominance interactions (*A by D*, ω_{kl}) which can be combined with additive and dominance effects to give rise to the following specification

Additive+Dominance+A by D (A+D+AD): $g_{ij} = \sum_{k=1}^{p} x_{ijk}\alpha_k + \sum_{k=1}^{p} \Delta_{ijk}\beta_k + \sum_{k=1}^{p}\sum_{l>k}^{p} x_{ijk}\Delta_{ijk}\omega_{kl}$ [4]

2.2.3. Parametric kernels for additive and non-additive effects

The number of effects entering in [1]-[4] can be extremely considerable. Therefore, in genomic models, effects are usually treated as random draws from some distribution, the most common one is the Normal distribution.

The terms in the right side of equations [1], [2], [3] and [4] are linear combinations of effects. Therefore, if effects follow normal distributions, $\alpha_k \underset{\sim}{iid} N(0, \sigma_a^2)$, $\beta_k \underset{\sim}{iid} N(0, \sigma_d^2)$, $\gamma_{kl} \underset{\sim}{iid} N(0, \sigma_{aA}^2)$ and $\omega_{kl} \underset{\sim}{iid} N(0, \sigma_{ad}^2)$, then, vectors containing additive $\boldsymbol{a} = \{a_{ij} =$

$\sum_{k=1}^{p} x_{ijk}\alpha_k \}$, dominance $\boldsymbol{d} = \{d_{ij} = \sum_{k=1}^{p} 1(x_{ijk} = 1)\,\beta_k \}$, additive-by-additive $\boldsymbol{aa} = \{aa_{ij} = \sum_{k=1}^{p}\sum_{l>k}^{p} x_{ijk}x_{ijl}\gamma_{kl} \}$, and additive-by-dominance epistatic interactions $\boldsymbol{ad} = \{ad_{ij} = \sum_{k=1}^{p}\sum_{l>k}^{p} x_{ijk}\Delta_{ijk}\omega_{kl} \}$ will follow multivariate normal distributions: $\boldsymbol{a}\sim MVN(\boldsymbol{0}, \boldsymbol{K}_a\sigma_a^2)$, $\boldsymbol{d}\sim MVN(\boldsymbol{0}, \boldsymbol{K}_d\sigma_d^2)$, $\boldsymbol{aa}\sim MVN(\boldsymbol{0}, \boldsymbol{K}_{aa}\sigma_{aa}^2)$ and $\boldsymbol{ad}\sim MVN(\boldsymbol{0}, \boldsymbol{K}_{ad}\sigma_{ad}^2)$ where $\boldsymbol{K}_a$, $\boldsymbol{K}_d$, $\boldsymbol{K}_{aa}$ and $\boldsymbol{K}_{ad}$ are co-variance matrices for additive, dominance, additive-by-additive, and additive-by-dominance effects, respectively.

The covariance matrices for additive and dominance effects ($\boldsymbol{K}_a$ and $\boldsymbol{K}_d$) are well established (e.g., [36–38]), and can be computed using cross-products of genotypes codes: $\boldsymbol{K}_a = \frac{\boldsymbol{XX'}}{\boldsymbol{tr(XX')}/\boldsymbol{n}}$ where $\boldsymbol{X} = \{x_{ijk} - 2\theta_k\}$ is a matrix of (centered) hybrid genotypes (here θ_{jk} is the frequency of the allele counted at the k^{th} loci) and $\boldsymbol{K}_d = \frac{\boldsymbol{DD'}}{\boldsymbol{tr(DD')}/\boldsymbol{n}}$ where $\boldsymbol{D} = \{1(x_{ijk} = 1) - 2\theta_k(1 - \theta_k)\}$ is a matrix whose columns contain dummy variables for heterozygous genotypes centered around their respective means.

Unfortunately, computing the covariance structure for additive-by-additive and additive-by-dominance effects is more challenging because the number of contrasts involved can be very large. However, these covariance matrices can be computed using Hadamard products. For instance, the covariance matrix for additive-by-dominance can be computed using the Hadamard product (denoted by "$\odot$") between $\boldsymbol{K}_a$ and $\boldsymbol{K}_d$ (see [39,40]); hence, $\boldsymbol{K}_{ad} = \frac{\boldsymbol{K_a}\odot\boldsymbol{K_d}}{\boldsymbol{tr(K_a}\odot\boldsymbol{K_d)}/\boldsymbol{n}}$. It can be shown (Appendix 1) that the Hadamard product $\boldsymbol{K}_a \odot \boldsymbol{K}_a$ includes cross-products of contrasts for additive-by-additive effects and also cross-products of contrasts for dominance. Therefore, the correct covariance structure for additive-by-additive effects can be obtained by subtracting the contribution of dominance, that is: $\boldsymbol{K}_{aa} = \frac{(\boldsymbol{XX'})\odot(\boldsymbol{XX'})' - (\boldsymbol{X}\odot\boldsymbol{X})(\boldsymbol{X}\odot\boldsymbol{X})'}{\boldsymbol{tr}((\boldsymbol{XX'})\odot(\boldsymbol{XX'})' - (\boldsymbol{X}\odot\boldsymbol{X})(\boldsymbol{X}\odot\boldsymbol{X})')/\boldsymbol{n}}$

The covariance structures discussed in the previous section can be used in multivariate normal distributions to model the hybrid's genetic/genotypic values. For instance, for the model of expression [3], we have $\boldsymbol{g} = \boldsymbol{a} + \boldsymbol{d} + \boldsymbol{aa}$ and with

$$\boldsymbol{g}\sim MVN(\boldsymbol{0}, \boldsymbol{K}_a\sigma_a^2 + \boldsymbol{K}_d\sigma_d^2 + \boldsymbol{K}_{aa}\sigma_{aa}^2) \qquad [3b]$$

Likewise for the model of expression [4] we have $\boldsymbol{g} = \boldsymbol{a} + \boldsymbol{d} + \boldsymbol{ad}$ with

$$\boldsymbol{g}\sim MVN(\boldsymbol{0}, \boldsymbol{K}_a\sigma_a^2 + \boldsymbol{K}_d\sigma_d^2 + \boldsymbol{K}_{ad}\sigma_{ad}^2) \qquad [4b]$$

2.2.4. Semi-parametric procedures

The models of expressions [3b] and [4b] can be viewed as multi-kernel models where different kernels are used to accommodate different types of effects. Each of these kernels also defines a different degree of smoothness of genetic values with respect to genotypes, with $\boldsymbol{K}_a$ usually giving higher smoothness (i.e., more covariance) than dominance or epistatic kernels. In such multi-kernel models, the variance parameters act as weights which end up defining the smoothness of $\boldsymbol{g}$ concerning genotypes [34]. For semi-parametric smoothing, we can replace the parametric kernels with, for example, Gaussian kernels indexed with bandwidth parameters. For instance, one can assume

$$\boldsymbol{g} \sim MVN(\mathbf{0}, \boldsymbol{K}_{h_1}\sigma_1^2 + \boldsymbol{K}_{h_2}\sigma_2^2 + \boldsymbol{K}_{h_3}\sigma_3^2) \quad [5b]$$

This approach, referred as "kernel averaging" in de los Campos *et al* [34], can be used to infer smooth functions without making parametric assumptions. Recently, Lyra *et al.* [23] and Sousa *et al.*[41] used kernel regressions (with a single kernel) to predict hybrid performance. Here we consider multi-kernel methods based on three Gaussian kernels derived from an additive relationship matrix. The proposed approach derives a matrix of genetic distances from $\boldsymbol{K}_a$. These distances are then used as inputs in three Gaussian kernels with values of the bandwidth parameters chosen so that one of the kernels gives higher covariance than additive effects, another one gives lower covariances than additive effects, and the last one gives covariances smaller than the two former kernels. The proposed approach has a built-in standarization such that the values of the bandwidth parameters do not depend on the number of markers used. Further details are given in Appendix 2.

2.2.5. The classical approach to estimate the general and specific combining abilities

A widespread method to model the general and specific combining abilities for predicting the performance of non-tested hybrids based on molecular markers was proposed by Bernardo [42] based on the studies of Stuber and Cockerham [43]. This approach has been recently used by several authors in genomic prediction studies of single crosses in plants [18,24,31,44], and assumes that the covariance among two single crosses, considering absence of epistasis, is:

$$Cov_{(xy,x'y')} = K_{xx'}\sigma^2_{GCA(1)} + K_{yy'}\sigma^2_{GCA(2)} + K_{xx'}K_{yy'}\sigma^2_{SCA}, \quad [6]$$

in which, $K_{xx'}$ and $K_{yy'}$ is the additive relationship between the inbreed lines x and x', and y

and y' from the groups 1 and 2, respectively. $K_{xx'}K_{yy'}$ is the direct product (Hadamard product) between the relationship of the hybrids parents. $\sigma^2_{GCA(1)}$ and $\sigma^2_{GCA(2)}$ are the variance due the general combining ability of parentals in groups 1 and 2 and represents the additive variance of each of them. σ^2_{SCA} is the specific combining ability, and, as commonly assumed, under absence of epistasis represents only the dominance variance. But, assuming a complete diallel design (when the group 1 is equal to 2) or even for partial diallels (different populations), where, in general, the largest proportion of markers is the same for both populations, the product $K_{xx'}K_{yy'}$ models both intra-loci and inter-loci interactions (Appendix 1). Furthermore, assuming a large number of loci for estimating the relationship the kernels, the product $K_{xx'}K_{yy'}$ will explain basically inter-loci interactions (for more details see [45]). However, $\sigma^2_{GCA(1)}$, $\sigma^2_{GCA(2)}$, and σ^2_{SCA} cannot be used to make inferences about the importance of the genetic effects for the phenotypic variation due to the lack of orthogonality between then [30,46].

2.2.6. Making the general and specific combining abilities orthogonal in genomic regressions

Lehermeier et al [30] highlighted that in a regression involving multiple terms, when predictors are not mutually orthogonal, genetic variance parameters (e.g., σ^2_a, σ^2_d, σ^2_{aa} and , σ^2_{ad}) cannot be used to decompose the variance into components because such decomposition ignores covariances. For this reason, in a multi-kernel model, these parameters cannot be directly used to decompose the genetic variance into orthogonal components such the classical definition of the σ^2_{GCA} and σ^2_{SCA}. Lehermeier et al [30] discussed how variance components can be estimated when predictors are not mutually orthogonal. Here, we adapted the ideas discussed by those author for estimating σ^2_{GCA} and σ^2_{SCA} .

In a multi-kernel model, $\mathbf{g} = \mathbf{g}_1 + \mathbf{g}_2 + \cdots + \mathbf{g}_q$, the amount of variance explained by the model (or **total genomic variance**, σ^2_G) is a function of the variance of each term plus twice the covariance of each pair of them: $\sigma^2_G = Var\left(\sum_{j=1}^{q} \mathbf{g}_j\right) = \sum_{j=1}^{q} Var\left(\mathbf{g}_j\right) + 2\sum_{j=1;k\neq j}^{q} Cov\left(\mathbf{g}_j, \mathbf{g}_k\right)$. Here, $Var\left(\mathbf{g}_j\right) = (n-1)^{-1}\sum_{i=1}^{n}\left(\mathrm{g}_{ij} - \bar{\mathrm{g}}_j\right)^2$ is the sample-variance of the j[th] random effect. As noted by [30], in a Bayesian setting, samples from the posterior distribution of σ^2_G can be obtained by evaluating, at each iteration of the sampler $\sigma^2_G = Var\left(\sum_{j=1}^{q} \mathbf{g}_j\right)$ where $\mathbf{g}_j$ represent realized samples of the vectors containing the random effects

and $Var()$ is the sample variance operator.

The **general combining ability variance** (σ^2_{GCA}) represents the amount of variance that can be captured by additive effects in a pure additive model (equation [1]) at each iteration of the sampler. The **specific combining ability variance** (σ^2_{SCA}) can be estimated by subtracting, at each iteration of the sampler, the σ^2_{GCA} from the total genomic variance estimated from models accounting non-additive effects (equations [2-4]). Thus, $\sigma^2_{SCA} = \sigma^2_G - \sigma^2_{GCA}$ where, e.g., $\sigma^2_G = Var(\boldsymbol{a} + \boldsymbol{d} + \boldsymbol{aa})$. Finally, the proportion of the total genomic variance attributable to SCA can be estimated using $D^2 = \frac{\sigma^2_{SCA}}{\sigma^2_G}$.

2.3. Application to a dataset of tropical maize hybrids derived from a convergent population

We used the models described above to study the contribution of additive and non-additive effects to predict hybrids obtained by crossing lines from a convergent population.

Data was available for a total of 906 maize single-crosses derived from forty-nine inbred lines, contrast in the use of nitrogen [47], crossed in an unbalanced diallel mating design . The hybrids were evaluated during the second growing season (January to May), of 2016 and 2017, in two locations, Piracicaba (PI; rainfed; 22°42'23"S, 47°38'14"W, 535 m) and Anhembi (AN; irrigated; 22°50'51"S, 48°01'06"W, 466 m), São Paulo State, Brazil. At each site, the material was evaluated under two nitrogen (N) regimes, ideal N (IN; 100 $kg\ N\ ha^{-1}$, 70 $kg\ N\ ha^{-1}$ at sowing and 30 $kg\ N\ ha^{-1}$ on the V8 plant stage) and low N (LN; 30 $kg\ N\ ha^{-1}$ being the totality applied at sowing). These two treatments, in combination with the two locations, were used to define four distinct environments (PI.IN, PI.LN, AN.IN, AN.LN).

Field trials were organized in an unreplicated augmented block design consisting of 47 (year 1) or 50 (year 2) blocks with 16 hybrids and two commercial checks evaluated in each block. **Three traits** were evaluated in each environment: grain yield (GY, $ton\ ha^{-1}$), plant height (PH, m), and ear height (EH, m). Plots were manually harvested and GY was corrected to 13% moisture. EH and PH were measured from soil surface until the insertion of the first ear and the flag leaf collar on five representative plants within each plot, respectively.

Phenotypes were pre-adjusted using a mixed model with an intercept, the fixed effect of the check, and the random effect of the block. We used this model to derive an adjusted phenotype for each trait, which consisted of the measured phenotype minus the estimated intercept minus the block effect. Finally, we averaged the adjusted phenotype of each hybrid

from years 1 and 2 to carry out the genomic analysis.

Genotypes for each one of the forty-nine parental inbred lines were obtained using the Affymetrix® Axiom® Maize Genotyping Array of 616 K SNPs [48]. Markers with call rate lower than 0.90, heterozygous loci in at least one parental line, and all non-mapped SNPs were removed. Posteriorly, the hybrids genotypes matrix was constructed by combining the parentals genotypes. Then, markers with a minor allele frequency smaller than 0.05 were removed from the hybrids SNP matrix, once we evaluated only a sample of all possible combination of the inbred lines. After that, we pruned the hybrids genotype matrix excluding markers with r^2 value (pairwise linkage disequilibrium -LD) greater than 0.9. All quality control procedures were made using the R package *synbreed* [49], and LD pruning was carried out using the *SNPRelate R* package [50]. After all quality control and LD pruning process, 34,571 high-quality SNPs were available to further analysis.

For genomic analyses *w*e used the multi-kernel regressions described above to a defined sequence of models of increasing complexity: from strictly additive models to semi-parametric regressions (Table 1)**.** We used the BGLR R-package [51] software to collect samples of the posterior distribution of effects, variance parameters (e.g., σ^2_ε, σ^2_a, σ^2_d, σ^2_{aa} and , σ^2_{ad}) and samples from the posterior distribution of variance components (σ^2_G, σ^2_{GCA}, σ^2_{SCA}). Samples from the posterior distribution of variance components and variance parameters were generated using the approach described by Lehermeier *et al.* [30] and discussed in the previous section. For this, we fitted each model to all the data available for each trait-environment combination (full-data analysis). Models were fitted within environment (defined as location-by-fertilization treatment combinations), separately for each trait. For each model, inferences were based on 30,000 samples collected after discarding 5,000 samples for burn-in and thinning of 5.

Prediction accuracy was evaluated using replicated training-testing (TRN-TST) partitions. In each partition, 75% of the data (approximately 680 hybrids) was randomly selected and used for model training. The predictive performance was evaluated using the data of the 25% of the hybrids saved for each validation set. None data from hybrids used for TST was included in the TRN set. Therefore, our evaluation of prediction accuracy is similar to the method labeled as CV1 in Burgueño *et al.* [52]. This validation scheme mimics, in our case, the prediction problem that one faces when predicting the performance of un-tested hybrids. The same partitions were used to fit each of the models, and this allowed us to compute the proportion of times that one model achieved higher prediction accuracy than the other ones while accounting for variance in prediction accuracy due the sampling of TRN and TST sets. Predictive performance was measured using Pearson's product moment correlation between

adjusted phenotypes and genomic estimated genetic values ($r_{y\hat{y}}$) in each of the TST sets. For each model/trait/environment, we carried out a total of 100 TRN-TST partitions, totaling 100 correlations estimates.

2.4. Results

The average ear height, plant height, and grain yield were higher in the irrigated environment (Anhembi) than in the rainfed one (Piracicaba) and higher with ideal nitrogen (especially in well-watered conditions) than with low-nitrogen availability (Figure 2). For all the traits and environments, the observed distributions of phenotypes were somewhat symmetric and there were no significant differences in variances (except for grain yield, for this trait the variance of phenotypes was higher in well-watered conditions).

2.4.1. Variance components

Genomic variance and broad-sense genomic heritability (H^2). The proportion of variance of phenotypes explained by the model ($H^2 = \frac{\sigma^2_G}{\sigma^2_G+\sigma^2_\varepsilon}$) was highest for EH (ranging from 0.7 to ~ 0.8, depending on the environment and model, Figure 3A), intermediate for PH and lowest for GY (for this trait values ranged from ~0.3 to ~0.6). The comparison across environments shows that the proportion of variance that can be explained by genetic factors was highest in the best environmental conditions (AN.IN) and lowest in AN.LN and with either low or ideal N in Piracicaba, where trials were not irrigated. As one would expect, the proportion of variance explained by the model increased when terms accounting for non-additive effects were included in the model (Figure 3).

In general, there was a sizable increase in the proportion of variance explained when D (dominance) was included in the model and relatively small increases in σ^2_G when other effects ere added to the A+D model. The difference in σ^2_G between the A and A+D models was smaller for EH and larger for GY (Figure 3A). The RKHS model showed the highest estimates of the H^2 by the model. However, in general, this model did not explain much more variance than the A+D model.

The inclusion of non-additive effects reduced the estimate of the additive parameter (σ^2_a). For instance, for EH the σ^2_a was always the largest estimated parameter. However, for GY the estimates of individual non-additive components were usually higher, with values similar to

that of the additive parameter (Figure 3b, Tabs. S1,S2,S3,S4 and S5).

Covariances between additive and non-additive effects: Different covariance patterns were observed for the evaluated traits (Figure 4). Among them, EH was the trait that appeared to be mostly additive (Figure 3A). The average covariance between additive and additive-by-additive variances, and those among additive and additive-by-dominance were slightly positive. On the other hand, for PH and GY most of the covariances were close to zero, with a few exceptions (e.g., PH in PI.IN).

Variance components (σ^2_G, σ^2_{GCA} and σ^2_{SCA}) were used to compute the ***proportion of variance explained by non-additive effects*** ($D^2 = \frac{\sigma^2_{SCA}}{\sigma^2_G}$, Table 2). D^2 was highest for grain yield (D^2 values ranging from ~0.236 to ~0.47) and lowest for EH (D^2 estimates ranged from ~0.08 to ~0.17). PH was a compromising situation with D^2 ranging from ~0.12 to ~0.29 (Table 2). Regarding the estimates for the ratio among the SCA and the GCA variance components (SCA_{ratio}, Table S6), in agreement with the D^2 results, SCA_{ratio} estimates were the highest for GY, lowest for EH, and intermediate for PH. In most cases, non-additive effects contributed more to the variance under low N conditions. The optimal environment (AN.IN, ideal nitrogen regime and irrigated conditions) showed the smallest mean importance of non-additive effects for ear height, grain yield, and plant height.

2.4.2. Prediction accuracy

The cross-validation analysis yielded moderately high prediction correlations ($r_{y\hat{y}}$), ranging from ~0.46 to ~0.81 (Table 3). Prediction accuracy was highest for EH, smaller but still high for PH, and moderate for GY. In general, the lowest mean correlations were obtained in AN.LN. For EH the predictive performance was very similar in the other three environments. On the other hand, for GY and PH, the prediction accuracies were smaller in stressed conditions (low nitrogen availability) than in "ideal" conditions (Table 3).

Overall, the differences in the prediction accuracy achieved through different models were moderate. For instante, for EH almost no differences were observed in prediction accuracy between models. However, for GY and PH, there was a clear superiority of models including dominance and the RKHS regression relative to the additive model.

For GY, the superiority of the A+D model over the A model was consistent across the validation sets in more than 95 of the 100 sets conducted the A+D model gave higher prediction correlation than the A model (Figure 5). On the other hand, the proportion of times that the

A+D model outperformed the A model was much more modest for EH. Plant height was in an intermediate situation, where the A+D model was in average better than the A model, but the superiority was not as consistent across CV as observed for GY. The same trend was observed in other environments (Figure S1).

2.4.3. Predicting hybrid performance for observed and un-observed crosses

We used the fitted models to predict the total genetic value of all possible hybrids that can be obtained from the 49 inbred lines available (Figure 6). In the heatmaps, the parental lines were sorted according to the predicted genetic values from the additive model. Based on that it is possible to note that there is a smooth increase on predicted genotypic values along the diagonal of the heatmap (values increase in "top-right" direction). This trend also appears in the heatmaps displaying predictions from non-additive models. However, when dominance was included the patterns in the heatmaps were less smooth (this is particularly clear for grain yield). Overall, the best crosses that one would choose using an additive model (i.e., those in the top-right corner of each plot) are also predicted to have high genotypic value under the non-additive model. Nevertheless, for grain yield, there are also a few cases where the additive model predicts intermediate genetic values (points in the center of the heat maps) and the non-additive model predicts a higher genotypic value (this corresponds to yellow-green points in the center of the heatmap).

2.5. Discussion

In crops where new varieties are inbred lines (e.g., wheat, soybeans), F_1 seeds (e.g., hybrids in maize, sunflower), or clones (e.g., potato, cassava, sugarcane, eucalyptus) advantageous gene combinations can be fixed and multiplied. In these cases, non-additive effects can be effectively exploited and maintained [32]. However, identifying the best genotypes requires extensive field evaluations, especially for F_1 hybrids. For instance, in single-cross selection obtained from N inbreed lines there would be possible $N(N-1)/2$ crosses. Therefore, even for small values of N, evaluating all possible crosses can be extremely costly and may not be logistically feasible.

Genetic similarity (derived from either pedigrees or molecular markers) can be leveraged to induce borrowing of information between crosses and this can be used for prediction of performance of un-tested hybrids. The strength of borrowing information between hybrids

depends on the genetic similarity among the inbred lines, and on the mode of gene action. Additive effects give rise to a smooth surface where the expected performance of a hybrid is the average of the general combining ability of the two parental lines (Figure 1). Deviations from this plane can be accommodated using non-additive effects such as dominance or epistatic interactions or using semi-parametric procedures. All these models can be formulated as multi-kernel regressions (e.g., [34,53]), where different kernels are used to model different types of effects.

Disentangling the contribution of dominance and epistatic effects is not always possible. We found, for all traits, successive reductions on the estimates of genetic variance parameters (σ_a^2, σ_d^2, σ_{aa}^2, and σ_{ad}^2) according to the model complexity. It suggests that the genetic parameters were partially confounded, which was confirmed by the covariance's analysis (Figure 4; Figure S2). Furthermore, modeling non-additive effects, for traits in which these effects showed small importance induces to larger covariances between them. Covariance among genetic effects may occur due to the non-orthogonality of components. Also, an orthogonal partition of the genetic variance into additive and non-additive effects occurs only under idealized conditions that are not met using breeding populations [46,54,55]. Within locus, it is possible to make additive effects orthogonal to dominance contrasts (e.g., [40]). However, it does not guarantee orthogonality between loci. Moreover, to generate an orthogonal parametrization for models involving epistasis is difficult, especially in breeding populations. Indeed, selection induces linkage disequilibrium (LD, i.e., the covariance of alleles at different loci) and it results in a correlation between additive and non-additive terms [45]. Overall, our results suggest that while it is clear that non-additive models can capture signals that are not captured by additive models, disentangle the gene action is challenging once the modeled genetic effects are often confounded.

Additive effects dominate but "one-size-(does not)-fit-all" traits/populations. For the three traits analyzed, additive effects explained the majority of the genetic variance. The comparison of the broad-sense genomic heritability estimates obtained via models including additive and non-additive effects (e.g., model A+D+AA+AD) relative to the amount of variance explained by the additive model suggest that near to 88, 78, and 65% of the genetic variance of EH, PH, and GY can be captured by modeling only additive effects, respectively. Moreover, the components estimates indicate that the three traits analyzed have a different genetic architecture concerning heritability and relative importance of additive and non-additive gene action. EH showed the highest broad-sense heritability (~0.8), and a high proportion of genetic variance explained by additive effects (D^2 was only ~0.12). On the other hand, GY showed moderate broad-sense heritability (~0.5-0.6 for models including non-additive effects), and a sizable

fraction of the total heritability accounted for non-additive effects (D^2 of 0.3~0.48). Finally, PH represented an intermediate situation between EH and GY concerning broad-sense heritability and the relative importance of non-additive effects. Indeed, our results are in agreement with those reported by [56], who indicated that additive effects explained a very large fraction of genetic variance for EH and PH. Furthermore, the variance components (σ^2_G, σ^2_{GCA} and σ^2_{SCA}) indicate that for PH and EH selection based on GCA may be effective. It has important implications for breeding, because the selection in early stages of the breeding process based on additive models may result in gains at the hybrid level as well [29]. However, for GY accounting for non-additive effects seems to be more critical.

Genetic diversity affects the ratio of SCA to GCA. Average estimates of SCA_{ratio} across the evaluated models and environments were 0.14, 0.28, and 0.56 for EH, PH, and GY, respectively. The estimates of SCA_{ratio} were higher than those previously reported for GY and PH in studies in which genomic kernels were employed to fit the prediction models [18,25,44]. Some authors have shown that genetic divergence between inbred lines affects the SCA_{ratio} [22,29,57]. Indeed, empirical evidence suggests that the SCA_{ratio} is higher for hybrids originated by crossing materials from genetically homogeneous pools (i.e., sets of inbred lines with similar allele frequencies). Therefore, lower SCA_{ratio} is expected for hybrids obtained by crossing lines from two divergent populations (*i.e.,* heterotic groups). Most of the published studies on maize hybrids are based on data originated by crossing lines from different heterotic groups [18,22,24,31,44]. In this context, non-additive effects are often absorbed in the population mean or are highly confounded with the additive effects [58]. This reduces the relative importance of the SCA and justifies selection based only on the GCA [26,27].

In contrast, in this study, we used data from hybrids generated from an unbalanced diallel where the parental lines did not show a clear population structure/differentiation (see Figure S3). Therefore, our dataset can be regarded as one in which hybrids were produced by intra-group crosses, and it may explain the relative high SCA_{ratio} observed.

Non-additive effects have an important role under stress conditions. In all but a case (PH in PI), for all traits, the environments under low nitrogen regime showed higher SCA_{ratio} than those under ideal nitrogen (Table S6). Similar results were reported by [59] and [60], who concluded that for grain yield in maize non-additive variation appears to be more important in low nitrogen growing conditions. They also reported the higher importance of non-additive effects under drought stress. Our results indicate substantial importance of non-additive effects in non-irrigated conditions, especially for GY. Thus, to take account of non-additive effects may be important when predicting for stressed environments.

Prediction of un-tested hybrids can reach moderate-to high accuracy and, within the model, it was linearly related to trait heritability. Our results indicate that GP can achieve a high level of prediction accuracy. Also, for any given model, there was a direct relationship between the proportion of variance explained by the model (H^2) and the prediction accuracy achieved in the prediction of un-tested hybrids. Interestingly, within the model, this relationship was very close to linear (Figures S4 and S5). For instance, prediction accuracy was highest (~0.8) for EH (the most heritable of the three traits analyzed), intermediate for PH (~0.7) and lowest (~0.5) for GY. Likewise, environments with lower heritability (those under stress conditions), were the one with lower prediction accuracy either. These results agree with the theoretical and empirical evidence, which support a direct relationship between trait heritability and prediction accuracy (e.g., [61,62]).

The models that fitted the data better were not always the ones that gave the highest prediction accuracy. Indeed, the relationship between the proportion of variance explained and prediction accuracy was not linear when comparing (within a trait or environment) results across models (Figure S5). For instance, while the RKHS model was in all cases the one that had the highest proportion of variance explained (Figure 3A) the predictive performance of this model was not the highest one. ***Overall, the best performing model across traits and environments was the A+D model*** (Table 3). Models including two or more non-additive (e.g., A+D+AA+AD) terms fitted the data better than models based on A+D (Figure 3). However, these models had poorer predictive performance than the A+D model.

Prediction accuracy depends on the proportion of variance that can be explained by the model and on the accuracy of estimates of effects (e.g., [63]). There is a trade-off between these two factors: more complex models often explain a larger amount of variance. On the other hand, they also involved more effects to be estimated and hence, for any given sample size, the accuracy of estimated effects is higher for the simpler models. It seems that the A+D model offers, at least for the sample size considered here, a very good balance between these two factors because it captures non-additive effects with a much less complex specification than other non-additive models.

Modeling non-additive effects increased prediction accuracy for traits with high SCA_{ratio} (Table S1), e.g., GY, had a small effect for PH and almost no effect for EH, the trait with smallest SCA_{ratio}. This results are in agreement with those of [11], who concluded that the impact of the inclusion of non-additive effects on the prediction accuracy depended on the trait architecture.

Genomic prediction can be effectively used for pre-screening, thus reducing the

number of hybrids to be tested in field evaluations. How can the genomic prediction be incorporated in hybrid selection? One possibility is to use GP to select a subset of promising hybrids which will be tested at field evaluations. This approach can significantly reduce the time and costs involved in generating hybrids and could reduce the probability that superior hybrids do not reach the field testing stage [18,64,65]. To assess how accurate genomic prediction could be at capturing in pre-screening a set of superior hybrids we estimated, using cross-validation predictions, the proportion of the top-5% of the hybrids (from the ranking based on the observed trait) that is captured within a set of hybrids selected using genomic prediction (Figure 7). Selecting the best 30% of the crosses based on genomic prediction leads to a subset of hybrids that contained between 85-95% of the top-5% of hybrids with the highest ear height. For PH, the best 30% of the hybrids in the genomic screening contained between 70-80% of the top-5% best hybrids. Finally, the set containing the 30% of the hybrids with highest genomic prediction values for GY included between 70-85% of the hybrids with highest GY in field evaluations. These results are in agreement with [66], who found high concordance among superior wheat lines selected by GS and phenotypic selection from multi-environment trials. Since final decisions regarding what hybrids should be advanced to commercial productions must be supported on extensive field trials, pre-screening seems to be an effective approach for incorporating GP into hybrid selection programs.

Predicting the performance of newly developed hybrids through genomic models accounting for non-additive effects can lead to higher predictive ability than a pure additive model. Furthermore, modeling non-additive effects provided higher genomic heritabilities, indicating the importance of these effects for the phenotypic variation of the evaluated traits and suggesting larger genetic gains, especially for grain yield. As pointed by some authors [12,67,68], modeling non-additive effects into genomic prediction frameworks may reduce the overestimation of the additive variance and improve the estimation of non-additive effects, which has large importance for accurately predicting the genetic gains in hybrids breeding programs. Hybrid's prediction can be done under two perspectives, pre-screening of promising hybrids for further field evaluations and for hybrids breeding programs. For the former, as we previously showed, accurately predicting the performance of new hybrids will lead to a larger proportion of coincidence between single crosses selected based on genomic and phenotypic information. It is advantageous when the breeder aims to pre-screen superior hybrids from a set of superior inbred lines. On the other hand, as we know, hybrid breeding is based on the Reciprocal Recurrent Selection (RRS, [56]), where the selection of superior inbred lines to the intrapopulational breeding (inside each heterotic group) is made based on the performance of

interpopulational (across heterotic groups) hybrids. Thus, increasing the prediction abilities of hybrids will allow a more accurate selection of superior lines in each heterotic group. Moreover, accurately estimating the importance of non-additive effects is necessary, once the hybrids breeding process is designed to maximize the heterosis in single-crosses.

2.6. Conclusions

We proposed a new method to obtain an orthogonal partition of the total genetic variance into general and specific combining ability components. This approach can be useful to study the influence of additive and non-additive effect on the phenotypic expression of complex traits in hybrids.

Also, we showed that additive relationship kernels can be used to derive genetic distances for computing gaussian kernels. It has important implications on genomic prediction, once it permits to standardize the bandwidth parameters values for Reproducing Kernel Hilbert Spaces regressions in which multiple kernels are included in the prediction model (as for the kernel averaging method).

Finally, our results indicate that non-additive effects play a major role in grain yield, a moderate part in plant height, and a limited for ear height. We also found that, in general, non-additive effects seem to be more important for the expression of traits under stress conditions. For traits/environments exhibiting high SCA_{ratio}, modeling non-additive effects increased prediction accuracy.

REFERENCES

1. Longin CFH, Mühleisen J, Maurer HP, Zhang H, Gowda M, Reif JC. Hybrid breeding in autogamous cereals. Theor Appl Genet. 2012;125:1087–96.

2. Schrag TA, Möhring J, Melchinger AE, Kusterer B, Dhillon BS, Piepho H-P, et al. Prediction of hybrid performance in maize using molecular markers and joint analyses of hybrids and parental inbreds. Theor Appl Genet. 2010;120:451–61.

3. Meuwissen TH, Hayes BJ, Goddard ME. Prediction of total genetic value using genome-wide dense marker maps. Genetics. 2001;157:1819–29.

4. Meuwissen T, Hayes B, Goddard M. Accelerating Improvement of Livestock with Genomic Selection. Annu Rev Anim Biosci. 2013;1:221–37.

5. Hayes BJ, Bowman PJ, Chamberlain AJ, Goddard ME. Invited review: Genomic selection in dairy cattle: Progress and challenges. J Dairy Sci. 2009;92:433–43.

6. C.M. Dekkers J. Application of Genomics Tools to Animal Breeding. Curr Genomics. 2012;13:207–12.

7. de los Campos G, Hickey JM, Pong-Wong R, Daetwyler HD, Calus MPL. Whole-Genome Regression and Prediction Methods Applied to Plant and Animal Breeding. Genetics. 2013;193:327–45.

8. Resende MFR, Muñoz P, Acosta JJ, Peter GF, Davis JM, Grattapaglia D, et al. Accelerating the domestication of trees using genomic selection: accuracy of prediction models across ages and environments. New Phytol. 2012;193:617–24.

9. Muranty H, Troggio M, Sadok I Ben, Rifaï M Al, Auwerkerken A, Banchi E, et al. Accuracy and responses of genomic selection on key traits in apple breeding. Hortic Res. 2015;2:15060.

10. Muñoz PR, Resende MFR, Gezan SA, Resende MDV, de los Campos G, Kirst M, et al. Unraveling Additive from Nonadditive Effects Using Genomic Relationship Matrices. Genetics. 2014;198:1759–68.

11. de Almeida Filho JE, Guimarães JFR, e Silva FF, de Resende MD V, Muñoz P, Kirst M, et al. The contribution of dominance to phenotype prediction in a pine breeding and simulated population. Heredity (Edinb). 2016;117:33–41.

12. Bouvet J-M, Makouanzi G, Cros D, Vigneron P. Modeling additive and non-additive effects in a hybrid population using genome-wide genotyping: prediction accuracy implications. Heredity (Edinb). 2016;116:146–57.

13. Bernardo R, Yu J. Prospects for Genomewide Selection for Quantitative Traits in Maize. Crop Sci. 2007;47:1082.

14. Crossa J, Campos G d. l., Perez P, Gianola D, Burgueno J, Araus JL, et al. Prediction of Genetic Values of Quantitative Traits in Plant Breeding Using Pedigree and Molecular Markers. Genetics. 2010;186:713–24.

15. Crossa J, Beyene Y, Kassa S, Pérez P, Hickey JM, Chen C, et al. Genomic prediction in maize breeding populations with genotyping-by-sequencing. G3 Genes|Genomes|Genetics. 2013;3:1903–26.

16. Crossa J, Pérez P, Hickey J, Burgueño J, Ornella L, Cerón-Rojas J, et al. Genomic prediction in CIMMYT maize and wheat breeding programs. Heredity (Edinb). 2014;112:48–60.

17. Nakaya A, Isobe SN. Will genomic selection be a practical method for plant breeding? Ann Bot. 2012;110:1303–16.

18. Kadam DC, Potts SM, Bohn MO, Lipka AE, Lorenz AJ. Genomic Prediction of Single Crosses in the Early Stages of a Maize Hybrid Breeding Pipeline. G3 Genes|Genomes|Genetics. 2016;6:3443–53.

19. Zhao Y, Zeng J, Fernando R, Reif JC. Genomic Prediction of Hybrid Wheat Performance. Crop Sci. 2013;53:802–10.

20. Philipp N, Liu G, Zhao Y, He S, Spiller M, Stiewe G, et al. Genomic Prediction of Barley Hybrid Performance. Plant Genome. 2016;9.

21. Xu S, Zhu D, Zhang Q. Predicting hybrid performance in rice using genomic best linear unbiased prediction. Proc Natl Acad Sci. 2014;111:12456–61.

22. Technow F, Riedelsheimer C, Schrag TA, Melchinger AE. Genomic prediction of hybrid performance in maize with models incorporating dominance and population specific marker effects. Theor Appl Genet. 2012;125:1181–94.

23. Lyra DH, de Freitas Mendonça L, Galli G, Alves FC, Granato ÍSC, Fritsche-Neto R. Multi-trait genomic prediction for nitrogen response indices in tropical maize hybrids. Mol Breed. 2017;37:80.

24. Massman JM, Gordillo A, Lorenzana RE, Bernardo R. Genomewide predictions from maize single-cross data. Theor Appl Genet. 2013;126:13–22.

25. Cantelmo NF, Von Pinho RG, Balestre M. Genome-wide prediction for maize single-cross hybrids using the GBLUP model and validation in different crop seasons. Mol Breed. 2017;37:51.

26. Melchinger AE. Genetic diversity and heterosis. In: Coors J., Pandey S, editors. Genet Exploit heterosis Crop. Madson: American Society of Agronomy, Crop Science Society of America and Soil Science Society of America; 1999. p. 99–118.

27. Dhillon BS, Gurrath PA, Pollmer WG, Klein Stuttgart (Germany, F.R.). Inst. of Plant Breeding, Seed Science and Population Genetics) D (Hohenhein U, Zimmer E, Wermke Braunschweig Voelkenrode (Germany, F.R.) Inst. of Grassland and Foddes Research) M (Federal ARS. Analysis of diallel crosses of maize for variation and covariation in agronomic traits at silage and grain harvests [in Germany Federal Republic]. Maydica (Italy). 1990.

28. Sprague GF, Tatum LA. General vs. specific combining ability in single crosses of corn. J Am Soc Agron. 1942;34:923–32.

29. Reif JC, Gumpert F-M, Fischer S, Melchinger AE. Impact of Interpopulation Divergence on Additive and Dominance Variance in Hybrid Populations. Genetics. 2007;176:1931–4.

30. Lehermeier C, de los Campos G, Wimmer V, Schön C-C. Genomic variance estimates: With or without disequilibrium covariances? J Anim Breed Genet. 2017;134:232–41.

31. Acosta-Pech R, Crossa J, de los Campos G, Teyssèdre S, Claustres B, Pérez-Elizalde S, et al. Genomic models with genotype × environment interaction for predicting hybrid performance: an application in maize hybrids. Theor Appl Genet. 2017;130:1431–40.

32. Wolfe MD, Kulakow P, Rabbi IY, Jannink J-L. Marker-Based Estimates Reveal Significant Non-additive Effects in Clonally Propagated Cassava (Manihot esculenta): Implications for the Prediction of Total Genetic Value and the Selection of Varieties. G3 Genes|Genomes|Genetics. 2016;6:3497–506.

33. Gianola D. Genomic-Assisted Prediction of Genetic Value With Semiparametric Procedures. Genetics. 2006;173:1761–76.

34. de los Campos G, Gianola D, Rosa GJM, Weigel KA, Crossa J. Semi-parametric genomic-enabled prediction of genetic values using reproducing kernel Hilbert spaces methods. Genet Res (Camb). 2010;92:295–308.

35. Lynch M, Walsh B. Genetics and analysis of quantitative traits. Sunderland, MA: Sinauer Associates; 1998.

36. VanRaden PM. Efficient Methods to Compute Genomic Predictions. J Dairy Sci. 2008;91:4414–23.

37. Su G, Christensen OF, Ostersen T, Henryon M, Lund MS. Estimating Additive and Non-Additive Genetic Variances and Predicting Genetic Merits Using Genome-Wide Dense Single Nucleotide Polymorphism Markers. Palmer AA, editor. PLoS One. 2012;7.

38. Vitezica ZG, Varona L, Legarra A. On the Additive and Dominant Variance and Covariance of Individuals Within the Genomic Selection Scope. Genetics. 2013;195:1223–30.

39. Martini JWR, Wimmer V, Erbe M, Simianer H. Epistasis and covariance: how gene interaction translates into genomic relationship. Theor Appl Genet. 2016;129:963–76.

40. Vitezica ZG, Legarra A, Toro MA, Varona L. Orthogonal Estimates of Variances for Additive, Dominance, and Epistatic Effects in Populations. Genetics. 2017;206:1297–307.

41. e Souza MB, Cuevas J, Couto EG de O, Pérez-Rodríguez P, Jarquín D, Fritsche-Neto R, et al. Genomic-Enabled Prediction in Maize Using Kernel Models with Genotype × Environment Interaction. G3 Genes|Genomes|Genetics. 2017;7:1995–2014.

42. Bernardo R. (1996) Best Linear Unbiased Prediction of Maize Single-Cross Performance. 1996;

43. Stuber CW, Cockerham CC. Gene effects and variances in hybrid populations. Genetics. 1966;54:1279–86.

44. Technow F, Schrag TA, Schipprack W, Bauer E, Simianer H, Melchinger AE. Genome Properties and Prospects of Genomic Prediction of Hybrid Performance in a Breeding Program of Maize. Genetics. 2014;197:1343–55.

45. Jiang Y, Reif JC. Modeling Epistasis in Genomic Selection. Genetics. 2015;201:759–68.

46. Huang W, Mackay TFC. The Genetic Architecture of Quantitative Traits Cannot Be Inferred from Variance Component Analysis. Zhu X, editor. PLOS Genet. 2016;12.

47. Mendonça L de F, Granato ÍSC, Alves FC, Morais PPP, Vidotti MS, Fritsche-Neto R. Accuracy and simultaneous selection gains for N-stress tolerance and N-use efficiency in maize tropical lines. Sci Agric. 2017;74:481–8.

48. Unterseer S, Bauer E, Haberer G, Seidel M, Knaak C, Ouzunova M, et al. A powerful tool for genome analysis in maize: development and evaluation of the high density 600 k SNP genotyping array. BMC Genomics. 2014;15:823.

49. Wimmer V, Albrecht T, Auinger H-J, Schön C-C. synbreed: a framework for the analysis of genomic prediction data using R. Bioinformatics. 2012;28:2086–7.

50. Zheng X, Levine D, Shen J, Gogarten SM, Laurie C, Weir BS. A high-performance computing toolset for relatedness and principal component analysis of SNP data. Bioinformatics. 2012;28:3326–8.

51. Pérez P, De Los Campos G. Genome-wide regression and prediction with the BGLR statistical package. Genetics. Genetics Society of America; 2014;198:483–95.

52. Burgueño J, de los Campos G, Weigel K, Crossa J. Genomic Prediction of Breeding Values when Modeling Genotype × Environment Interaction using Pedigree and Dense Molecular Markers. Crop Sci. 2012;52:707–19.

53. de los Campos G, Gianola D, Rosa GJM. Reproducing kernel Hilbert spaces regression: A general framework for genetic evaluation. J Anim Sci. Crop Science Society of America; 2009;87:1883–7.

54. Wittenburg D, Melzer N, Reinsch N. Including non-additive genetic effects in Bayesian methods for the prediction of genetic values based on genome-wide markers. BMC Genet. 2011;12:74.

55. Gianola D, de los Campos G, Hill WG, Manfredi E, Fernando R. Additive Genetic Variability and the Bayesian Alphabet. Genetics. 2009;183:347–63.

56. Carena MJ, Hallauer AR, Miranda Filho JB. Quantitative Genetics in Maize Breeding. New York, NY: Springer New York; 2010.

57. Larièpe A, Moreau L, Laborde J, Bauland C, Mezmouk S, Décousset L, et al. General and specific combining abilities in a maize (Zea mays L.) test-cross hybrid panel: relative importance of population structure and genetic divergence between parents. Theor Appl Genet. 2017;130:403–17.

58. Werner CR, Qian L, Voss-Fels KP, Abbadi A, Leckband G, Frisch M, et al. Genome-wide regression models considering general and specific combining ability predict hybrid performance in oilseed rape with similar accuracy regardless of trait architecture. Theor Appl Genet. 2018;131:299–317.

59. Betrán FJ, Ribaut JM, Beck D, de León DG. Genetic Diversity, Specific Combining Ability, and Heterosis in Tropical Maize under Stress and Nonstress Environments. Crop Sci. 2003;43:797–806.

60. Makumbi D, Betrán JF, Bänziger M, Ribaut J-M. Combining ability, heterosis and genetic diversity in tropical maize (Zea mays L.) under stress and non-stress conditions. Euphytica. 2011;180:143–62.

61. Combs E, Bernardo R. Accuracy of Genomewide Selection for Different Traits with Constant Population Size, Heritability, and Number of Markers. Plant Genome. 2013;6.

62. Daetwyler HD, Pong-Wong R, Villanueva B, Woolliams JA. The Impact of Genetic Architecture on Genome-Wide Evaluation Methods. Genetics. 2010;185:1021–31.

63. Goddard M. Genomic selection: prediction of accuracy and maximisation of long term response. Genetica. 2009;136:245–57.

64. Marulanda JJ, Mi X, Melchinger AE, Xu J-L, Würschum T, Longin CFH. Optimum breeding strategies using genomic selection for hybrid breeding in wheat, maize, rye, barley, rice and triticale. Theor Appl Genet. 2016;129:1901–13.

65. Viana JMS, Pereira HD, Mundim GB, Piepho H-P, e Silva FF. Efficiency of genomic prediction of non-assessed single crosses. Heredity (Edinb). 2018;120:283–95.

66. Michel S, Ametz C, Gungor H, Akgöl B, Epure D, Grausgruber H, et al. Genomic assisted selection for enhancing line breeding: merging genomic and phenotypic selection in winter wheat breeding programs with preliminary yield trials. Theor Appl Genet. 2017;130:363–76.

67. Cros D, Denis M, Sánchez L, Cochard B, Flori A, Durand-Gasselin T, et al. Genomic selection prediction accuracy in a perennial crop: case study of oil palm (Elaeis guineensis Jacq.). Theor Appl Genet. Springer Berlin Heidelberg; 2015;128:397–410.

68. A. Sofi P. Implications of Epistasis in Maize Breeding. Int J Plant Breed Genet. 2007;1–11.

69. Jarquín D, Crossa J, Lacaze X, Du Cheyron P, Daucourt J, Lorgeou J, et al. A reaction norm model for genomic selection using high-dimensional genomic and environmental data. Theor Appl Genet. 2014;127:595–607.

Appendix 1: Constructing kernels for additive-by-additive epistatic interactions

In this section we show that Hadamard products of additive relationship matrices provide a covariance structure that represents not only additive-by-additve contrasts but also dominance. We then describe a simple way to remove the dominance contribution to the epistasis relationship matrix. We employed this approach in our study to model additive-by-additive epistasis.

Hadamard products and covariance matrices for interactions: general case

Let $\boldsymbol{X}_{n\times p}$ and $\boldsymbol{Z}_{n\times q}$ represent two incidence matrices of effects and consider modelling all possible first order interactions between the columns of $\boldsymbol{X}$ and $\boldsymbol{Z}$. Here, $\boldsymbol{X}$ and $\boldsymbol{Z}$ may: (i) represent different information sets (e.g., $\boldsymbol{X}$ may be a matrix with SNP genotypes and $\boldsymbol{Z}$ may be a matrix with environmental covariates, as in Jarquin *et al.* [69]), (ii) be different types of contrasts derived from the same information set (e.g., $\boldsymbol{X}$ may code additive effects and $\boldsymbol{Z}$ may provide contrasts for dominance) or, (iii) $\boldsymbol{Z}=\boldsymbol{X}$ (this will be the case when modeling additive-by-additive interactions).

The incidence matrix containing contrasts for all possible interactions between the columns of $\boldsymbol{X}$ and $\boldsymbol{Z}$ can be formed using Kronecker products of the rows of $\boldsymbol{X}$ and $\boldsymbol{Z}$. Specifically,

$$\boldsymbol{W}=\begin{bmatrix}\boldsymbol{x}_1'\otimes\boldsymbol{z}_1'\\ \boldsymbol{x}_2'\otimes\boldsymbol{z}_2'\\ \vdots\\ \boldsymbol{x}_n'\otimes\boldsymbol{z}_n'\end{bmatrix}, \qquad [1]$$

where $\boldsymbol{x}_i'$ and $\boldsymbol{z}_i'$ are the ith rows of matrices $\boldsymbol{X}$ and $\boldsymbol{Z}$, respectively, is a matrix containing interactions. Indeed, the Kronecker products entering in the righ-hand side of [1], $\boldsymbol{x}_i'\otimes\boldsymbol{z}_i'=\left[x_{i1}z_{i1},x_{i1}z_{i2},\ldots,x_{i1}z_{iq},x_{i2}z_{i1},\ldots x_{ip}z_{iq-1},x_{ip}z_{iq}\right]$, generating all possible interactions beteween the colums of $\boldsymbol{X}$ and $\boldsymbol{Z}$.

A covariance structure for a linear model for $\boldsymbol{W}$ takes the form

$$\boldsymbol{K}=\boldsymbol{W}\boldsymbol{W}'=\begin{bmatrix}\boldsymbol{x}_1'\otimes\boldsymbol{z}_1'\\ \boldsymbol{x}_2'\otimes\boldsymbol{z}_2'\\ \vdots\\ \boldsymbol{x}_n'\otimes\boldsymbol{z}_n'\end{bmatrix}[(\boldsymbol{x}_1'\otimes\boldsymbol{z}_1')',\quad\ldots\quad,(\boldsymbol{x}_n'\otimes\boldsymbol{z}_n')'] \qquad [2]$$

The ij^{th} element of this kernel is

$$\boldsymbol{K}_{ij}=(\boldsymbol{x}_i'\otimes\boldsymbol{z}_i')\left(\boldsymbol{x}_j'\otimes\boldsymbol{z}_j'\right)'=(\boldsymbol{x}_i'\otimes\boldsymbol{z}_i')\left(\boldsymbol{x}_j\otimes\boldsymbol{z}_j\right)=\left(\boldsymbol{x}_i'\boldsymbol{x}_j\otimes\boldsymbol{z}_i'\boldsymbol{z}_j\right)=\boldsymbol{x}_i'\boldsymbol{x}_j\times\boldsymbol{z}_i'\boldsymbol{z}_j. \qquad [3]$$

This entry is equal to the *ij*th element of the Haddmard product $\boldsymbol{XX'} \odot \boldsymbol{ZZ'}$. Indeed the *ij*th element of this product is the product of the *ij*th element of $\boldsymbol{XX'}$, $\boldsymbol{XX'}_{ij} = \boldsymbol{x}_i'\boldsymbol{x}_j$, times the *ij*th element of $\boldsymbol{ZZ'}$, $\boldsymbol{ZZ'}_{ij} = \boldsymbol{z}_i'\boldsymbol{z}_j$. Therefore

$$\boldsymbol{XX'} \odot \boldsymbol{ZZ'} = \boldsymbol{WW'} \quad [4]$$

The result in [4] shows that a covariance structure for all possible interactions between the predictors included in $\boldsymbol{X}$ and $\boldsymbol{Z}$ can be computed by first computing a kernel for each of these matrices, $\boldsymbol{K}_X = \boldsymbol{XX'}$ and $\boldsymbol{K}_Z = \boldsymbol{ZZ'}$, and then producing the Haddmard product between these two kernels $\boldsymbol{K}_X \odot \boldsymbol{K}_Z$. This result was used, for example, by Jarquin *et al.* [69] to compute kernels for all possible interactions between SNPs and environmental covariates. The same result can be use to compute additive-by-dominance epistatic interactions, indeed, setting $\boldsymbol{X}$ and $\boldsymbol{Z}$ to be matrices with contrasts for additive and dominance effects (denoted as $\boldsymbol{D}$ in our manuscript), respectively, and computing the expression in [4] renders a covariance structure additive-by-dominance epistatic interactions.

Computing kernels for additive-by-additive epistatic interactions

For additive-by-additive interactions we need to set $\boldsymbol{Z} = \boldsymbol{X}$ with $\boldsymbol{X}$ being a matrix with contrasts for additive effects. However, in this case the interactions included in the columns of $\boldsymbol{W}$ (expression [1]) include not only interactions between loci but also interactions within loci, $x_{ij}x_{ij} = x_{ij}^2$, indeed, if $\boldsymbol{Z} = \boldsymbol{X}$,

$$\boldsymbol{x}_i' \otimes \boldsymbol{x}_i' = \left[x_{i1}^2, x_{i1}x_{i2}, \ldots, x_{i1}x_{ip}, x_{i2}x_{1i}, x_{i2}^2, \ldots, x_{ip}^2\right]$$

The within-loci interactions correspond to dominance; therefore, computting the Hadamard product of additive relationship matrices, $\boldsymbol{XX'} \odot \boldsymbol{XX'}$ gives a kernel that accounts not only for additive-by-additive effects but also for dominance.

A simple way to remove the contribution to dominance is to set the kernel for additive an additive effects to be $\boldsymbol{K}_{aa} = \boldsymbol{XX'} \odot \boldsymbol{XX'} - (\boldsymbol{X} \odot \boldsymbol{X})(\boldsymbol{X} \odot \boldsymbol{X})'$ where the second term represents a kernel for intra loci interactions. Substracting this from $\boldsymbol{XX'} \odot \boldsymbol{XX'}$ removes the contribution to dominance. In our application we further standardize this kernel to have an average diagonal value of one, therefore, for additive-by-additive effects we used:

$$\boldsymbol{K}_{aa} = \frac{(\boldsymbol{XX'}) \odot (\boldsymbol{XX'})' - (\boldsymbol{X} \odot \boldsymbol{X})(\boldsymbol{X} \odot \boldsymbol{X})'}{\boldsymbol{tr}\left((\boldsymbol{XX'}) \odot (\boldsymbol{XX'})' - (\boldsymbol{X} \odot \boldsymbol{X})(\boldsymbol{X} \odot \boldsymbol{X})'\right)/\boldsymbol{n}} \quad [5]$$

Appendix 2: Computing gaussian kernels from additive relationship matrices

Gaussian Kernels are often used in genomic kernel regressions. The ij^{th} entry of a Gaussian kernel is computed as follows: $\boldsymbol{K}_{ij} = e^{-h\left\|\boldsymbol{x}_i-\boldsymbol{x}_j\right\|^2}$. Here, $\left\|\boldsymbol{x}_i - \boldsymbol{x}_j\right\|^2 = \sum_{k=1}^{p}\left(x_{ik} - x_{jk}\right)^2$ is the squared-Euclidean distance between the genotypes of the i^{th} and j^{th} individual and h is a bandwidth parameter that controls how fast the kernel drop with the distance between genotypes. Determining the appropiate value of h can be challenging and values of h used in one study cannot be authomatically considered for other studies because the distance between genotypes depends on both how closely related the genotypes are but also on how many markers were used (because the distance is a sum over markers and it monotonically increases with the number of SNPs).

Additive relationship matrices can be used to derive squared-Euclidean distances and have an embeded standarization that makes the choice of the bandwith parameter relatively straightforward. Therefore, Gaussian kernels can be directly comptued from additive relationship matrices.

Deriving squared-Euclidean distances from relationship matrices

Kernels for linear models for additive effects are often computed using $\boldsymbol{K}_a = \boldsymbol{X}\boldsymbol{X}'$ where $\boldsymbol{X}$ is an incidence matrix for additive effect containing centered (and possibly-scaled) SNP genotypes. Additive relationship matrices provide a measure of genetic similarity between pairs of individuals. However, similarity matrices also define distances, more specifically, the distance between the *i* and *j* genotype is defined as

$$D_{ij} = \boldsymbol{X}\boldsymbol{X}'_{ii} + \boldsymbol{X}\boldsymbol{X}'_{jj} - 2\boldsymbol{X}\boldsymbol{X}'_{ij} \quad [6]$$

The ij^{th} element of this kernel is $\boldsymbol{X}\boldsymbol{X}'_{ij} = \boldsymbol{x}'_i\boldsymbol{x}_j$; therefore, $D_{ij} = \boldsymbol{x}'_i\boldsymbol{x}_i + \boldsymbol{x}'_j\boldsymbol{x}_j - 2\boldsymbol{x}'_i\boldsymbol{x}_j = \sum_{k=1}^{p} x_{ik}^2 + \sum_{k=1}^{p} x_{jk}^2 - 2\sum_{k=1}^{p} x_{ik}x_{jk}$. This quantidy is the squared-Euclidean distance $\left\|\boldsymbol{x}_i - \boldsymbol{x}_j\right\| = \sum_{k=1}^{p}\left(x_{ik} - x_{jk}\right)^2 = \sum_{k=1}^{p} x_{ik}^2 + x_{jk}^2 - 2x_{ik}x_{jk} = \sum_{k=1}^{p} x_{ik}^2 + \sum_{k=1}^{p} x_{jk}^2 - 2\sum_{k=1}^{p} x_{ik}x_{jk}$.

Therefore, squared-Euclidean distances can be directly computed from additive relationship matrices. These distances can then be used into a Gaussian kernel for semi-parameteric regression.

Bandwidht parameters

If the additive relationship matrix was standarized (e.g., if it had, by construction, an average diagonal value of one) that standarization carries over the distances. Using distances computed from [6] with a bandwidth parameter equal to one leads to a kernel that have off-diagonal covariances similar to that of the original additive relationship matrix (Figure 1). Using higher values of the bandwith parameter will lead to more a 'local kernel' which may be more in line with the covariance structures induce by epistatic terms.

Multi-kernel models (aka, "Kernel Averaging", e.g., [34]) use kernels that represent different degree of smoothness with repsect to genotype differences. Often, using three kernels is enough. One possiblity is to derive distances according to [6] and then derive three kernels, one with h=0.5 (this gives higher covariances than the additive relationship matrices), one with h=1 (this gives a kernel with covariances similar to that of the additive kernel, Figure 8) and one with h=2, which gives a kernel that is more local than the one representing additive relationship matrices. This is illustrated in the figure below. We use these three kernels in the study for our RKHS regression.

TABLES

Table 1. Models implemented and genetic effects considered in each model

Model	Effect				
	Additive	**Dominance**	**Additive-Additive**	**Additive-Dominance**	**Non-Linear Kernels**
A	×				
A+D	×	×			
A+AA	×		×		
A+AD	×			×	
A+D+AA	×	×	×		
A+D+AD	×	×		×	
A+D+AA+AD	×	×	×	×	
RKHS					×

A: Additive model, A+D: Additive-dominance model, A+AA: Additive - additive × additive epistatic model, A+AD: Additive – additive × dominance epistatic model, A+D+AD: Additive - dominance - additive × additive epistatic model, A+D+AA+AD: Additive - dominance - additive × additive – additive × dominance epistatic model, RKHS: Reproducing Kernel Hilbert Spaces model.

Table 2. Proportion of non-additive variance ($D^2 \pm SE$) explained by each model by trait and environment

Trait	Env	Models						
		A+D	**A+AA**	**A+AD**	**A+D+AA**	**A+D+AD**	**A+D+AA+AD**	**Mean**
EH	AN.IN	$0.099^{\pm 0.001}$	$0.088^{\pm 0.001}$	$0.097^{\pm 0.001}$	$0.120^{\pm 0.001}$	$0.123^{\pm 0.001}$	$0.135^{\pm 0.001}$	0.110
	AN.LN	$0.117^{\pm 0.001}$	$0.104^{\pm 0.001}$	$0.111^{\pm 0.001}$	$0.150^{\pm 0.001}$	$0.153^{\pm 0.001}$	$0.172^{\pm 0.001}$	0.135
	PI.IN	$0.115^{\pm 0.001}$	$0.094^{\pm 0.001}$	$0.114^{\pm 0.001}$	$0.134^{\pm 0.001}$	$0.140^{\pm 0.001}$	$0.150^{\pm 0.001}$	0.124
	PI.LN	$0.119^{\pm 0.001}$	$0.097^{\pm 0.001}$	$0.125^{\pm 0.001}$	$0.138^{\pm 0.001}$	$0.143^{\pm 0.001}$	$0.154^{\pm 0.001}$	0.129
PH	AN.IN	$0.150^{\pm 0.001}$	$0.130^{\pm 0.001}$	$0.123^{\pm 0.001}$	$0.172^{\pm 0.001}$	$0.171^{\pm 0.001}$	$0.186^{\pm 0.001}$	0.155
	AN.LN	$0.238^{\pm 0.001}$	$0.204^{\pm 0.001}$	$0.210^{\pm 0.001}$	$0.269^{\pm 0.001}$	$0.273^{\pm 0.001}$	$0.292^{\pm 0.001}$	0.248
	PI.IN	$0.220^{\pm 0.001}$	$0.184^{\pm 0.001}$	$0.202^{\pm 0.001}$	$0.243^{\pm 0.001}$	$0.243^{\pm 0.001}$	$0.254^{\pm 0.001}$	0.224
	PI.LN	$0.213^{\pm 0.001}$	$0.183^{\pm 0.001}$	$0.172^{\pm 0.001}$	$0.236^{\pm 0.001}$	$0.236^{\pm 0.001}$	$0.249^{\pm 0.001}$	0.215
GY	AN.IN	$0.302^{\pm 0.001}$	$0.284^{\pm 0.001}$	$0.236^{\pm 0.001}$	$0.331^{\pm 0.001}$	$0.333^{\pm 0.001}$	$0.352^{\pm 0.001}$	0.306
	AN.LN	$0.307^{\pm 0.002}$	$0.326^{\pm 0.002}$	$0.260^{\pm 0.002}$	$0.379^{\pm 0.001}$	$0.352^{\pm 0.001}$	$0.399^{\pm 0.001}$	0.337
	PI.IN	$0.286^{\pm 0.001}$	$0.253^{\pm 0.001}$	$0.282^{\pm 0.001}$	$0.335^{\pm 0.001}$	$0.339^{\pm 0.001}$	$0.361^{\pm 0.001}$	0.309
	PI.LN	$0.405^{\pm 0.001}$	$0.380^{\pm 0.001}$	$0.395^{\pm 0.001}$	$0.446^{\pm 0.001}$	$0.440^{\pm 0.001}$	$0.466^{\pm 0.001}$	0.422

A: Additive, D: Dominance, AA: Additive × Additive, AD: Additive × Dominance effects, RKHS: Reproducing Kernel Hilbert Spaces model. AN.IN: Anhembi ideal nitrogen regime, AN.LN: Anhembi low nitrogen regime, PI.IN: Piracicaba ideal nitrogen regime, PI.LN: Piracicaba low nitrogen regime. EH, GY, and PH: ear height, grain yield, and plant height, respectively.

Table 3. Prediction accuracy (± standard error) of models by environments and traits

Models	Environment: AN.IN			Environment: AN.LN		
	EH	**PH**	**GY**	**EH**	**PH**	**GY**
A	$0.805^{\pm 0.002}$	$0.74^{\pm 0.004}$	$0.58^{\pm 0.004}$	$0.710^{\pm 0.004}$	$0.595^{\pm 0.005}$	$0.462^{\pm 0.004}$
A+D	$0.809^{\pm 0.002}$	$0.750^{\pm 0.004}$	$0.618^{\pm 0.004}$	$0.711^{\pm 0.003}$	$0.611^{\pm 0.004}$	$0.481^{\pm 0.004}$
A+AA	$0.805^{\pm 0.002}$	$0.74^{\pm 0.004}$	$0.597^{\pm 0.004}$	$0.708^{\pm 0.004}$	$0.601^{\pm 0.005}$	$0.478^{\pm 0.004}$
A+AD	$0.804^{\pm 0.002}$	$0.74^{\pm 0.004}$	$0.579^{\pm 0.004}$	$0.708^{\pm 0.004}$	$0.594^{\pm 0.005}$	$0.463^{\pm 0.005}$
A+D+AA	$0.806^{\pm 0.002}$	$0.745^{\pm 0.004}$	$0.612^{\pm 0.004}$	$0.707^{\pm 0.003}$	$0.607^{\pm 0.004}$	$0.48^{\pm 0.004}$
A+D+AD	$0.805^{\pm 0.002}$	$0.738^{\pm 0.004}$	$0.583^{\pm 0.004}$	$0.708^{\pm 0.004}$	$0.60^{\pm 0.005}$	$0.466^{\pm 0.004}$
A+D+AA+ AD	$0.805^{\pm 0.002}$	$0.742^{\pm 0.004}$	$0.607^{\pm 0.004}$	$0.705^{\pm 0.003}$	$0.604^{\pm 0.004}$	$0.475^{\pm 0.005}$
RKHS	$0.802^{\pm 0.002}$	$0.735^{\pm 0.004}$	$0.602^{\pm 0.004}$	$0.699^{\pm 0.003}$	$0.599^{\pm 0.004}$	$0.47^{\pm 0.005}$
Models	**Environment: PI.IN**			**Environment: PI.LN**		
	EH	**PH**	**GY**	**EH**	**PH**	**GY**
A	$0.791^{\pm 0.002}$	$0.701^{\pm 0.005}$	$0.527^{\pm 0.004}$	$0.800^{\pm 0.002}$	$0.676^{\pm 0.005}$	$0.456^{\pm 0.005}$
A+D	$0.797^{\pm 0.002}$	$0.720^{\pm 0.004}$	$0.543^{\pm 0.004}$	$0.806^{\pm 0.002}$	$0.699^{\pm 0.004}$	$0.487^{\pm 0.005}$
A+AA	$0.792^{\pm 0.002}$	$0.706^{\pm 0.005}$	$0.534^{\pm 0.004}$	$0.799^{\pm 0.002}$	$0.685^{\pm 0.004}$	$0.476^{\pm 0.005}$
A+AD	$0.790^{\pm 0.002}$	$0.702^{\pm 0.005}$	$0.526^{\pm 0.004}$	$0.799^{\pm 0.002}$	$0.677^{\pm 0.005}$	$0.457^{\pm 0.005}$
A+D+AA	$0.794^{\pm 0.002}$	$0.714^{\pm 0.004}$	$0.54^{\pm 0.004}$	$0.803^{\pm 0.002}$	$0.694^{\pm 0.004}$	$0.483^{\pm 0.005}$
A+D+AD	$0.794^{\pm 0.002}$	$0.705^{\pm 0.005}$	$0.537^{\pm 0.004}$	$0.803^{\pm 0.002}$	$0.679^{\pm 0.004}$	$0.475^{\pm 0.005}$
A+D+AA+ AD	$0.793^{\pm 0.002}$	$0.712^{\pm 0.004}$	$0.539^{\pm 0.004}$	$0.803^{\pm 0.002}$	$0.690^{\pm 0.004}$	$0.483^{\pm 0.005}$
RKHS	$0.791^{\pm 0.002}$	$0.708^{\pm 0.004}$	$0.539^{\pm 0.004}$	$0.802^{\pm 0.002}$	$0.683^{\pm 0.004}$	$0.484^{\pm 0.005}$

A: Additive, D: Dominance, AA: Additive × Additive, AD: Additive × Dominance effects, RKHS: Reproducing Kernel Hilbert Spaces model. AN.IN: Anhembi ideal nitrogen regime, AN.LN: Anhembi low nitrogen regime, PI.IN: Piracicaba ideal nitrogen regime, PI.LN: Piracicaba low nitrogen regime. EH, GY, and PH: ear height, grain yield, and plant height, respectively.

FIGURES

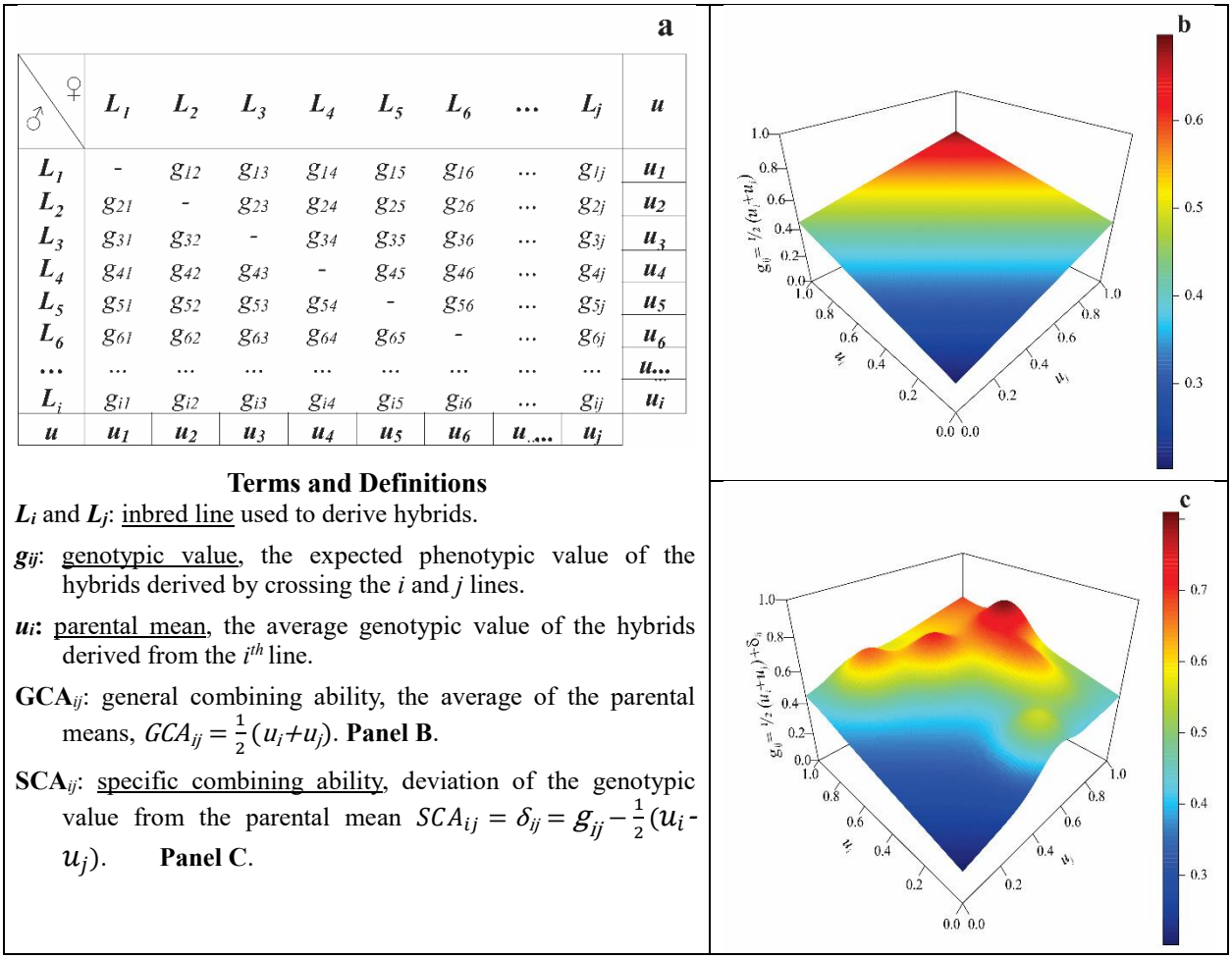

Terms and Definitions

L_i and L_j: inbred line used to derive hybrids.

g_{ij}: genotypic value, the expected phenotypic value of the hybrids derived by crossing the *i* and *j* lines.

u_i: parental mean, the average genotypic value of the hybrids derived from the i^{th} line.

GCA$_{ij}$: general combining ability, the average of the parental means, $GCA_{ij} = \frac{1}{2}(u_i + u_j)$. **Panel B**.

SCA$_{ij}$: specific combining ability, deviation of the genotypic value from the parental mean $SCA_{ij} = \delta_{ij} = g_{ij} - \frac{1}{2}(u_i - u_j)$. **Panel C**.

Figure 1. Prediction of hybrid performance using genomic regression models. **a-** Grid is showing all possible crosses between *n* lines ($i = j$) in a diallel mating design. **b-** Hyper-plane generated by the general combining abilities of females and males. **c-** Hypothetical hybrid performance surface influenced by both additive and non-additive effects (module).

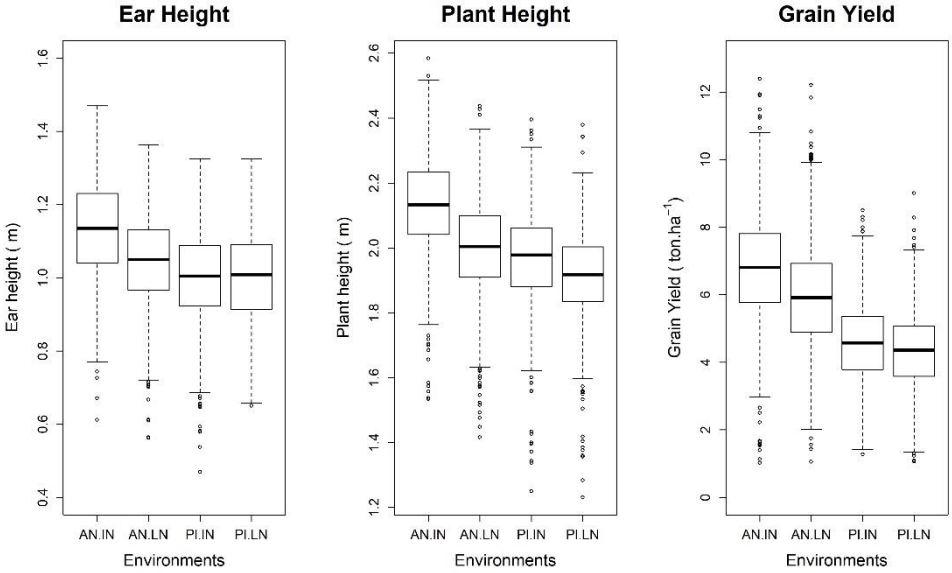

Figure 2. Boxplot of phenotypes by trait and environments. AN.IN: Anhembi ideal nitrogen regime; AN.LN: Anhembi low nitrogen regime; PI.IN: Piracicaba ideal nitrogen regime; PI.LN: Piracicaba low nitrogen regime.

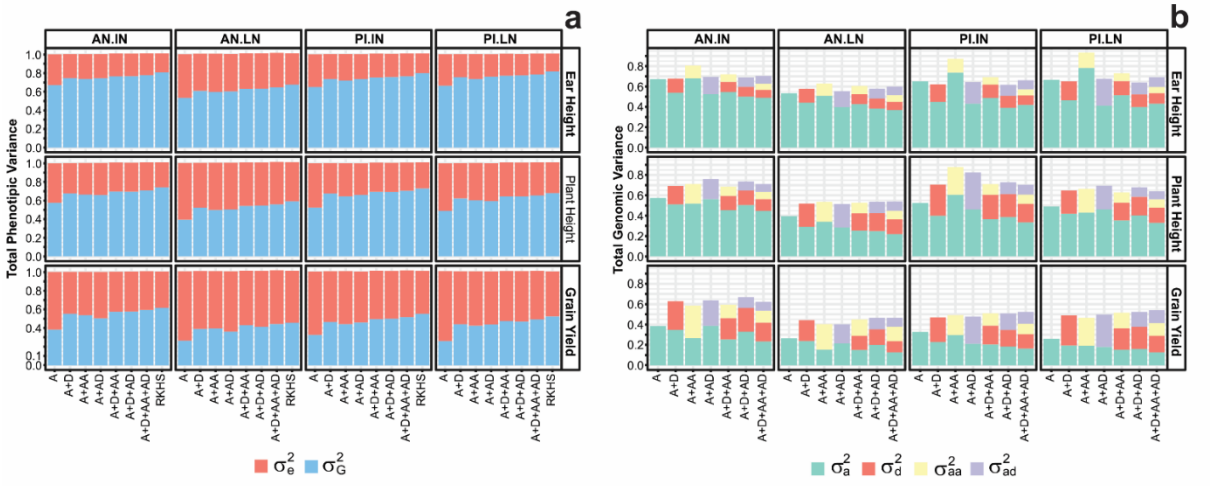

Figure 3. Variance components and variance parameters. (a) Estimated genetic variance explained by the model (σ^2_G), and estimated error variance (σ^2_e). (b) Individual variance estimates. (AN.IN: Anhembi ideal nitrogen regime; AN.LN: Anhembi low nitrogen regime; PI.IN: Piracicaba ideal nitrogen regime; PI.LN: Piracicaba low nitrogen regime. A: Additive, D: Dominance, AA: Additive × additive, and AD: Additive × dominance effects. RKHS: Reproducing Kernel Hilbert Spaces model). σ^2_a, σ^2_d, σ^2_{aa} and , σ^2_{ad}, additive, dominance, additive by additive, additive by dominance genetic parameters, respectively.

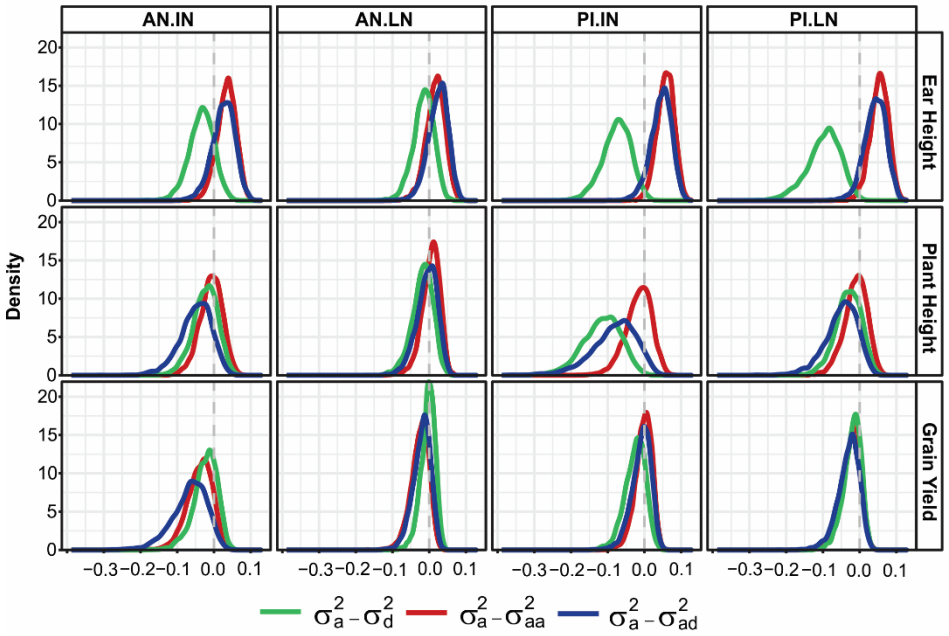

Figure 4. Posterior density of the covariance between the additive and non-additive genetic components of models including two genetic terms by environment and traits. A+D=σ_a^2- σ_d^2 ; A+AA=σ_a^2- σ_{aa}^2; A+AD=σ_a^2- σ_{ad}^2.

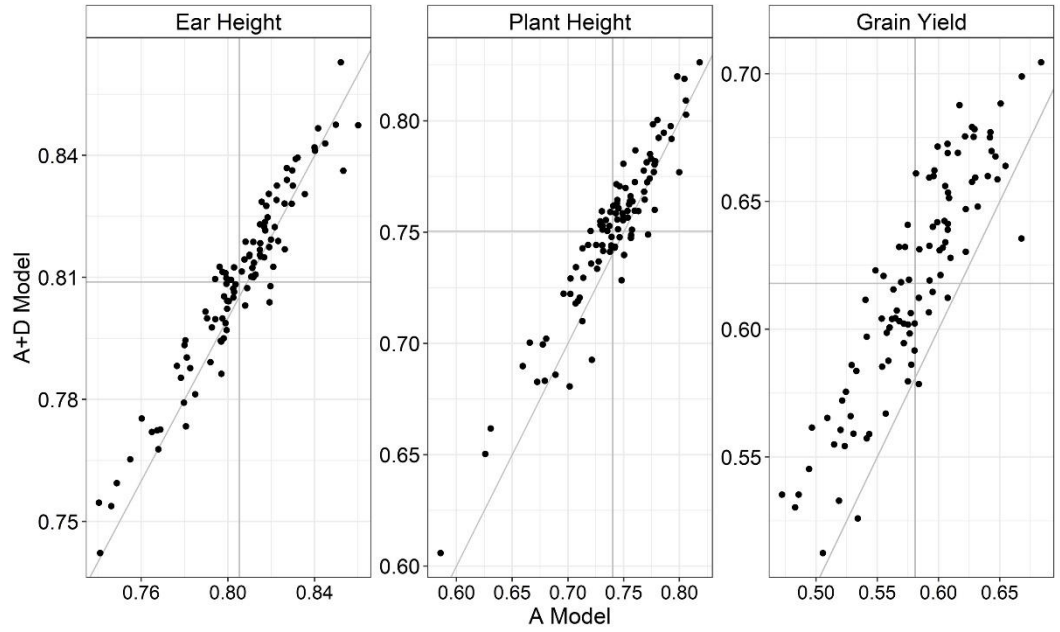

Figure 5. Comparison of correlations between observed and predicted values obtained by the A+D model (Additive-dominance) and A (Additive) model by trait at Anhembi with ideal nitrogen availability (AN.IN). Each point represents one replicate of the validation considering the same population partitions across models.

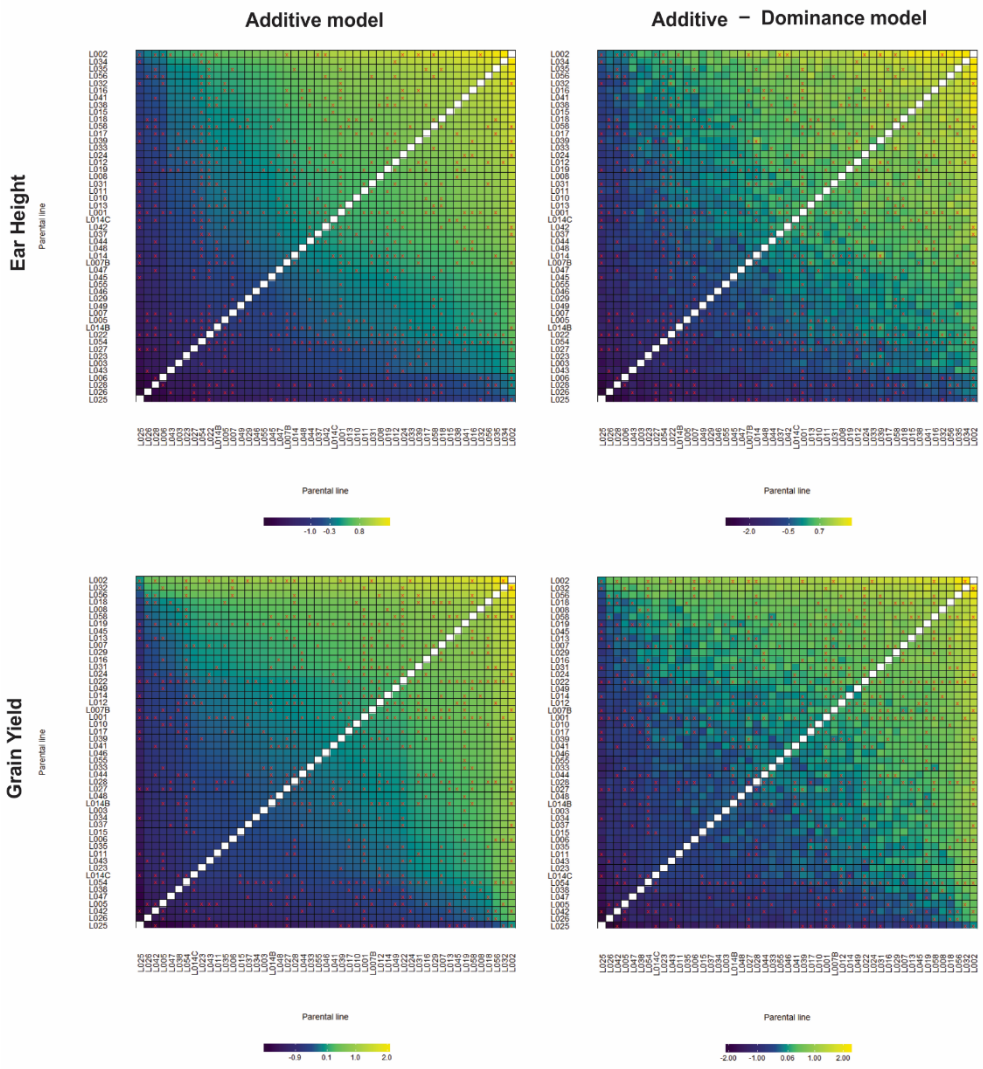

Figure 6. Heatmaps of genomic estimated genetic/genotypic values of all possible single-crosses by models (columns) and traits (rows) at Anhembi with ideal nitrogen (AN.IN). Red cross (×) correspond to non-tested hybrids. Lines and columns of each plot were sorted by the mean performance of parental inbred lines at all crosses considering the Additive model predicted values.

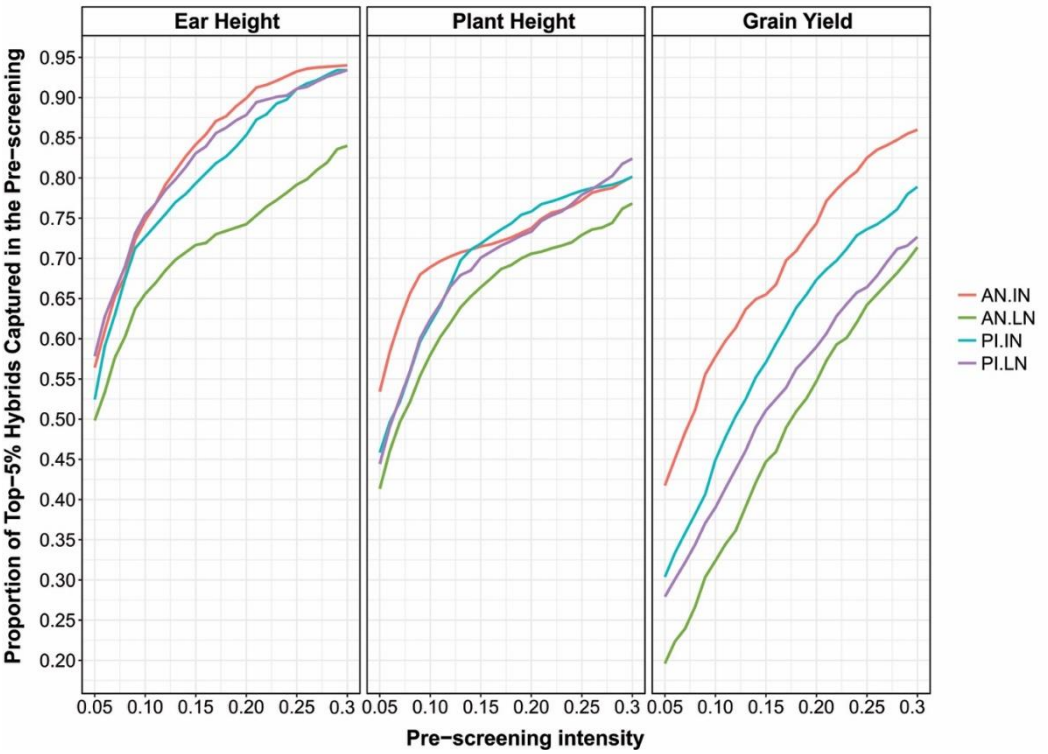

Figure 7. Proportion of the top-5% hybrids (according to phenotypic rank) that is captured by pre-screening based on (cross-validation) genomic prediction using the additive-dominance model at a different intensity of selection (x-axis). Each panel corresponds to an evaluated trait, lines within a plot represent different environments. AN: Anhembi; PI: Piracicaba; LN: Low nitrogen; IN: Ideal nitrogen.

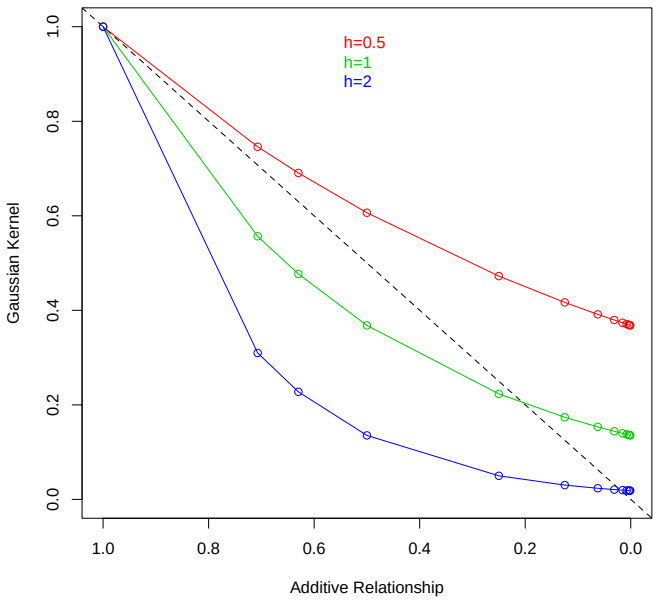

Figure 8. Entries of a Gaussian Kernel versus Additive Relationships, by value of the bandwidth parameter.

SUPPLEMENTARY TABLES

Table S1. Posterior means (± posterior standard deviations) of variance components and broad-sense genomic heritability ($\boldsymbol{H^2}$) by traits and models at Anhembi with ideal nitrogen availability (AN.IN).

		Model						
Trait	**Comp**	**A**	**A+D**	**A+AA**	**A+AD**	**A+D+AA**	**A+D+AD**	**A+D+AA+AD**
EH	σ_a^2	0.672±0.031	0.545±0.065	0.68±0.07	0.525±0.073	0.547±0.084	0.5±0.074	0.489±0.085
	σ_d^2	-	0.136±0.029	-	-	0.1±0.027	0.09±0.025	0.08±0.022
	σ_{aa}^2	-	-	0.129±0.03	-	0.074±0.02	-	0.062±0.018
	σ_{ad}^2	-	-	-	0.171±0.044	-	0.09±0.029	0.075±0.025
	σ_G^2	0.672±0.031	0.747±0.031	0.738±0.031	0.746±0.032	0.765±0.031	0.767±0.03	0.778±0.03
	σ_e^2	0.329±0.004	0.258±0.012	0.265±0.013	0.257±0.015	0.245±0.012	0.24±0.013	0.234±0.013
	H^2	0.671±0.011	0.743±0.014	0.736±0.015	0.744±0.016	0.757±0.014	0.76±0.014	0.769±0.014
GY	σ_a^2	0.383±0.032	0.348±0.065	0.271±0.061	0.392±0.08	0.256±0.067	0.32±0.074	0.236±0.078
	σ_d^2	-	0.28±0.055	-	-	0.213±0.053	0.24±0.053	0.183±0.053
	σ_{aa}^2	-	-	0.311±0.067	-	0.131±0.044	-	0.116±0.043
	σ_{ad}^2	-	-	-	0.253±0.074	-	0.11±0.036	0.088±0.032
	σ_G^2	0.383±0.033	0.553±0.04	0.538±0.043	0.505±0.044	0.575±0.039	0.577±0.04	0.594±0.04
	σ_e^2	0.62±0.007	0.45±0.024	0.467±0.027	0.496±0.033	0.429±0.024	0.43±0.025	0.417±0.024
	H^2	0.381±0.021	0.55±0.028	0.534±0.031	0.505±0.036	0.574±0.026	0.57±0.028	0.587±0.027
PH	σ_a^2	0.575±0.034	0.511±0.066	0.518±0.068	0.563±0.076	0.46±0.075	0.50±0.077	0.442±0.086
	σ_d^2	-	0.186±0.04	-	-	0.138±0.037	0.14±0.035	0.113±0.033
	σ_{aa}^2	-	-	0.191±0.048	-	0.088±0.028	-	0.075±0.026
	σ_{ad}^2	-	-	-	0.193±0.056	-	0.09±0.029	0.077±0.027
	σ_G^2	0.575±0.034	0.677±0.034	0.664±0.035	0.659±0.036	0.697±0.034	0.69±0.034	0.709±0.033
	σ_e^2	0.425±0.005	0.324±0.016	0.341±0.017	0.345±0.019	0.313±0.016	0.31±0.016	0.302±0.016
	H^2	0.575±0.014	0.677±0.019	0.66±0.02	0.655±0.022	0.69±0.018	0.69±0.018	0.702±0.018

σ_a^2, σ_d^2, σ_{aa}^2, σ_{ad}^2, σ_G^2, σ_e^2: Additive, dominance, additive-additive, and additive-dominance variance parameters, total genomic and error variances, respectively.

H^2: Genomic broad-sense heritability

Table S2. Posterior means (± posterior standard deviations) of variance components and broad-sense genomic heritability (H2) by traits and models at Anhembi with low nitrogen availability (AN.LN).

		Model						
Trait	**Comp**	**A**	**A+D**	**A+AA**	**A+AD**	**A+D+AA**	**A+D+AD**	**A+D+AA+AD**
EH	σ_a^2	$0.534^{\pm 0.033}$	$0.444^{\pm 0.063}$	$0.51^{\pm 0.065}$	$0.399^{\pm 0.072}$	$0.429^{\pm 0.076}$	$0.384^{\pm 0.074}$	$0.373^{\pm 0.08}$
	σ_d^2	-	$0.129^{\pm 0.032}$	-	-	$0.098^{\pm 0.028}$	$0.096^{\pm 0.027}$	$0.08^{\pm 0.025}$
	σ_{aa}^2	-	-	$0.12^{\pm 0.03}$	-	$0.08^{\pm 0.024}$	-	$0.068^{\pm 0.02}$
	σ_{ad}^2	-	-	-	$0.156^{\pm 0.046}$	-	$0.097^{\pm 0.032}$	$0.079^{\pm 0.027}$
	σ_G^2	$0.534^{\pm 0.034}$	$0.61^{\pm 0.036}$	$0.599^{\pm 0.035}$	$0.603^{\pm 0.036}$	$0.63^{\pm 0.035}$	$0.633^{\pm 0.034}$	$0.647^{\pm 0.034}$
	σ_e^2	$0.468^{\pm 0.005}$	$0.401^{\pm 0.016}$	$0.409^{\pm 0.016}$	$0.403^{\pm 0.018}$	$0.384^{\pm 0.017}$	$0.381^{\pm 0.017}$	$0.371^{\pm 0.017}$
	H^2	$0.533^{\pm 0.016}$	$0.602^{\pm 0.02}$	$0.594^{\pm 0.019}$	$0.599^{\pm 0.022}$	$0.621^{\pm 0.019}$	$0.623^{\pm 0.02}$	$0.636^{\pm 0.018}$
GY	σ_a^2	$0.264^{\pm 0.03}$	$0.24^{\pm 0.052}$	$0.15^{\pm 0.044}$	$0.212^{\pm 0.055}$	$0.151^{\pm 0.05}$	$0.201^{\pm 0.057}$	$0.132^{\pm 0.05}$
	σ_d^2	-	$0.197^{\pm 0.047}$	-	-	$0.131^{\pm 0.038}$	$0.153^{\pm 0.044}$	$0.108^{\pm 0.039}$
	σ_{aa}^2	-	-	$0.258^{\pm 0.062}$	-	$0.166^{\pm 0.055}$	-	$0.142^{\pm 0.049}$
	σ_{ad}^2	-	-	-	$0.197^{\pm 0.057}$	-	$0.114^{\pm 0.038}$	$0.089^{\pm 0.032}$
	σ_G^2	$0.264^{\pm 0.03}$	$0.391^{\pm 0.041}$	$0.396^{\pm 0.042}$	$0.361^{\pm 0.041}$	$0.43^{\pm 0.043}$	$0.411^{\pm 0.039}$	$0.443^{\pm 0.041}$
	σ_e^2	$0.745^{\pm 0.008}$	$0.624^{\pm 0.026}$	$0.612^{\pm 0.029}$	$0.645^{\pm 0.03}$	$0.587^{\pm 0.028}$	$0.602^{\pm 0.027}$	$0.576^{\pm 0.029}$
	H^2	$0.261^{\pm 0.022}$	$0.381^{\pm 0.031}$	$0.394^{\pm 0.035}$	$0.361^{\pm 0.034}$	$0.421^{\pm 0.031}$	$0.407^{\pm 0.031}$	$0.435^{\pm 0.031}$
PH	σ_a^2	$0.395^{\pm 0.033}$	$0.284^{\pm 0.059}$	$0.344^{\pm 0.063}$	$0.282^{\pm 0.065}$	$0.251^{\pm 0.066}$	$0.25^{\pm 0.064}$	$0.217^{\pm 0.07}$
	σ_d^2	-	$0.232^{\pm 0.053}$	-	-	$0.174^{\pm 0.051}$	$0.171^{\pm 0.048}$	$0.141^{\pm 0.046}$
	σ_{aa}^2	-	-	$0.192^{\pm 0.05}$	-	$0.109^{\pm 0.036}$	-	$0.093^{\pm 0.034}$
	σ_{ad}^2	-	-	-	$0.235^{\pm 0.065}$	-	$0.119^{\pm 0.042}$	$0.094^{\pm 0.035}$
	σ_G^2	$0.395^{\pm 0.032}$	$0.524^{\pm 0.041}$	$0.5^{\pm 0.039}$	$0.503^{\pm 0.041}$	$0.543^{\pm 0.039}$	$0.546^{\pm 0.04}$	$0.56^{\pm 0.038}$
	σ_e^2	$0.609^{\pm 0.007}$	$0.48^{\pm 0.024}$	$0.509^{\pm 0.024}$	$0.501^{\pm 0.028}$	$0.464^{\pm 0.024}$	$0.463^{\pm 0.024}$	$0.451^{\pm 0.024}$
	H^2	$0.393^{\pm 0.021}$	$0.521^{\pm 0.027}$	$0.494^{\pm 0.029}$	$0.501^{\pm 0.031}$	$0.541^{\pm 0.026}$	$0.541^{\pm 0.027}$	$0.555^{\pm 0.026}$

σ_a^2, σ_d^2, σ_{aa}^2, σ_{ad}^2, σ_G^2, σ_e^2: Additive, dominance, additive-additive, and additive-dominance variance parameters, total genomic and error variances, respectively.

H^2: Genomic broad-sense heritability

Table S3. Posterior means (± posterior standard deviations) of variance components and broad-sense genomic heritability (H2) by traits and models at Piracicaba with ideal nitrogen availability (PI.IN).

		Model						
Trait	**Comp.**	**A**	**A+D**	**A+AA**	**A+AD**	**A+D+AA**	**A+D+AD**	**A+D+AA+AD**
EH	σ_a^2	$0.651^{\pm 0.032}$	$0.447^{\pm 0.065}$	$0.734^{\pm 0.076}$	$0.421^{\pm 0.074}$	$0.489^{\pm 0.085}$	$0.394^{\pm 0.069}$	$0.42^{\pm 0.088}$
	σ_d^2	-	$0.176^{\pm 0.04}$	-	-	$0.13^{\pm 0.037}$	$0.12^{\pm 0.032}$	$0.096^{\pm 0.03}$
	σ_{aa}^2	-	-	$0.135^{\pm 0.031}$	-	$0.075^{\pm 0.02}$	-	$0.061^{\pm 0.018}$
	σ_{ad}^2	-	-	-	$0.224^{\pm 0.056}$	-	$0.106^{\pm 0.036}$	$0.09^{\pm 0.033}$
	σ_G^2	$0.651^{\pm 0.032}$	$0.737^{\pm 0.032}$	$0.72^{\pm 0.032}$	$0.736^{\pm 0.034}$	$0.753^{\pm 0.031}$	$0.758^{\pm 0.032}$	$0.766^{\pm 0.031}$
	σ_e^2	$0.35^{\pm 0.004}$	$0.267^{\pm 0.014}$	$0.285^{\pm 0.013}$	$0.264^{\pm 0.016}$	$0.256^{\pm 0.014}$	$0.25^{\pm 0.015}$	$0.244^{\pm 0.014}$
	H^2	$0.65^{\pm 0.012}$	$0.734^{\pm 0.016}$	$0.716^{\pm 0.015}$	$0.736^{\pm 0.018}$	$0.746^{\pm 0.015}$	$0.752^{\pm 0.016}$	$0.759^{\pm 0.015}$
GY	σ_a^2	$0.327^{\pm 0.032}$	$0.222^{\pm 0.053}$	$0.298^{\pm 0.06}$	$0.21^{\pm 0.06}$	$0.203^{\pm 0.06}$	$0.182^{\pm 0.057}$	$0.165^{\pm 0.058}$
	σ_d^2	-	$0.247^{\pm 0.059}$	-	-	$0.186^{\pm 0.056}$	$0.167^{\pm 0.053}$	$0.136^{\pm 0.049}$
	σ_{aa}^2	-	-	$0.195^{\pm 0.052}$	-	$0.117^{\pm 0.037}$	-	$0.097^{\pm 0.034}$
	σ_{ad}^2	-	-	-	$0.268^{\pm 0.073}$	-	$0.145^{\pm 0.055}$	$0.123^{\pm 0.05}$
	σ_G^2	$0.327^{\pm 0.032}$	$0.465^{\pm 0.043}$	$0.442^{\pm 0.042}$	$0.46^{\pm 0.046}$	$0.496^{\pm 0.043}$	$0.499^{\pm 0.044}$	$0.516^{\pm 0.043}$
	σ_e^2	$0.68^{\pm 0.008}$	$0.543^{\pm 0.028}$	$0.57^{\pm 0.029}$	$0.546^{\pm 0.035}$	$0.522^{\pm 0.029}$	$0.519^{\pm 0.03}$	$0.503^{\pm 0.03}$
	H^2	$0.324^{\pm 0.022}$	$0.462^{\pm 0.032}$	$0.436^{\pm 0.033}$	$0.458^{\pm 0.038}$	$0.485^{\pm 0.032}$	$0.486^{\pm 0.033}$	$0.504^{\pm 0.033}$
PH	σ_a^2	$0.525^{\pm 0.034}$	$0.401^{\pm 0.064}$	$0.603^{\pm 0.086}$	$0.458^{\pm 0.081}$	$0.366^{\pm 0.08}$	$0.388^{\pm 0.074}$	$0.338^{\pm 0.081}$
	σ_d^2	-	$0.304^{\pm 0.06}$	-	-	$0.237^{\pm 0.06}$	$0.224^{\pm 0.053}$	$0.178^{\pm 0.053}$
	σ_{aa}^2	-	-	$0.273^{\pm 0.064}$	-	$0.102^{\pm 0.033}$	-	$0.091^{\pm 0.03}$
	σ_{ad}^2	-	-	-	$0.361^{\pm 0.08}8$	-	$0.115^{\pm 0.041}$	$0.098^{\pm 0.036}$
	σ_G^2	$0.525^{\pm 0.034}$	$0.676^{\pm 0.036}$	$0.645^{\pm 0.036}$	$0.66^{\pm 0.04}$	$0.695^{\pm 0.036}$	$0.694^{\pm 0.036}$	$0.705^{\pm 0.035}$
	σ_e^2	$0.477^{\pm 0.005}$	$0.327^{\pm 0.019}$	$0.357^{\pm 0.02}$	$0.342^{\pm 0.024}$	$0.314^{\pm 0.019}$	$0.312^{\pm 0.019}$	$0.303^{\pm 0.019}$
	H^2	$0.523^{\pm 0.017}$	$0.673^{\pm 0.021}$	$0.643^{\pm 0.023}$	$0.658^{\pm 0.025}$	$0.688^{\pm 0.021}$	$0.689^{\pm 0.021}$	$0.699^{\pm 0.02}$

σ_a^2, σ_d^2, σ_{aa}^2, σ_{ad}^2, σ_G^2, σ_e^2: Additive, dominance, additive-additive, and additive-dominance variance parameters, total genomic and error variances, respectively.

H^2: Genomic broad-sense heritability

Table S4. Posterior means (± posterior standard deviations) of variance components and broad-sense genomic heritability (H^2) by traits and models at Piracicaba with low nitrogen availability (PI.LN)

		Model						
Trait	**Comp.**	**A**	**A+D**	**A+AA**	**A+AD**	**A+D+AA**	**A+D+AD**	**A+D+AA+AD**
EH	σ_a^2	$0.665^{\pm 0.032}$	$0.46^{\pm 0.067}$	$0.784^{\pm 0.081}$	$0.417^{\pm 0.077}$	$0.518^{\pm 0.087}$	$0.397^{\pm 0.071}$	$0.431^{\pm 0.088}$
	σ_d^2	-	$0.191^{\pm 0.043}$	-	-	$0.141^{\pm 0.04}$	$0.127^{\pm 0.035}$	$0.102^{\pm 0.034}$
	σ_{aa}^2	-	-	$0.15^{\pm 0.036}$	-	$0.075^{\pm 0.022}$	-	$0.061^{\pm 0.018}$
	σ_{ad}^2	-	-	-	$0.261^{\pm 0.064}$	-	$0.116^{\pm 0.039}$	$0.097^{\pm 0.036}$
	σ_G^2	$0.665^{\pm 0.032}$	$0.756^{\pm 0.031}$	$0.737^{\pm 0.032}$	$0.761^{\pm 0.033}$	$0.772^{\pm 0.031}$	$0.776^{\pm 0.031}$	$0.786^{\pm 0.03}$
	σ_e^2	$0.337^{\pm 0.004}$	$0.246^{\pm 0.015}$	$0.267^{\pm 0.014}$	$0.242^{\pm 0.017}$	$0.236^{\pm 0.015}$	$0.228^{\pm 0.015}$	$0.223^{\pm 0.015}$
	H^2	$0.664^{\pm 0.011}$	$0.755^{\pm 0.016}$	$0.734^{\pm 0.016}$	$0.759^{\pm 0.018}$	$0.765^{\pm 0.016}$	$0.773^{\pm 0.015}$	$0.779^{\pm 0.015}$
GY	σ_a^2	$0.26^{\pm 0.029}$	$0.194^{\pm 0.053}$	$0.195^{\pm 0.052}$	$0.177^{\pm 0.055}$	$0.153^{\pm 0.051}$	$0.159^{\pm 0.052}$	$0.129^{\pm 0.05}$
	σ_d^2	-	$0.292^{\pm 0.065}$	-	-	$0.209^{\pm 0.061}$	$0.209^{\pm 0.06}$	$0.169^{\pm 0.058}$
	σ_{aa}^2	-	-	$0.266^{\pm 0.063}$	-	$0.149^{\pm 0.051}$	-	$0.124^{\pm 0.046}$
	σ_{ad}^2	-	-	-	$0.318^{\pm 0.084}$	-	$0.16^{\pm 0.061}$	$0.121^{\pm 0.051}$
	σ_G^2	$0.26^{\pm 0.029}$	$0.441^{\pm 0.047}$	$0.425^{\pm 0.047}$	$0.437^{\pm 0.054}$	$0.474^{\pm 0.045}$	$0.469^{\pm 0.046}$	$0.492^{\pm 0.046}$
	σ_e^2	$0.751^{\pm 0.008}$	$0.567^{\pm 0.035}$	$0.588^{\pm 0.036}$	$0.571^{\pm 0.045}$	$0.539^{\pm 0.034}$	$0.541^{\pm 0.035}$	$0.522^{\pm 0.036}$
	H^2	$0.256^{\pm 0.022}$	$0.437^{\pm 0.039}$	$0.416^{\pm 0.039}$	$0.432^{\pm 0.048}$	$0.465^{\pm 0.036}$	$0.465^{\pm 0.037}$	$0.484^{\pm 0.037}$
PH	σ_a^2	$0.49^{\pm 0.034}$	$0.419^{\pm 0.067}$	$0.429^{\pm 0.068}$	$0.459^{\pm 0.079}$	$0.352^{\pm 0.076}$	$0.402^{\pm 0.074}$	$0.332^{\pm 0.081}$
	σ_d^2	-	$0.227^{\pm 0.046}$	-	-	$0.171^{\pm 0.042}$	$0.182^{\pm 0.043}$	$0.145^{\pm 0.04}$
	σ_{aa}^2	-	-	$0.236^{\pm 0.055}$	-	$0.099^{\pm 0.031}$	-	$0.087^{\pm 0.029}$
	σ_{ad}^2	-	-	-	$0.231^{\pm 0.064}$	-	$0.09^{\pm 0.03}$	$0.076^{\pm 0.026}$
	σ_G^2	$0.49^{\pm 0.034}$	$0.624^{\pm 0.036}$	$0.603^{\pm 0.038}$	$0.594^{\pm 0.039}$	$0.644^{\pm 0.036}$	$0.644^{\pm 0.036}$	$0.655^{\pm 0.036}$
	σ_e^2	$0.511^{\pm 0.006}$	$0.379^{\pm 0.019}$	$0.4^{\pm 0.02}$	$0.409^{\pm 0.023}$	$0.367^{\pm 0.018}$	$0.365^{\pm 0.019}$	$0.357^{\pm 0.019}$
	H^2	$0.49^{\pm 0.018}$	$0.622^{\pm 0.022}$	$0.601^{\pm 0.023}$	$0.592^{\pm 0.026}$	$0.636^{\pm 0.021}$	$0.637^{\pm 0.022}$	$0.646^{\pm 0.021}$

σ_a^2, σ_d^2, σ_{aa}^2, σ_{ad}^2, σ_G^2, σ_e^2: Additive, dominance, additive-additive, and additive-dominance variance parameters, total genomic and error variances, respectively.

H^2: Genomic broad-sense heritability

Table S5. Posterior means (± posterior standard deviations) of variance components and broad-sense genomic heritability (H^2) by traits and environments estimated using the RKHS model

		Environments			
Trait	**Comp.**	**AN.IN**	**AN.LN**	**PI.IN**	**PI.LN**
EH	σ^2_{K1}	$0.061^{\pm 0.015}$	$0.075^{\pm 0.02}$	$0.07^{\pm 0.018}$	$0.068^{\pm 0.017}$
	σ^2_{K2}	$0.098^{\pm 0.033}$	$0.112^{\pm 0.043}$	$0.112^{\pm 0.043}$	$0.106^{\pm 0.04}$
	σ^2_{K3}	$0.536^{\pm 0.084}$	$0.405^{\pm 0.08}$	$0.492^{\pm 0.087}$	$0.53^{\pm 0.091}$
	σ^2_G	$0.808^{\pm 0.03}$	$0.676^{\pm 0.035}$	$0.801^{\pm 0.03}$	$0.818^{\pm 0.029}$
	σ^2_e	$0.203^{\pm 0.013}$	$0.338^{\pm 0.018}$	$0.209^{\pm 0.014}$	$0.191^{\pm 0.014}$
	H^2	$0.799^{\pm 0.014}$	$0.666^{\pm 0.02}$	$0.793^{\pm 0.015}$	$0.81^{\pm 0.015}$
GY	σ^2_{K1}	$0.094^{\pm 0.028}$	$0.104^{\pm 0.034}$	$0.122^{\pm 0.038}$	$0.156^{\pm 0.055}$
	σ^2_{K2}	$0.137^{\pm 0.054}$	$0.145^{\pm 0.053}$	$0.167^{\pm 0.064}$	$0.176^{\pm 0.073}$
	σ^2_{K3}	$0.394^{\pm 0.081}$	$0.216^{\pm 0.06}$	$0.248^{\pm 0.071}$	$0.215^{\pm 0.074}$
	σ^2_G	$0.618^{\pm 0.04}$	$0.457^{\pm 0.042}$	$0.552^{\pm 0.044}$	$0.524^{\pm 0.048}$
	σ^2_e	$0.388^{\pm 0.027}$	$0.557^{\pm 0.03}$	$0.463^{\pm 0.033}$	$0.482^{\pm 0.041}$
	H^2	$0.616^{\pm 0.028}$	$0.452^{\pm 0.033}$	$0.543^{\pm 0.035}$	$0.522^{\pm 0.042}$
PH	σ^2_{K1}	$0.069^{\pm 0.018}$	$0.102^{\pm 0.032}$	$0.076^{\pm 0.02}$	$0.074^{\pm 0.02}$
	σ^2_{K2}	$0.101^{\pm 0.037}$	$0.15^{\pm 0.063}$	$0.115^{\pm 0.041}$	$0.115^{\pm 0.043}$
	σ^2_{K3}	$0.742^{\pm 0.033}$	$0.591^{\pm 0.04}$	$0.73^{\pm 0.034}$	$0.68^{\pm 0.036}$
	σ^2_G	$0.513^{\pm 0.078}$	$0.3^{\pm 0.085}$	$0.482^{\pm 0.082}$	$0.444^{\pm 0.078}$
	σ^2_e	$0.27^{\pm 0.017}$	$0.42^{\pm 0.026}$	$0.283^{\pm 0.019}$	$0.332^{\pm 0.02}$
	H^2	$0.733^{\pm 0.018}$	$0.584^{\pm 0.028}$	$0.719^{\pm 0.02}$	$0.672^{\pm 0.021}$

σ^2_{K1}, σ^2_{K2}, σ^2_{K3}: K_1 (h=0.5), K_2 (h=1), K_3 (h=2) variances, respectively, where K is a non-linear kernel; σ^2_G, σ^2_e: : total genomic and error variances; H^2 : Genomic broad-sense heritability; AN.IN: Anhembi ideal nitrogen availability; AN.LN: Anhembi low nitrogen availability; PI.IN: Piracicaba ideal nitrogen availability; PI.LN: Piracicaba low nitrogen availability.

Table S6. Ratio between non-additive and additive variances ($\boldsymbol{SCA_{ratio}}$±SE) by trait, environment, and model

		Model						
Trait	**Env**	**A+D**	**A+AA**	**A+AD**	**A+D+AA**	**A+D+AD**	**A+D+AA+AD**	**Mean**
EH	AN.IN	$0.114^{\pm 0.001}$	$0.101^{\pm 0.001}$	$0.112^{\pm 0.001}$	$0.141^{\pm 0.001}$	$0.144^{\pm 0.001}$	$0.160^{\pm 0.001}$	0.129
	AN.LN	$0.141^{\pm 0.001}$	$0.125^{\pm 0.001}$	$0.134^{\pm 0.001}$	$0.184^{\pm 0.001}$	$0.189^{\pm 0.001}$	$0.216^{\pm 0.001}$	0.165
	PI.IN	$0.135^{\pm 0.001}$	$0.109^{\pm 0.001}$	$0.134^{\pm 0.001}$	$0.160^{\pm 0.001}$	$0.168^{\pm 0.001}$	$0.180^{\pm 0.001}$	0.148
	PI.LN	$0.140\pm^{0.001}$	$0.112^{\pm 0.001}$	$0.148^{\pm 0.001}$	$0.164^{\pm 0.001}$	$0.171^{\pm 0.001}$	$0.186^{\pm 0.001}$	0.153
GY	AN.IN	$0.450^{\pm 0.002}$	$0.416^{\pm 0.002}$	$0.329^{\pm 0.002}$	$0.513^{\pm 0.002}$	$0.519^{\pm 0.002}$	$0.561^{\pm 0.002}$	0.465
	AN.LN	$0.479^{\pm 0.003}$	$0.520^{\pm 0.003}$	$0.387^{\pm 0.003}$	$0.649^{\pm 0.004}$	$0.578^{\pm 0.003}$	$0.700^{\pm 0.004}$	0.552
	PI.IN	$0.429^{\pm 0.003}$	$0.364^{\pm 0.003}$	$0.420^{\pm 0.003}$	$0.530^{\pm 0.003}$	$0.540^{\pm 0.003}$	$0.592^{\pm 0.003}$	0.479
	PI.LN	$0.722^{\pm 0.004}$	$0.652^{\pm 0.004}$	$0.700^{\pm 0.004}$	$0.844^{\pm 0.004}$	$0.827^{\pm 0.004}$	$0.913^{\pm 0.004}$	0.777
PH	AN.IN	$0.183^{\pm 0.001}$	$0.157^{\pm 0.001}$	$0.148^{\pm 0.001}$	$0.215^{\pm 0.001}$	$0.213^{\pm 0.001}$	$0.236^{\pm 0.001}$	0.192
	AN.LN	$0.329^{\pm 0.002}$	$0.274^{\pm 0.002}$	$0.282^{\pm 0.002}$	$0.384^{\pm 0.002}$	$0.393^{\pm 0.002}$	$0.428^{\pm 0.002}$	0.348
	PI.IN	$0.291^{\pm 0.002}$	$0.234^{\pm 0.002}$	$0.262^{\pm 0.002}$	$0.330^{\pm 0.002}$	$0.329^{\pm 0.002}$	$0.349^{\pm 0.002}$	0.299
	PI.LN	$0.282^{\pm 0.002}$	$0.235^{\pm 0.002}$	$0.218^{\pm 0.002}$	$0.319^{\pm 0.002}$	$0.319^{\pm 0.002}$	$0.342^{\pm 0.002}$	0.286

The ratio between non-additive and additive variance was estimated by : $SCA_{Ratio} = \frac{\sigma^2_{SCA}}{\sigma^2_{GCA}}$; σ^2_{GCA} is the estimate of additive variance using a purely additive -effects model (A model). Non-additive variance components (σ^2_{SCA}) were estimated by subtracting from the total genomic variance of each model the additive variance (σ^2_{GCA})

SUPPLEMENTARY FIGURES

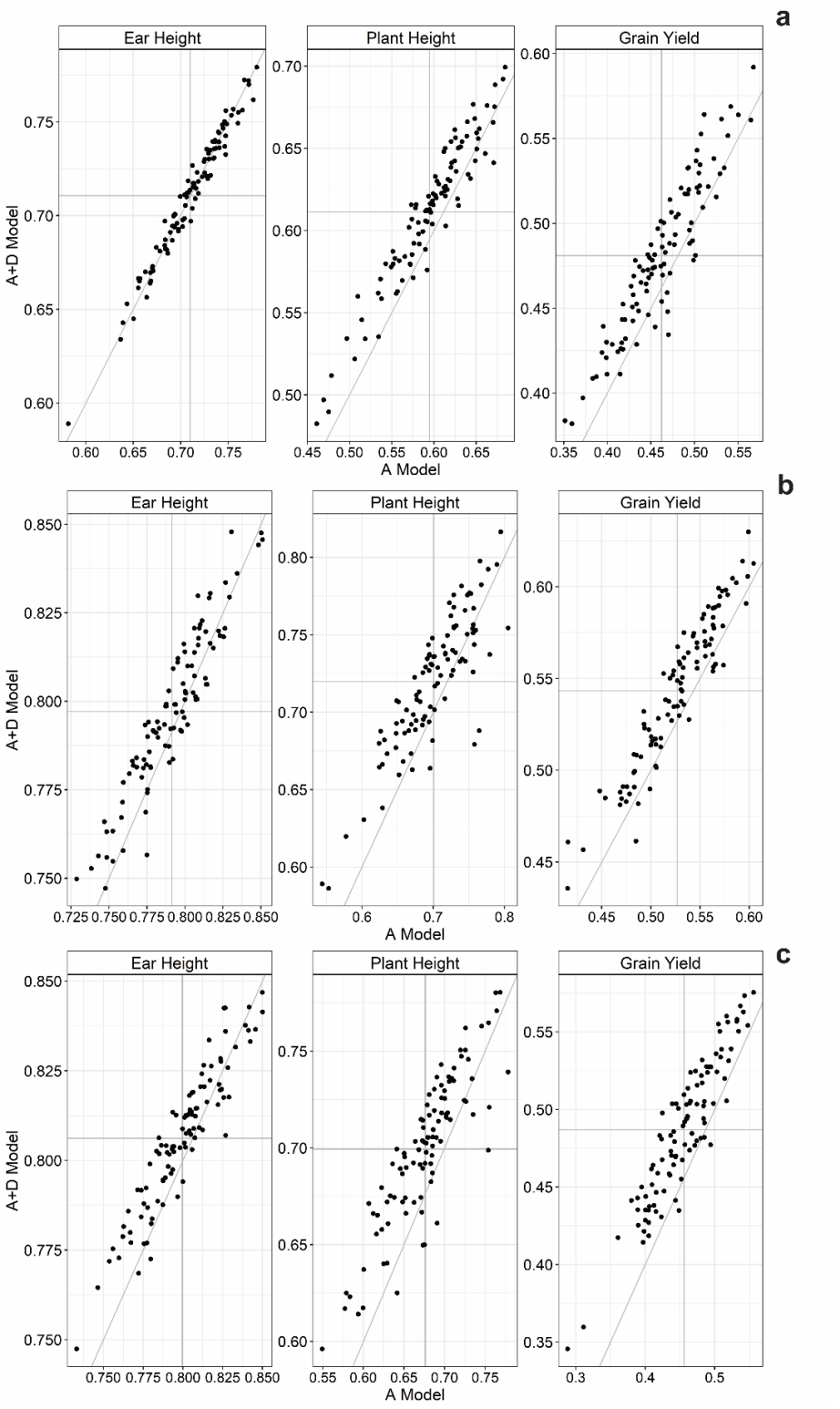

Figure S1. Comparison of correlations between observed and predicted values obtained by the A+D model (Additive-dominance) and A (Additive) model by trait. A: AN.LN: Anhembi low nitrogen availability; B: PI.IN: Piracicaba ideal nitrogen availability; C: PI.LN: Piracicaba low nitrogen availability.

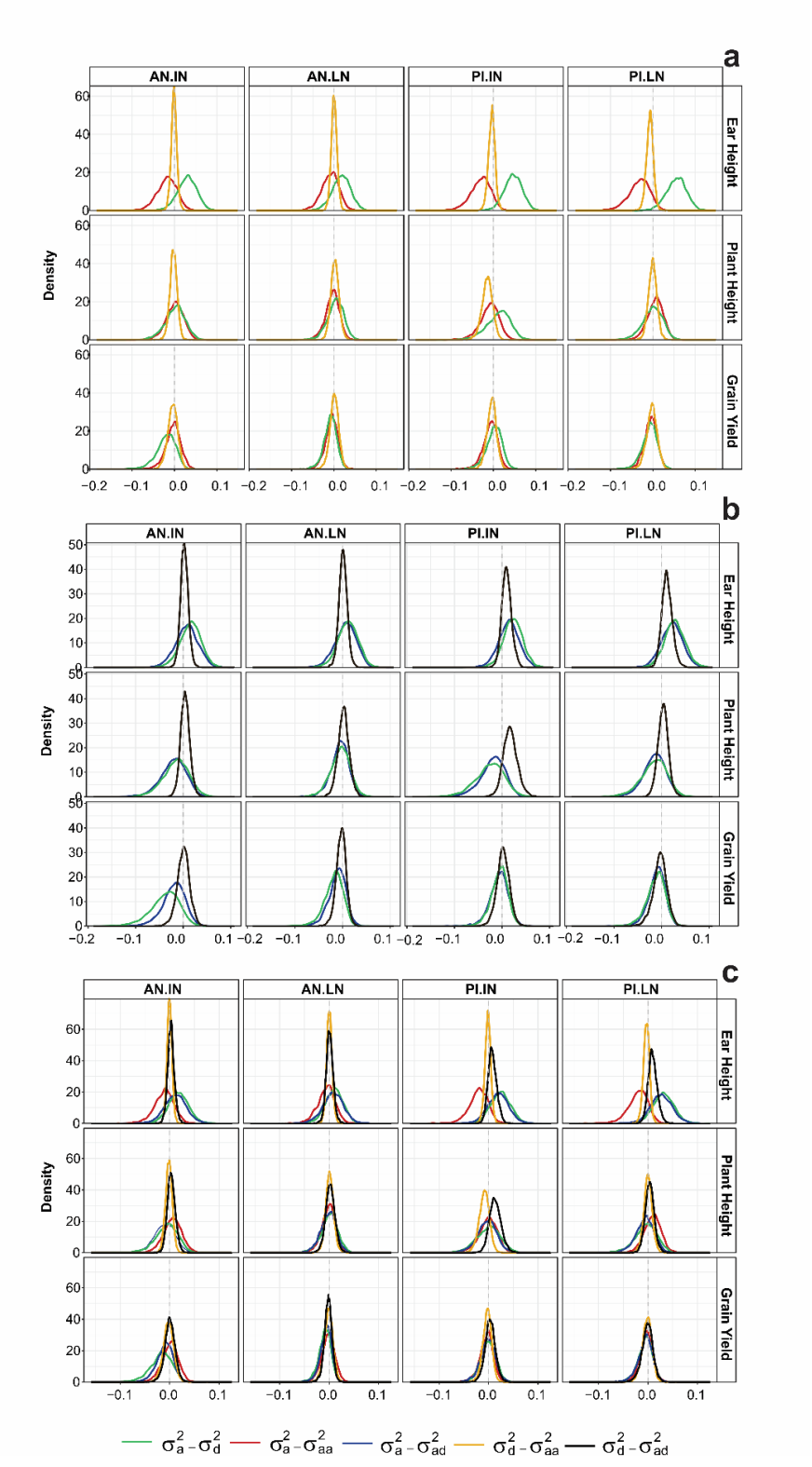

Figure S2. Posterior density of the covariance between the additive and nonadditive genetic components by environment and traits, for: A: A+D+AA, B: A+D+AD, and C: A+D+AA+AD models. A: Additive effect, D: Dominance, AA: Additive-additive, and AD: Additive-dominance effects.

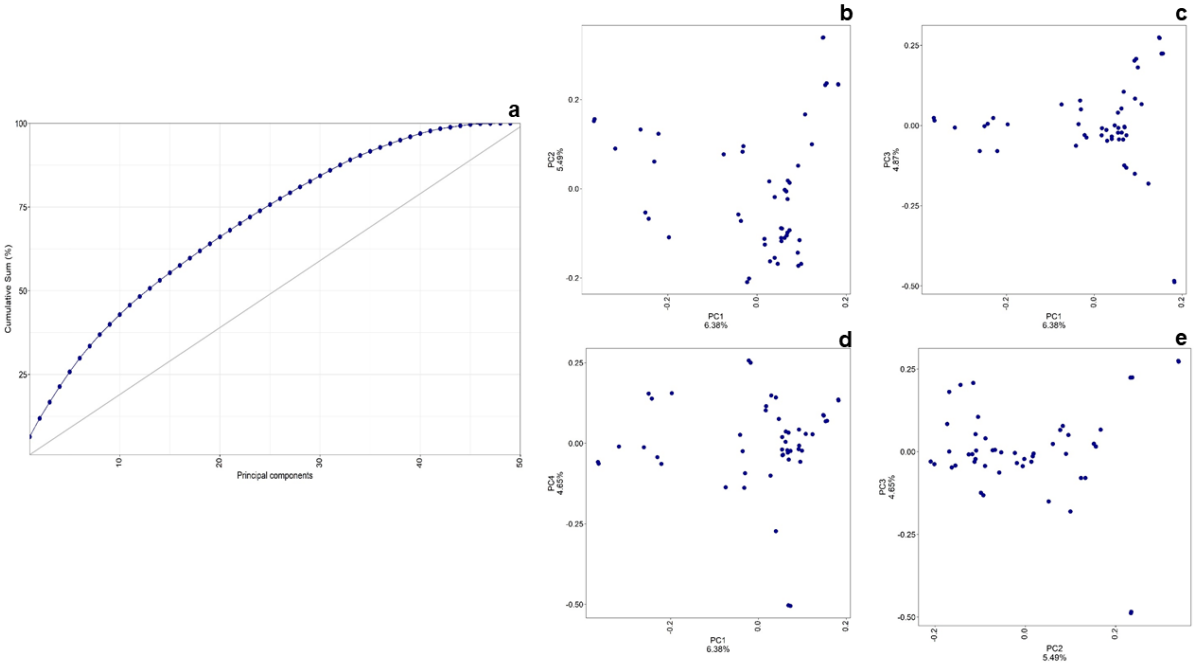

Figure S3. Population structure of 49 inbred lines in maize. **a:** Cumulative proportion of variance explained by the principal components (PC). **b:** PC2 vs. PC1. **c:** PC3 vs. PC1. **d:** PC4 vs. PC1. **e:** PC3 vs. PC2.

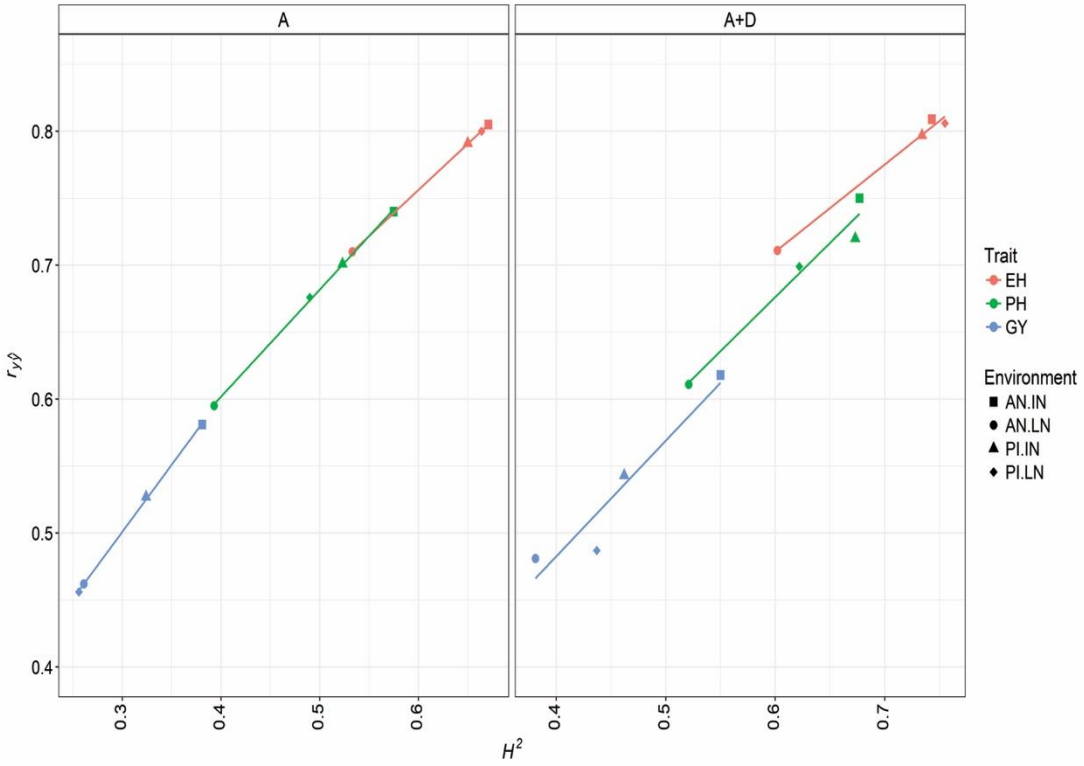

Figure S4. Linearity among prediction accuracy ($r_{y\hat{y}}$) and broad-sense genomic heritability (H^2) by trait/environment within prediction model. EH: Ear height, PH: Plant height, and GY: Grain yield. AN: Anhembi, PI: Piracicaba, IN: Ideal nitrogen, and LN: Low nitrogen. A: Additive effect, and D: Dominance effects.

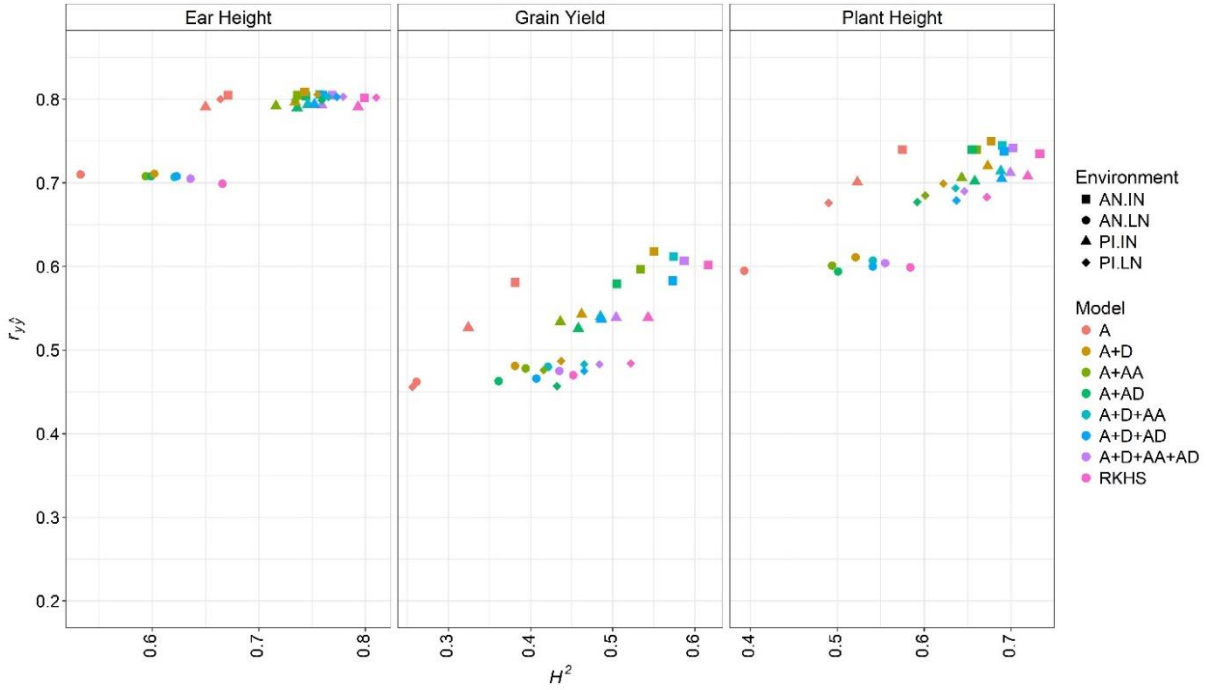

Figure S5. Cross-validation prediction accuracy (r_{yy}) versus broad-sense genomic heritability (H^2) by trait, environment, and model. A: Additive, D: Dominance, AA: Additive x additive, and AD: Additive x dominance effects. RKHS: Reproducing Kernel Hilbert Spaces model). AN: Anhembi, PI: Piracicaba, LN: Low nitrogen, IN: Ideal nitrogen.

3. UNDERSTANDING HOW THE COMPLEXITY OF GENOTYPE BY ENVIRONMENT MAY AFFECT THE PREDICTIVE ACCURACY OF MAIZE HYBRIDS THROUGH MULTI-ENVIRONMENT MODELS ACCOUNTING ADDITIVE AND DOMINANCE EFFECTS

ABSTRACT

Prediction accuracy of multi-environment prediction models can be affected by the complexity of the genotype by environment interaction. Moreover, depending on the genetic architecture of a trait, modeling for non-additive effects, as dominance, can increase the genomic prediction accuracy. In this study we aimed to verify: *i)* the impact of the genotype by environment complexity on the prediction accuracy of grain yield of maize hybrids; *ii)* the advantage of modeling dominance effects for prediction of maize hybrids in multi-environment trials; *iii)* which genetic effect, additive or dominance, interact more with environments; and *iii)* how parents information impacts the prediction accuracy of hybrids in multi-environment genomic models. For this, we used data of 614 maize hybrids evaluated during two growing seasons, under two nitrogens regimes at two locations. Based on the hybrid's adjusted phenotypes by trials, we derived eighth scenarios differing in the genotype by environment interaction complexity. For each of the scenarios, we estimated genetic parameters, and the prediction accuracy obtained by four different validation systems (based on hybrids and half-sib families allocation). We reported that sampling entire half-sib families by environments instead of individual hybrids can lead to very similar accuracy when employing multi-environment prediction models. Moreover, the inclusion of dominance deviations in multi-environment prediction model increases the prediction accuracy. Also, there is a linear relation between prediction accuracy and complexity of the interaction, in which was observed an increasiang on the prediction accuracy according to the genotype by environment reduction. Furthermore, we observed significant increases in prediction accuracy of lowly correlated environments when information of a linking trial/environment is included in the prediction model.

Keywords: non-additive effects, half-sib families, crossover interaction, tropical maize

3.1. INTRODUCTION

The evaluation of newly developed materials in extensive multi-environment trials (MET) is a common and fundamental step for the development and releasing of new commercial cultivars. Usually, the environments that compose the MET net have specific pedoclimatic characteristics and represent the conditions for the crop development in a particular region.

These differences among them often lead to the occurrence of genotype by environment interaction (G×E). According to Bernardo (2010), it is possible to deal with the G×E by three manners: ignoring, reducing, or exploiting it. One may adopt the two first options when the importance of this interaction is low or when the breeder aims to select broadly adapted genotypes. Nevertheless, even for low degrees of G×E, exploring it is recommended.

Several methods have been used to manage G×E, *i.e.*, linear-bilinear models as the Site regressions (Crossa and Cornelius 1997), Additive Main effect and Multiplicative Interaction (AMMI; Gauch, 2006), GGE-biplot (Yan 2001), and mixed modeling (Burgueño et al. 2012; Crossa 2012). Another interesting approach to reduce or exploit the G×E is grouping the most correlated environments into "mega-environments." According to several authors, this allows the targeting of promising genotypes for specific mega-environments by reducing the G×E, and consequently, increasing heritability and genetic gains (Bernardo 2010; Windhausen et al. 2012; Heslot et al. 2015).

Due to the development of feasible genotyping tools, and the increasing of phenotyping costs, approaches based on whole spread molecular markers for predicting the performance of non-phenotyped materials, as genomic prediction (GP; Meuwissen et al., 2001), has been extensively employed into breeding programs (Crossa et al. 2016; Lado et al. 2016). Predicting the performance of new materials based on GP is advantageous especially for those cases in which traits are difficult, time-consuming, and expensive to measure. Also, GP can be helpful when a genotype must be evaluated in several environments. In this case, due to the occurrence of the G×E, it is worthwhile to account for the interaction in prediction models, once it can boost the predictive accuracy and the genetic gains (Jarquín et al. 2014; Zhang et al. 2014; Lopez-Cruz et al. 2015; Cuevas et al. 2016; Sousa et al. 2017).

Therefore, several authors have proposed distinct prediction models accounting for the G×E that differ in their manner of modeling the interaction (Burgueño et al. 2012; Heslot et al. 2014; Jarquín et al. 2014; Lopez-Cruz et al. 2015). For instance, Burgueño et al. (2012) were the first to propose a model accounting for the G×E effects into GP. They suggested modeling $G \times E$ in a mixed model framework using factor analytic structures (FA). On the other hand, the model developed by Heslot et al. (2014) integrates environmental covariates and molecular markers associated with crop modeling. In its turn, Jarquín et al. (2014) suggested a reaction norm model in which the G×E is modeled through Hadamard product of two random linear effects, the genetic (represented by the single nucleotide polymorphism [SNP] based relationship matrix), and a relationship matrix of environmental covariates. Finally, Lopez-Cruz et al. (2015) proposed that the genotypic value of an individual should be partitioned into main effects, which

are stable among environments, and specific effects for each environment (marker by environment interaction-here denoted as the marker by environment model, MGE). Thus, it permits to identify the environments that most contribute to the G×E and those genomic regions that most interact with the environment. This model is especially valuable because can be easily extended to account for non-additive effects, such as dominance deviations or epistatic interactions, and can be implemented using priors that produce shrinkage and variable selection (Crossa et al. 2016). However, its main disadvantage is the requirement of positive correlations between environments.

Quantitative traits, as grain yield, are profoundly influenced by the environment. Thus, a substantial interaction of the genetic components with the environments is expected. In quantitative loci (QTL) analyses, the occurrence of QTL x environment interaction for additive and non-additive effects is well known (Liu et al. 2008; Shang et al. 2016). This suggests that accounting for both of them, especially dominance, can be highly useful for the prediction of non-tested materials. Recently, Dias et al. (2018) and Acosta-Pech et al. (2017) found substantial increases in the predictive accuracy of genomic models by modeling additive and non-additive effects for maize hybrids. However, to the best of our knowledge, the marker by environment model proposed by Lopez-Cruz et al. (2015) has not yet been extended to account both additive and dominance effects. Furthermore, studies reporting the effect of different magnitudes of G×E complexity (crossover G×E) and its influence on the prediction accuracy of the MGE models are no available in the literature.

Besides the prediction of non-tested genotypes, the use of multi-environment trials enables to target parents for specific environments. The inclusion of parental information in training sets establishment through its progenies in genomic prediction models to single environment analysis has been proven to impact prediction accuracy (Technow et al. 2012, 2014; Zhao et al. 2015; Kadam et al. 2016). Nevertheless, it has been shown that the inclusion of information from at least one parental line leads to intermediate prediction accuracies when compared to situations in which two or none parental are represented in the training set. However, the effect of G×E on the inclusion of parental information in training sets has not been reported yet. This result may allow a rational reduction in the number parents per site, enabling a projected genetic imbalance by the breeder, which may lead to considerable increases in prediction accuracy, and reduces the costs, labor, and time-consuming.

Therefore, we aimed to answer the following questions when using MGE models: *i)* What is the impact of the G×E complexity on the prediction accuracy of maize hybrids?; *ii)* Are there advantages of modeling dominance effects for hybrid prediction in MET?; *iii)* Which

genetic effect, additive or dominance, is the most affected by G×E?; *iii)* How does the parent information impact the hybrid prediction in MET? To address these questions, we performed an empirical study using the MGE model (Lopez-Cruz et al. 2015), accounting for additive (A) and dominance (D) effects, and considering 614 maize hybrids in different scenarios of G×E complexity obtained by environmental stratification and different adjustment methods.

3.2. MATERIAL AND METHODS

3.2.1. Phenotypic data

A panel of 906 single-cross hybrids from an unbalanced full diallel mating design involving 49 inbred lines with tropical genetic background contrasting for nitrogen use efficiency (Mendonça et al. 2017) was used in this study. Hybrids were evaluated over two growing seasons (2016 and 2017 winter season), two locations, Piracicaba (PI; rainfed; 22°42'23"S, 47°38'14"W, 535 m), and Anhembi (AN; irrigated; 22°50'51"S, 48°01'06"W, 466 m), in the state of São Paulo, Brazil. Within each location, two separated trials were considered in adjacent fields, one considering ideal nitrogen (N) fertilization (IN; 30 kg N ha^{-1} at sowing and 70kg N ha^{-1} for top-dressing) and another with low N fertilization (LN; 30 kg N ha^{-1} at sowing without top-dressing). Each combination of N fertilization, location, and growing season was considered as an environment, totalizing eight trials. The experimental design employed for each trial was the unreplicated augmented blocks (Federer 1961) with two checks. Each plot consisted of a 7-m row containing 25 plants. Grain yield (GY, $ton.ha^{-1}$) was measured in each experiment and corrected for 13% of moisture.

3.2.2. Accounting different degrees of G×E interaction (scenarios)

Environments can be determined according to the environmental conditions in which a determined trial was conducted. Thus, one can consider individual trials as different environments, also, these trials can be grouped according to environmental conditions, as years, climate patterns, altitude, locations, fertilizer regimes, or even the combination between these conditions, as for example, years x locations. According to the mode of grouping individual trials, different degrees of G×E's complexities among environments are obtained. Therefore, in our study, we adjusted the phenotypic records using five models differing in the stratification of trials to obtain scenarios differing in their G×E's complexity between environments. The first scenario

(*Scenario 1*) comprises the adjustment at trial level (combination between location, nitrogen regime and year, *i.e*, AN.IN.1, AN.IN.2, etc). The adjustment was performed by subtracting the block effects from the measured phenotype of each trial. The blocks effects were obtained by fitting a model considering the effects of check (fixed) and blocks (random). Based on the adjusted phenotypes from Scenario 1, we derived four additional scenarios by stratifying the trials according to: *i)* Scenario 2- the combination of locations (AN or PI) and nitrogen regimes (IN or LN), totalling four distinct environments (AN.IN, AN.LN, PI.IN, PI.LN); *ii)* Scenario 3- by year (2016 and 2017); *iii)* Scenario 4- by nitrogen regime (IN and LN); *iv)* Scenario 5- by location (AN and PI).

For each obtained environment within Scenarios 2 to 5 the pre-adjusted phenotypes from Scenario 1 were adjusted by a joint analyses considering the model:

$$y_{ij} = \mu + a_j + h_i + ah_{ij}$$

in which, μ is the overall mean; a_j is the fixed effect of the environmental variables whitin each environment by scenario (year effects, combination between location x nitrogen regime, location x year, and year x notrogen regime for Scenario 2, 3, 4 and 5, respectively); h_i is the fixed effects of genotypes; and ah_{ij} is the interaction between the environmental variables and genotypes. Given that our trials were conducted using unreplicated augmented blocks, the ah_{ij} term comprises both interaction and residual effects (Moehring et al. 2014).

Due to the small degree of interaction obtained for each of the former scenarios, three additional setups were obtained (sixth to eighth) based on GGEBiplot analyses using the R package GGEBiplots (Dumble 2017) of trials presented in Scenario 1. These new scenarios were derived aiming to determine situations in which the hybrid's performance is predicted using: *i)* Scenario 6 - data from lowest correlated trials; *ii)* Scenario 7 - phenotypic records from a set of positively correlated trials within a "mega-environment"; *iii)* Scenario 8 - phenotypes from two low correlated and one connecting trial. Further information about these scenarios is shown in the Results section.

Within each scenario, the Spearman's correlation coefficients (s) was estimated between the environments as an indicator of the presence and the magnitude of crossover G×E. In order to circumvent unbalanced data during the genomic analyses, we considered only the hybrids present in all trials. Thus, all the analyses were carried out considering only the 614 constant hybrids.

3.2.3. Genotype

The 49 parental inbred lines were genotyped using the Affymetrix® Axiom® Maize Genotyping Array of 616 K SNPs (Unterseer et al. 2014). The quality control procedures were performed in two steps using the R package *synbreed* (Wimmer et al. 2012). First, we removed all non-mapped SNPs, *loci* with at least one heterozygous, and the SNPs with call rate lower than 0.90. All missing data were imputed using the Beagle algorithm (Browning and Browning 2016). Then, the genotype of each hybrid was constructed by combining the genotype of its parents. In the second quality control step, SNPs with minor allele frequency smaller than 0.05 were removed. After these quality control procedures, we performed a linkage disequilibrium (LD) pruning on the genotype matrix of hybrids, removing those markers with pairwise linkage disequilibrium (r^2) greater than 0.9. This step was carried out using the *SNPRelate R* package (Zheng et al. 2012). After these procedures, 34,571 high-quality SNPs were retained for the further genomic analyses.

3.2.4. Genomic Models

Lopez-Cruz et al. (2015) proposed a genomic model that accounts for main genetic effects and marker by environment interactions (MGE). Here, we extended this model to regard additive and dominance effects. In addition, we considered the heterogeneity of residual variance among environments, according to the proposed by Crossa et al. (2016). Thus, the MGE model was defined as follows:

$$\boldsymbol{y} = \boldsymbol{\mu}\mathbf{1} + \mathrm{Z}\boldsymbol{a} + \mathrm{W}\boldsymbol{d} + \mathrm{Z}_1\boldsymbol{a_1} + \mathrm{W}_1\boldsymbol{d_1} + \boldsymbol{\varepsilon},$$

where $\boldsymbol{y}$ is the vector of adjusted phenotypes by environments, being $\boldsymbol{y}' = \{\boldsymbol{y_1}', \boldsymbol{y_2}', \ldots, \boldsymbol{y_n}'\} = \{y_{11}, y_{21}, \ldots, y_{kE}\}$, where k refers to the k^{st} hybrid and E is the E^{st} environment; $\boldsymbol{\mu}$ is the intercept, being $\boldsymbol{\mu}' = \{\mu_1, \mu_2, \ldots, \mu_E\}$; $\boldsymbol{a}$ is the vector of additive effects, with $\boldsymbol{a} \sim N(\mathbf{0}, \mathbf{J_E} \otimes G_a\sigma_a^2)$; $\boldsymbol{d}$ is the vector of dominance effects, with $\boldsymbol{d} \sim N(\mathbf{0}, \mathbf{J_E} \otimes G_d\sigma_d^2)$. G_a and G_d are additive and dominance relationship matrices. Z, W, Z_1, and W_1corresponds to incidence matrices and $\otimes$ is the Kronecker product of matrices. ε are the residuals, with $\boldsymbol{\varepsilon} \sim \boldsymbol{N}(\mathbf{0}, \boldsymbol{\Sigma})$, where $\boldsymbol{\Sigma}$ is:

$$\boldsymbol{\Sigma} = \begin{bmatrix} \sigma^2_{\varepsilon_1} & \ldots & 0 \\ \vdots & \ddots & \vdots \\ 0 & \ldots & \sigma^2_{\varepsilon_E} \end{bmatrix}$$

Additive and dominance by environment interactions assume $\boldsymbol{a_1} \sim N(\mathbf{0}, \mathrm{A})$ and

$\boldsymbol{d}_1 \sim N(\mathbf{0}, \mathrm{D})$, respectively, where A is:

$$\mathrm{A} = \begin{bmatrix} G_a\sigma^2_{a\times1} & \dots & 0 \\ \vdots & \ddots & \vdots \\ 0 & \dots & G_a\sigma^2_{a\times E} \end{bmatrix} = \begin{bmatrix} G_a\sigma^2_{a\times1} & \dots & 0 \\ \vdots & \ddots & \vdots \\ 0 & \dots & 0 \end{bmatrix} + \dots + \begin{bmatrix} 0 & \dots & 0 \\ \vdots & \ddots & \vdots \\ 0 & \dots & G_a\sigma^2_{a\times E} \end{bmatrix},$$

and D assumes the same form of A, but replacing G_a by G_D and $\sigma^2_{a\times E}$ by $\sigma^2_{d\times E}$. $\mathbf{J_E}$ is a square matrix of ones with dimensions E (number of environments); $\sigma^2_{a\times E}$ and $\sigma^2_{d\times E}$ are the additive and dominance by environment variance component.

Furthermore, a model accounting only for main genetic effects (MG) was fitted following the model:

$$\boldsymbol{y} = \boldsymbol{\mu}\mathbf{1} + \mathrm{Z}\boldsymbol{a} + \mathrm{W}\boldsymbol{d} + \boldsymbol{\varepsilon},$$

where all factor definitions correspond to the ones presented for MGE.

The kinship matrices were obtained according to Vitezica et al. (2013). Therefore, the additive relationship kernel was obtained by:

$$\boldsymbol{G_a} = \frac{\mathbf{XX'}}{tr(\mathbf{XX'})/_n} \text{ where } x_{ij} = \begin{cases} \mathrm{AA} = 2 - 2p \\ \mathrm{Aa} = 1 - 2p \\ \mathrm{aa} = 0 - 2p \end{cases}$$

The dominance kinship kernel was obtained by:

$$\boldsymbol{G_d} = \frac{\mathbf{SS'}}{tr(\mathbf{SS'})/_n} \text{ where } s_{ij} = \begin{cases} \mathrm{AA} = 0 - 2pq \\ \mathrm{Aa} = 1 - 2pq \\ \mathrm{aa} = 0 - 2pq \end{cases}$$

The matrices $\mathbf{X}$ and $\mathbf{S}$ correspond to the SNP matrices with dimension $i \times j$, where i is the number of genotyped individuals and j the number of SNP markers; p and q are the alleles frequencies observed for the j^{th} SNP . To assess the advantage of modeling additive and dominance effects for hybrids prediction over a strict additive model, we also fitted the models as mentioned above (MGE and MG) considering only additive effects.

3.2.5. Variance components and genetic parameters

Variance components (e.g., σ^2_ε, σ^2_a, σ^2_d, σ^2_{axE}, σ^2_{dxE}, etc.) were estimated considering the entire dataset (614 hybrids phenotypes) using the BGLR R-package (Pérez and De Los Campos 2014). For that, we fitted a multi-environment genomic model taking into account 60,000 Gibbs samples, a burning of 10,000 and a thinning of 5. The occurrence of covariance between the modeled effects was disregarded for the estimation of variance components. Thus, $\sigma^2_G = Var(\boldsymbol{a} + \boldsymbol{d} + \boldsymbol{a}\times\boldsymbol{E} + \boldsymbol{d}\times\boldsymbol{E}) = Var\left(\sum_{k=1}^{q}\boldsymbol{g}_k\right) = \sum_{k=1}^{q} Var\left(\boldsymbol{g}_k\right)$, in which σ^2_G is the total genomic variance explained by the model and $\boldsymbol{g}$ represents the genetics effects included in the

model (additive $[\boldsymbol{a}]$, dominance $[\boldsymbol{d}]$, and their interactions with the environment).

For each environment, the broad-sense genomic heritability was estimated by:

$$H^2 = \frac{\sigma_G^2}{\sigma_G^2 + \sigma_{\varepsilon_E}^2}$$

where σ_a^2 is the main additive variance, σ_d^2 is the main dominance variance, and $\sigma_{\varepsilon_E}^2$ is the residual variance estimated for the E^{th} environment. Additionally, narrow-sense genomic heritability (h^2) was estimated for each environment by:

$$h^2 = \frac{\sigma_a^2 + \sigma_{axE}^2}{\sigma_G^2 + \sigma_{\varepsilon_E}^2}$$

The variance explained by dominance effects (d^2) was also estimated for each environment following the equation:

$$d^2 = \frac{\sigma_d^2 + \sigma_{dxE}^2}{\sigma_G^2 + \sigma_{\varepsilon_E}^2}$$

According to Lopez-Cruz et al. (2015), the variance of main effects obtained by the MGE model represents the mean pairwise covariance (stable effects) between the environments considered in the prediction model. Thus, for each scenario evaluated, we estimated the Pearson's correlation (p) of the total genetic values predicted by the MGE model between each pair of environments, within a determined scenario, based on:

$$p = \frac{COV(G_i, G_j)}{\sigma_{G_i} \times \sigma_{G_j}},$$

where, $COV(G_i, G_j)$ is the covariance between environments *i* and *j*, obtained by $COV(G_i, G_j) = \sigma_a^2 + \sigma_d^2$; and σ_{G_i} and σ_{G_j} represent the standard deviation of total genomic variance estimated in environments *i* and *j*, respectively, calculated by $\sigma_{\cdot} = \sqrt{\sigma_a^2 + \sigma_{d_i}^2 + \sigma_{a\times E_{\cdot}}^2 + \sigma_{d\times E_{\cdot}}^2}$. Finally, the correlation between additive and dominance effects based in the former equation was estimated.

3.2.6. Validation Systems

We simulated different scenarios using validation schemes that may occur in a maize breeding program in which genomic prediction is employed for multi-environment trials prediction. For this, we portioned the population into training-test partitions sets (TRN-TST). The first situation that may occur in a breeding program is the classic CV1 proposed by Burgueño et al. (2012), where the performance of genotypes that have not been evaluated in any

of the observed environments is predicted (Supplementary Figure 1A). In this case, the performance of a material is predicted mainly using the information from the kinship of individuals from the test population (TST) and the training population (TRN). The second scenario called CV2 (Burgueño et al. 2012) implies predicting the performance of genotypes that have been evaluated in some environments, but not in others – also known as sparse testing (Supplementary Figure 1B). Here, the model recovers information based on hybrids phenotypic records from the TST in different trials and the kinship with the training set.

Since our hybrids were generated from an unbalanced full diallel, i.e., mating all parental lines, different from what is usually done in maize breeding programs (partial diallel between heterotic groups), we elaborated two other validation schemes in which there is no phenotypic information of the progeny of specific inbred lines. For example, when there are no phenotypic records of the hybrids derived from parental one. A similar approach was described by (Technow et al., 2012; T1 validation system), but we expanded this scheme for a multi-environment framework in our study. The first validation system simulates a scenario in which the progenies of a given parental is not evaluated in any environment (Supplementary Figure 2A). This is a special CV1 situation. However, the recovered information comes from the relationship between families constituting the TRN and those present in the TST. This validation system was denoted as CV3.1. Another tested validation scheme is a special CV2 condition called CV3.2, and comprises the situation when the family was evaluated in at least one environment/trial (Supplementary Figure 2B).

For or each validation scheme, 100 training-testing partitions (TRN-TST) were generated considering a training set of 430 individuals (70%) and a testing set of 184 individuals (30%), maintaining the same TRN sets within validation scheme for additive and additive-dominance models. It is important to point out that for CV3.1 and CV3.2, the sampling of families to construct the TST was consistently performed to maintain a TST of nearly 184 hybrids, which comprises the sampling of six to eight families per partition. For each of the TRN-TST partitions, the following parameters were estimated: prediction accuracy ($r_{g\hat{g}}$) by the Pearson's product moment correlation between the predicted hybrids genetic values from the TST and its observed adjusted phenotypic record; and prediction bias (b) by the linear regression coefficient obtained by regressing the predicted genetic values into their adjusted phenotype. For both $r_{g\hat{g}}$ and b, we reported the average and standard deviation of 100 partitions.

3.3. RESULTS

3.3.1. Presence of G×E between environments

The Spearman's correlation coefficients (s) were positive (Tables 1 and 2) for all scenarios, and varied according to the phenotype adjusting method. This coefficient measures proportional changes of ranking between two variables. Thus, under a plant breeding perspective, s is an indication of the crossover genotype by environment magnitude, where the lower correlation, the larger the changes in the genotypes ranking over environments. Considering each trial as an independent environment (Scenario 1) the Spearman's correlation coefficient ranged from ~0.24 to ~0.50 (Table 1). That suggests critical changes in the phenotypes ranking, indicating the presence of strong crossover $G \times E$ interactions between environments. For scenarios 2, 3, 4, and 5, the correlation estimates were in general of moderate magnitude ranging from ~0.44 to ~0.68 (Table 2).

3.3.2. Generating new scenarios based on the Stratification of Scenario 1

Individual trials showed different patterns of relationship (Figure 1). According to the GGEBiplot analyses, the first two principal components explained 68.76% of the data variability. The less related environments are 2.AN.IN and 1.PI.LN, once the angle between their vectors is the largest in comparison to the others (Figure 1A). This result differs from those obtained considering the Spearman's correlation coefficient, where the less related environments were 2.AN.LN and 1.PI.LN (s =0.24). Furthermore, this MET can be split into 3 "mega-environments" (Figure 1B): The first comprises six environments (1.AN.IN, 1.AN.LN, 1.PI.IN,2.PI.LN, 1.PI.LN, and 2.PI.IN), and the other two involve one environment each, 2.AN.LN and 2.AN.IN.

According to the GGEBiplot analyses, we generated three additional scenarios based on stratification of the Scenario 1. The first one is based on the relationship between environments and considers the less related environments (2.PI.LN and 2.AN.IN) denoted as "Less Related" scenario and was considered the Scenario 6. The second comprises all environments of mega-environment 1, named as "Mega" (Scenario 7). The third considered a representant environment of each mega-environment, referred as "Representative" (Scenario 8). To generate the latter, we selected the environments 2.AN.LN (mega-environment 2), 2.AN.IN (mega-environment 3), and 1.PI.LN (mega-environment 1).

All evaluated scenarios in our study and the average Spearman's correlation coefficients among environments are shown in Table 3. As one can observe, the average Spearman's

correlation coefficients varied from 0.32 (Scenario 6) to 0.68 (Scenario 4), suggesting that the Scenario 6 has the largest crossover G×E.

3.3.3. Variance Components

When the dominance effects were considered, this component was more important than the additive for most scenarios (Supplementary Tables S1-S8 and Figure 2). Estimates of d^2 were higher than h^2 for all scenarios, especially when interaction effects were modeled. Furthermore, scenarios 3 and 8 showed the lowest and highest σ_d^2/σ_a^2 ratios, respectively. Moreover, for scenarios 2, 3, 4, and 5, the average G×E variance component estimated across all environments was smaller than the variance of main genetic effects (additive and dominance). For the remaining scenarios, this component was higher than at least one of the main genetic effects variance component, generally the additive. As expected, scenario 6 (less correlated environments) showed the highest proportion of the total genomic variance related to G×E. On the other hand, the smallest contribution of this component to the genomic variance was found in scenario 4, where we observed the largest Spearman's correlation estimates.

Modeling dominance effects highly increased the total genomic variance recovered by the model when compared to the estimates obtained by the strictly additive model within MG and MGE (Figure 2, and H^2estimates in Supplementary Tables S1-S8). In this case, the smaller contribution of dominance effects was found in Scenario 6, where the average total genomic variance was boosted in 67.8 and 75.9% for MG and MGE models, respectively. In contrast, the greatest contributions were found in Scenario 4, with increases of 118 and 116% in MG and MGE models, respectively.

The advantage of modeling additive and dominance by environments interaction effects for variance components estimation can be assessed by comparing the average total genomic variance obtained by the MG and MGE models (Figure 2, Supplementary Tables S1-S8). Therefore, it is expected the difference between estimates from them is due to the interaction effects modeling. In this case, the gains depended on the G×E magnitude expected in the scenarios (here represented by the mean Spearman's correlation estimates – Tables 1, 2, 3). Where s presented moderate magnitudes (scenarios 2, 3, 4, and 5), the advantage of modeling additive and dominance by environment interactions was moderate since the increment varied from ~7 and 6% to ~19 and 20.5% when modeling additive and additive plus dominance effects in scenarios 4 and 2, respectively. For those scenarios in which the G×E magnitude was expected

to be high (weak correlation estimates – Scenarios 1, 6, 7, and 8), the gains were more consistent, with values superior than 34% for all scenarios.

Modeling dominance effects and its interactions into genomic prediction model largely increased the magnitude of G×E when compared to the multi-environment model accounting only for additive effects (and its A×E interactions) for all scenarios (Figure 2, and 3A). In this case, the increasing rates ranged from ~16.6 to 41% for scenarios 5 and 1, respectively. It is interesting to note that the smallest advantage of modeling dominance by environment interactions was found for scenarios were s achieved high values, ~ 32, 26, 21 and 16% for Scenarios 2, 3, 4, and 5, respectively. On the other hand, for those showing small Spearman's correlation coefficients estimates (Scenarios 1, 6, 7, and 8), the increment on the genotype by environment were always superior to 38%. It suggests that dominance by environment effects play an important role in the phenotypic expression. In addition, with exception of scenarios 3 and 5, additive and dominance by environment interactions had similar contributions (~50%) to the total G×E (Figure 3B). For scenarios 3 and 5, the additive by environment interaction largely contributed to the G×E interaction.

As expected, modeling dominance for both MG and MGE models largely reduced the residual variance for all scenarios when compared to the pure additive models (Figure 4). Moreover, for all scenarios, the MGE model fitted the data better than the MG model (Figure 2 and Figure 4). We can also note that the average residual variance estimate magnitude was reduced according to the interaction complexity, being the smallest residual variance observed in those environments in which the smallest G×E is expected. Another interesting feature is the small variation of the estimates for Scenario 5.

3.3.4. Genetic effects correlations

Modeling additive plus dominance effects increased the Pearson's correlation coefficient (p) between the pairwise comparison of the total genomic variance recovered from different environments within scenarios to their respective pure additive model (Supplementary Tables S9-S11). The largest increases were observed for situations were the s among environments was small (for lowly correlated environments - scenarios 1, 6, 7, 8 - Tables 1 and 3). Nevertheless, for the A+D model, the correlation between dominance effects among environments had a larger magnitude than the observed for the additive effects in most of the scenarios

Positive weak to moderate p estimates for dominance and additive effects were found between environments for scenarios 1, 6, 7 and 8 (Tables S9-S11). Furthermore, we found

significant increases in the correlation estimates according to the complexity of the interaction and the number of environments. For example, in scenario six the Pearson's correlation coefficient between environments (2.AN.IN and 1.PI.LN, Table 4) for additive and dominance effects were 0.45 and 0.65 environments, respectively. Comparing the same pair of environments obtained in scenarios, 6, 8, and 1, the p estimate increased. In this case, the correlation of additive effects between these environments ranged from 0.45 to 0.65 for scenarios 6 and 1, respectively. The same trend was observed for dominance effects (0.65 to 0.70, scenarios 6 and 1), and total genomic variance for the A and A+D model (0.45 to 0.57 and 0.57 to 0.69, respectively).

3.3.5. Prediction Accuracies

The average prediction accuracy ($r_{g\hat{g}}$) across the environments obtained by fitting the MGE model reached the highest estimates for scenarios involving highly correlated (large values of s and p) environments (Figures 5 and 6). In addition, the mean prediction accuracy and the Spearman's correlation coefficient was linearly associated. For all regressions and validation systems, the determination coefficient (R^2) was superior to 0.7 for both additive and additive-dominance prediction model, indicating good data and genomic data fitting among scenarios. In general, cross-validation systems showed consistent performance according to the scenario's average $r_{g\hat{g}}$ (Figure 5 and 6). Thus, MET where at least one phenotypic record of a hybrid or family is present on the training set (CV2 and CV3.2) provided larger mean accuracies compared to schemes where the genotypes or families were not tested on field trials (CV1 and CV2). In general, the MGE model led to higher average prediction accuracies (within scenarios) than the MG model (Figure 6).

For most of the evaluated scenarios, modeling additive plus dominance effects resulted in higher prediction accuracies than accounting for only additive effects for both MG and MGE models (Figures 6, 7, and 8). The prediction accuracies broadly changed according to the validation system for all considered scenarios, being the CV2 and CV3.2 the ones that delivered the greatest estimates of prediction accuracies.

Considering the analyses by the environment within scenarios (Figure 7 and 8), one can observe that the inclusion of dominance effects in the prediction model by CV1 and CV3.1 led to small increases in prediction accuracy when compared to a strictly additive model for all scenarios. In contrast, the presence of phenotypic data from a hybrid/family highly increased the predictive accuracy of the additive-dominance model for CV2 and CV3.2. It is important to

highlight that, in general, fitting an additive model considering the CV2 provided very similar $r_{g\hat{g}}$ estimates to those observed for an additive and additive-dominance models fitted under a CV1 system (Figure 7 and 8). However, the same trend is not observed for the validation systems involving family sets. There is, for most of the environments, a great gain on the A and AD model's prediction accuracy when family information is included on the genomic prediction model (CV3.2) compared to both A and AD models under the CV3.1 scheme.

The advantage of modeling marker by environment effects for hybrids prediction can be assessed by comparing the prediction accuracies obtained from MGE and MG models. Overall, for scenarios in which the crossover G×E interaction was expected to be smaller (high s estimates – Scenarios 2, 3, 4 and 5), the MG model often had very similar or larger prediction accuracies compared to MGE, from what we infer is not worth it to model marker by environments effects (Figures 7 and 8). However, in situations where s among environments were small (Scenario 1, 6, 7 and 8), modeling marker environment-specific effects (MGE model) led to higher prediction accuracies (Figures 7 and 8).

3.3.6. Prediction unbiasedness

The prediction unbiasedness was significative for all validation systems in the MGE model, with most of the values varying between 0.8 and 1.1 (Table 5, 6, and 7). For scenarios 2, 3, 4, and 5, the estimates ranged from 0.744 to 1.07, 0.84 to 1.075, 0.8 to 1.12, and 0.82 to 1.072, respectively. For the other ones, the estimates varied from 0.63 (in 1.AN.LN in scenario 1 for CV3.2-AD) to 1.086 (2.PI.IN in scenario 1 for CV3.2-A).

For most scenarios, the CV2 led to the less biased estimates, followed by CV3.2, CV1, and CV3.1. It is interesting to note that validation schemes in which the entire family is sampled (CV3.1 and CV3.2) usually showed larger bias standard deviation than CV1 and CV2. Furthermore, modeling additive plus dominance effects drove to smaller prediction bias than fitting a strictly additive model only when the family or hybrid is not evaluated in any environment (CV3.1 and CV1). It indicates that dominance effects are better estimated and exploit when the phenotypic records of the crosses and parents are present in the training set.

3.4. DISCUSSION

3.4.1. Validation systems comparison

In maize breeding programs, the potential of inbred lines for crosses is assessed by the evaluation of testcrosses in multi-environment trials (Albrecht et al. 2011; Kadam et al. 2016). Recently, Fritsche-Neto et al. (2018) reported the superiority of factorial and full diallel mating designs over testcrosses for the performance prediction of untested single crosses in maize, and consequently to mate allocation. In our study, we employed a dataset containing hybrids obtained from an unbalanced full diallel mating design to evaluate the prediction performance of single crosses considering four different types of validation systems in a multi-environment context. Overall, our findings are in accordance with previous studies (Technow et al. 2012, 2014; Zhao et al. 2015; Kadam et al. 2016), and indicate that even using MGE models representing both parental lines in the training-set provides highest prediction accuracies and the smallest bias (Figures 6, 7, and 8, and Tables 4, 5, and 6).

Predicting non-tested hybrids/parents (CV1 and CV3.1) is more challenging than predicting genotypes previously evaluated in different environments (CV2 and CV3.2). The same pattern was already reported by several authors (Burgueño et al. 2012; Jarquín et al. 2014; Zhang et al. 2014; Lopez-Cruz et al. 2015; Saint Pierre et al. 2016; Sousa et al. 2017). Predicting non-tested hybrids/parents by CV1 and CV3.1 schemes led to a broad different accuracy and bias estimates. These two validation methods differ in the manner to construct the testing-set (TST). In the former scheme, the TST is composed by a group of hybrids randomly sampled from the total dataset, whereas the latter the contains whole half-sib families sampled from the total population. According to Technow et al. (2012, 2014), the difference in prediction accuracy of validation schemes based on hybrids and parents sampling can be explained by the representativeness of parental inbred line gametes/haplotypes in the training set. In this case, sampling hybrids maintain the gametes/haplotypes of the two parental lines in the training set, once each parental occurs in several crosses in the mating grid. Thus, it is expected that genetic effects are better estimated in this situation (Kadam et al. 2016). When half-sib families/parents are sampled, the entire half-sib family is removed and there are no representative gametes/haplotypes of the parental line in the training set for CV3.1. Therefore, maintaining the representativeness of the parental's gametes/haplotypes into the training population reduces the differences between validation schemes. This is evidenced by the small differences between accuracies and bias estimates within scenarios for CV2 and CV3.2 (Figures 6, 7, and 8 and Tables 4, 5 and 6).

Moreover, our results suggest that it is possible to target progenies of a determined parental line to specific environments, and it could be as efficient as the hybrid targeting for genomic prediction in multi-environmental trials. However, it is important to the clarify that,

some families (progeny of a specific inbred line) should be evaluated in all or most of the environments. It creates a connection among different trials, and this information will be borrowed in the genomic prediction process. Unfortunately, in our dataset, the inbred lines did not show a clear pattern of distribution across environments regarding the mean of their progenies, once the large proportion of them was grouped around the origin (Figure 9). Thus, as there was not an evident parent x environment stratification, to test this hypothesis we randomly sample families across environments. Nevertheless, further studies are necessary for the development of methods towards targeting families in multi-environment trials net in genomic prediction programs.

3.4.2. The inclusion of dominance effects for hybrid prediction under multiple environments

Modeling dominance effects in a genomic prediction framework can provide an increase on the prediction accuracy for those traits in which dominance effects are expected to play an important role in the phenotypic expression (Almeida Filho et al. 2016; Heidaritabar et al. 2016), which is a consensus for grain yield in maize. In our study, we showed the importance of modeling dominance effects under multi-environmental trials where several scenarios of G×E interaction complexity were explored. Our findings indicated that dominance effect largely interacts with the environments. The interaction of additive and non-additive genetic effects, especially dominance, with environments are known in QTL mapping studies (Liu et al. 2008; Shang et al. 2016), and recently was modeled into genomic prediction models (Acosta-Pech et al. 2017; Dias et al. 2018). The occurrence of dominance by environment interaction and the importance of main dominance effects for the phenotypic variation in maize suggest that these effects must be taken into account when predicting hybrids in multi-environment trials.

We observed a significant influence of non-additive effects for hybrid variation (Figure 2). Interestingly, the importance of dominance effects and its interactions on the phenotypic variation increased according to the complexity of the G×E. The opposite occurred for the additive effects (main and interactions effects).It suggests that the selection of specific combinations (hybrids) can be useful for each environment within scenario (Dhillon et al. 1990; Melchinger 1999), which permits the exploitation of the heterosis by environment interaction. That is confirmed by the "smaller" importance of the additive effects, especially in low correlated environments (Figure 2). Nevertheless, the inclusion of non-additive effects in genomic models can increase the prediction accuracy, the response to selection, and enable the mating allocation

(Varona et al. 2018).

Dias et al. (2018), using factor analytical structures for modeling the G×E interaction, found a large increase on the prediction accuracy for grain yield when modeling dominance by environment interaction in comparison with the strictly additive model for both CV1 and CV2. In our study, we also observed a substantial increase in the prediction accuracy of GY when modeling dominance into a multi-environment prediction model (Figure 6, 7, and 8). However, diverging from their findings, our gain was observed mainly when the validation scheme employed was the CV2 and CV3.2. On the other hand, for CV1 and CV3.1 the increases in accuracy were relatively small. It may be explained by the fact that Dias et al. (2018) predicted hybrids obtained by crossing different heterotic groups, being expected a large influence of dominance effects and a larger number of loci in heterozygosis (Varona et al. 2018). Whereas in our study, the population is derived from an unbalanced diallel of inbred lines without a clear heterotic pattern, which suggests a lower number of loci in heterozygosis and divergence degree between lines.

In order to compare the gains when the genotype by environment effects is incorporated on the predictions, we fitted a model accounting only for the main genetic effects (MG). In this case, we expected that the difference in prediction accuracy between MGE and MG models is mainly due to the effects of modeling the marker by environment interaction. However, the differences between the models were small, indicating the gains in accuracy using a multi-environment prediction model is mostly due to the influence of the main genetic effects. Small differences in prediction accuracy between the MGE and MG models were also reported in recent studies employing multi-environment prediction models (Crossa et al. 2016; Sousa et al. 2017).

According to Crossa et al. (2016), differences between MG and MGE models are due to the importance of the variance components from marker by environment interaction, being more evident in weakly correlated environments. Hence, if the environment-specific effects are expected to play an important role in the phenotypic variation, the MGE model will perform better than the MG model. Otherwise, for moderate to highly correlated environments, models are prone to perform similarly. This trend is explicit in scenarios 6 and 8 (see Figure 2, Figure 7 C-D, Supplementary Table S1-S8), where the MGE model performed better than the MG model for environments where the interaction effects for both dominance and additive were the largest variance components.

In addition, another plausible explanation for the small differences between the MG and MGE is the model fitting. As pointed out by Goddard (2009), prediction accuracy depends on

the balance between the proportion of genomic variance captured by the model and the accuracy in which the effects were estimated. Thus, even fitting better the data (more genomic variance recovered), the MGE model might show similar or lower prediction accuracies than the MG model due to less certainly estimation of the marker by environment effects. Furthermore, for both models, we considered heterogeneous residual variance among the environments which may be another explanation for the small differences in observed prediction accuracy between the two model.

3.4.3. Relationship between G×E magnitude and prediction accuracy

We stratified our dataset in eight different scenarios differing in their G×E magnitude. A clear linear relation between prediction accuracy and the G×E complexity (reflected by the s estimates) was found. According to several authors, the MGE model demands positive correlations among environments to perform better than single environment analyses (Crossa et al. 2017). In this case, under low degrees of G×E interaction (intermediate to high correlated environments), the main genetic effects are the most important on the prediction accuracy (Lopez-Cruz et al. 2015; Crossa et al. 2016; Cuevas et al. 2016; Sousa et al. 2017). Comparing scenarios (Figure 4 and 5), one can observe a consistent increase in prediction accuracy due to the correlation among environments within scenarios (Table 1 and 2). Moreover, the importance of main genetic effects decreases according to the G×E magnitude (Figure 2).

We observed a high increase on the prediction accuracy for the environments represented in scenarios 6 when the same environments were predicted in scenarios 7, 8, and 1 (Figure 7:A-D). The increases where more pronounced for CV2 and CV3.2, whereas for CV1 and CV3.1 the gains were small. This result was expected, once the increase in the number of environments (even with positive low correlated trials) is advantageous for CV2 and CV3.2. For these validation schemes, the model recovers the information based on the pairwise correlation between environments and the genetic covariance between training and testing set (Burgueño et al. 2012; Dias et al. 2018). On the other hand, the same trend was not observed for CV1 and CV3.1 Probably, because the information recovered by the model is based only on the genetic relationship between the hybrids/families used to training the model and those present on the candidate population (testing set). It suggests that grouping low to moderate positive correlated environments for the prediction of new materials/ families can be advantageous when employing the CV2 and CV3.2, even if these environments belong to different mega-environments.

3.4.4. Correlation of genetic effects between environments

Weak to moderate genomic correlation estimates among environments within scenario for both additive and dominance effects, and total genomic variance recovered by the model were found (Supplementary Tables S9-S11). In the MGE model, the main genetic effects represent the genetic covariance among the environments and stable effects (Lopez-Cruz et al. 2015; Cuevas et al. 2016; Sousa et al. 2017). Thus, an increase in genomic variance explained by the main genetic effects from the model will induce highest correlation estimates. Therefore, for environments with moderate to strong correlations, the preponderance of main effects over the interaction effects will lead to predicted values with high stability among the group of environments. This is evident by the comparison of p estimated for the environments within each scenario, especially when we contrast genetic values obtained in the strictly additive and the additive plus dominance models (Supplementary Tables S9-S11). In this case, modeling dominance considerably increase the total genomic variance recovered by the model, boosting p estimates, and then making the prediction among environments more similar.

Correlation estimates of additive and dominance effects largely vary according to the evaluated scenario. As expected for scenarios showing a small contribution of G×E for the phenotypic variation, the correlation was always superior to ~0.68 and 70 for additive and dominance effects, respectively. For scenarios where s was small (larger G×E interaction contribution) the correlations among the genetic effects were smaller than the former, showing values ranging from ~0.4 to 0.65 and 0.~65 to 0.74 for additive and dominance effects, respectively. Recently, Dias et al. (2018) observed more substantial dominance than additive correlations for grain yield in maize hybrids grown under water-stressed environments, suggesting that dominance contribute more to the G×E interaction than additive effects. Opposing to their findings, our results clearly indicate that additive interacts more with the environment than dominance effects.

3.5. Conclusions

In our study, we showed the importance of modeling additive and dominance effects, and its interactions with the environment, for hybrid prediction in multi-environment trials to increase the prediction accuracy of non-tested hybrids. Moreover, we showed the linear dependency of the MGE model to positive correlations among environments, and that reducing the G×E's there is an increasing in the prediction accuracy. Furthermore, the prediction accuracy

of hybrids in low correlated environments employing the MGE model can be increased through the inclusion of additional phenotypic information from other positive correlated trials.

Most studies in hybrids prediction consider the CV1 and CV2 as the main problem to predict hybrids in multi-environment trials (Acosta-Pech et al. 2017; Dias et al. 2018). Here, we evaluated the prediction accuracy of genomic models in which half-families were not evaluated in any or at least one environment. The results suggest that the evaluation of half-sib families in at least one location in a multi-environment trials net could lead to prediction accuracies similar to those observed in CV2. It has interesting implications, once the breeder can plan the trials to increase the prediction accuracy of non-tested families, targeting specific families for particular environments, raising the total number of families tested and reducing costs. Even though, further studies must be done to determine the best strategies for targeting families based on the parents x environment interaction.

REFERENCES

Acosta-Pech R, Crossa J, de los Campos G, et al (2017) Genomic models with genotype × environment interaction for predicting hybrid performance: an application in maize hybrids. Theor Appl Genet 130:1431–1440. doi: 10.1007/s00122-017-2898-0

Albrecht T, Wimmer V, Auinger H-J, et al (2011) Genome-based prediction of testcross values in maize. Theor Appl Genet 123:339–350. doi: 10.1007/s00122-011-1587-7

Almeida Filho JE, Guimarães JFR, e Silva FF, et al (2016) The contribution of dominance to phenotype prediction in a pine breeding and simulated population. Heredity (Edinb) 117:33–41. doi: 10.1038/hdy.2016.23

Bernardo R (2010) Breeding for quantitative traits, 2nd edn. Stemma Press, Woodbury

Browning BL, Browning SR (2016) Genotype Imputation with Millions of Reference Samples. Am J Hum Genet 98:116–126. doi: 10.1016/j.ajhg.2015.11.020

Burgueño J, de los Campos G, Weigel K, Crossa J (2012) Genomic prediction of breeding values when modeling genotype × environment interaction using pedigree and dense molecular markers. Crop Sci 52:707. doi: 10.2135/cropsci2011.06.0299

Crossa J (2012) From genotype × environment interaction to gene × environment interaction. Curr Genomics 13:225–44. doi: 10.2174/138920212800543066

Crossa J, Cornelius PL (1997) Sites regression and shifted multiplicative model clustering of cultivar trial sites under heterogeneity of error variances. Crop Sci 37:406–415. doi: 10.2135/cropsci1997.0011183X003700020017x

Crossa J, De Los Campos G, Maccaferri M, et al (2016) Extending the marker × Environment interaction model for genomic-enabled prediction and genome-wide association analysis in durum wheat. Crop Sci 56:2193–2209. doi: 10.2135/cropsci2015.04.0260

Crossa J, Pérez-Rodríguez P, Cuevas J, et al (2017) Genomic Selection in Plant Breeding: Methods, Models, and Perspectives. Trends Plant Sci 22:961–975. doi: 10.1016/j.tplants.2017.08.011

Cuevas J, Crossa J, Soberanis V, et al (2016) Genomic Prediction of Genotype × Environment Interaction Kernel Regression Models. Plant Genome 9:. doi: 10.3835/plantgenome2016.03.0024

Dhillon BS, Gurrath PA, Zimmer E, et al (1990) Analysis of diallel crosses of maize for variation and covariation in agronomic traits at silage and grain harvests. Maydica 35:297–302

Dias KODG, Gezan SA, Guimarães CT, et al (2018) Improving accuracies of genomic predictions for drought tolerance in maize by joint modeling of additive and dominance effects in multi-environment trials. Heredity (Edinb). doi: 10.1038/s41437-018-0053-6

Dumble S (2017) GGEBiplots: GGE Biplots with "ggplot2." R Packag version 011

Federer WT (1961) Augmented Designs with One-Way Elimination of Heterogeneity. Biometrics 17:447–473. doi: 10.2307/2527837

Flatt JP (1992) Body weight, fat storage, and alcohol metabolism. Nutr Rev 50:267–70. doi: 10.1186/1297-9686-33-6-605

Fritsche-Neto R, Akdemir D, Jannink J-L (2018) Accuracy of genomic selection to predict maize single-crosses obtained through different mating designs. Theor Appl Genet. doi: 10.1007/s00122-018-3068-8

Gauch HG (2006) Statistical Analysis of Yield Trials by AMMI and GGE. Crop Sci 46:1488–1500

Goddard M (2009) Genomic selection: prediction of accuracy and maximisation of long term response. Genetica 136:245–257. doi: 10.1007/s10709-008-9308-0

Heidaritabar M, Wolc A, Arango J, et al (2016) Impact of fitting dominance and additive effects on accuracy of genomic prediction of breeding values in layers. J Anim Breed Genet 133:334–346. doi: 10.1111/jbg.12225

Heslot N, Akdemir D, Sorrells ME, Jannink JL (2014) Integrating environmental covariates and crop modeling into the genomic selection framework to predict genotype by environment interactions. Theor. Appl. Genet. 127:1–18

Heslot N, Jannink J, Sorrells ME (2015) Perspectives for genomic selection applications and research in plants. Crop Sci 55:1–30. doi: 10.2135/cropsci2014.03.0249

Jarquín D, Crossa J, Lacaze X, et al (2014) A reaction norm model for genomic selection using high-dimensional genomic and environmental data. Theor Appl Genet 127:595–607. doi: 10.1007/s00122-013-2243-1

Kadam DC, Potts SM, Bohn MO, et al (2016) Genomic prediction of single crosses in the early stages of a maize hybrid breeding pipeline. G3:Genes|Genomes|Genetics 6:3443–3453. doi: 10.1534/g3.116.031286

Lado B, Barrios PG, Quincke M, et al (2016) Modeling genotype × Environment interaction for genomic selection with unbalanced data from a wheat breeding program. Crop Sci 56:2165–2179. doi: 10.2135/cropsci2015.04.0207

Liu G, Zhang Z, Zhu H, et al (2008) Detection of QTLs with additive effects and additive-by-environment interaction effects on panicle number in rice (Oryza sativa L.) with single-segment substitution lines. Theor Appl Genet 116:923–931. doi: 10.1007/s00122-008-0724-4

Lopez-Cruz M, Crossa J, Bonnett D, et al (2015) Increased Prediction Accuracy in Wheat Breeding Trials Using a Marker × Environment Interaction Genomic Selection Model. G3 Genes|Genomes|Genetics 5:569–582. doi: 10.1534/g3.114.016097

Melchinger AE (1999) Genetic diversity and heterosis. In: Coors J., Pandey S (eds) The genetics and exploitation of heterosis in crops. American Society of Agronomy, Crop Science Society of America and Soil Science Society of America, Madson, pp 99–118

Mendonça L de F, Granato ÍSC, Alves FC, et al (2017) Accuracy and simultaneous selection gains for N-stress tolerance and N-use efficiency in maize tropical lines. Sci Agric 74:481–488. doi: 10.1590/1678-992x-2016-0313

Meuwissen TH, Hayes BJ, Goddard ME (2001) Prediction of total genetic value using genome-wide dense marker maps. Genetics 157:1819–1829

Moehring J, Williams ER, Piepho H (2014) Efficiency of augmented p-rep designs in multi-environmental trials. Theor Appl Genet 127:1049–1060. doi: 10.1007/s00122-014-2278-y

Pérez P, De Los Campos G (2014) Genome-wide regression and prediction with the BGLR statistical package. Genetics 198:483–495. doi: 10.1534/genetics.114.164442

Saint Pierre C, Burgueño J, Crossa J, et al (2016) Genomic prediction models for grain yield of spring bread wheat in diverse agro-ecological zones. Sci Rep 6:1–11. doi: 10.1038/srep27312

Shang L, Liang Q, Wang Y, et al (2016) Epistasis together with partial dominance, over-

dominance and QTL by environment interactions contribute to yield heterosis in upland cotton. Theor Appl Genet 129:1429–1446. doi: 10.1007/s00122-016-2714-2

Sousa MB e, Cuevas J, Couto EG de O, et al (2017) Genomic-enabled prediction in maize using kernel models with genotype x environment interaction. G3 Genes|Genomes|Genetics 7:1995–2014. doi: 10.1534/g3.117.042341

Technow F, Riedelsheimer C, Schrag TA, Melchinger AE (2012) Genomic prediction of hybrid performance in maize with models incorporating dominance and population specific marker effects. Theor Appl Genet 125:1181–1194. doi: 10.1007/s00122-012-1905-8

Technow F, Schrag TA, Schipprack W, et al (2014) Genome properties and prospects of genomic prediction of hybrid performance in a breeding program of maize. Genetics 197:1343–1355. doi: 10.1534/genetics.114.165860

Unterseer S, Bauer E, Haberer G, et al (2014) A powerful tool for genome analysis in maize: development and evaluation of the high density 600 k SNP genotyping array. BMC Genomics 15:823. doi: 10.1186/1471-2164-15-823

Varona L, Legarra A, Toro MA, Vitezica ZG (2018) Non-additive Effects in Genomic Selection. Front Genet 9:. doi: 10.3389/fgene.2018.00078

Vitezica ZG, Varona L, Legarra A (2013) On the additive and dominant variance and covariance of individuals within the genomic selection scope. Genetics 195:1223–1230. doi: 10.1534/genetics.113.155176

Wimmer V, Albrecht T, Auinger H-J, Schön C-C (2012) synbreed: a framework for the analysis of genomic prediction data using R. Bioinformatics 28:2086–2087

Windhausen VS, Atlin GN, Hickey JM, et al (2012) Effectiveness of Genomic Prediction of Maize Hybrid Performance in Different Breeding Populations and Environments. G3 Genes|Genomes|Genetics 2:1427–1436. doi: 10.1534/g3.112.003699

Yan W (2001) GGEbiplot - A windows application for graphical analysis of multienvironment trial data and other types of two-way data. Agron J 93:1111–1118. doi: 10.2134/agronj2001.9351111x

Zhang X, Pérez-Rodríguez P, Semagn K, et al (2014) Genomic prediction in biparental tropical maize populations in water-stressed and well-watered environments using low-density and GBS SNPs. Heredity (Edinb) 114:291–299. doi: 10.1038/hdy.2014.99

Zhao Y, Li Z, Liu G, et al (2015) Genome-based establishment of a high-yielding heterotic pattern for hybrid wheat breeding. Proc Natl Acad Sci 112:201514547. doi: 10.1073/pnas.1514547112

Zheng X, Levine D, Shen J, et al (2012) A high-performance computing toolset for relatedness and principal component analysis of SNP data. Bioinformatics 28:3326–3328

TABLES

Table 1. Spearman's correlations for Scenario 1

	1.PI.IN	1.AN.LN	1.AN.IN	2.PI.LN	2.PI.IN	2.AN.LN	2.AN.IN
1_PI_LN	0.50	0.28	0.37	0.29	0.33	0.24	0.32
1_PI_IN	-	0.31	0.42	0.34	0.36	0.27	0.29
1_AN_LN		-	0.45	0.27	0.30	0.32	0.31
1_AN_IN			-	0.27	0.34	0.32	0.37
2_PI_LN				-	0.47	0.36	0.36
2_PI_IN					-	0.33	0.38
2_AN_LN						-	0.43

Table 2. Spearman's correlation coefficient for scenarios 2, 3, 4, and 5

	Scenario 2			Scenario 3		Scenario 4		Scenario 5	
	PI.IN	**AN.LN**	**AN.IN**		**Year 2**		**LN**		**PI**
PI.LN	0.60	0.44	0.48	**Year 1**	0.53	**IN**	0.68	**AN**	0.58
PI.IN	-	0.44	0.51						
AN.LN		-	0.55						

Table 3. Tested scenarios, number of environments and mean Spearman's correlation among its environments

Scenarios	nE*	*s*[1]
1- General	8	0.34
2- NxS	4	0.50
3- Year	2	0.53
4- N	2	0.68
5- Site	2	0.58
6- Less Related	2	0.32
7- Mega	6	0.35
8- Representative	3	0.33

*number of environments

[1]Mean Spearman's correlation between constituent environments

Table 4. Genomic correlations of common environments in Scenarios 1, 6 and 8.

Correlations of genetic values estimated from the additive and additive-dominance models among environments (upper and low diagonal, respectively)									
	Scenario 6			**Scenario 8**			**Scenario 1**		
	1.PI_LN	2.AN.LN	2.AN.IN	1.PI.LN	2.AN.LN	2.AN.IN	1.PI.LN	2.AN.LN	2.AN.IN
1.PI.LN	-	-	0.45	-	0.52	0.50	-	0.58	0.57
2.AN.LN	-	-	-	0.63	-	0.53	0.70	-	0.59
2.AN.IN	0.57	-	-	0.61	0.65	-	0.69	0.70	-
Correlations of additive and dominance effects among environments (upper and low diagonal, respectively)									
	Scenario 6			**Scenario 8**			**Scenario 1**		
	1.PI_LN	2.AN.LN	2.AN.IN	1.PI.LN	2.AN.LN	2.AN.IN	1.PI.LN	2.AN.LN	2.AN.IN
1.PI_LN	-	-	0.45	-	0.49	0.46	-	0.66	0.65
2.AN.LN	-	-	-	0.72	-	0.51	0.70	-	0.67
2.AN.IN	0.65	-	-	0.72	0.74	-	0.70	0.72	-

Table 5. Prediction bias for Scenarios 2, 3, 4 and 5.

		Scenario 2				Scenario 3		Scenario 4		Scenario 5	
CV	**Model**	**PI.LN**	**PI.IN**	**AN.LN**	**AN.IN**	**1**	**2**	**LN**	**IN**	**PI**	**AN**
CV1	A	$0.899^{\pm0.145}$	$0.945^{\pm0.114}$	$0.866^{\pm0.132}$	$0.955^{\pm0.122}$	$0.947^{\pm0.145}$	$0.979^{\pm0.132}$	$0.919^{\pm0.129}$	$0.961^{\pm0.139}$	$0.958^{\pm0.139}$	$0.97^{\pm0.113}$
	AD	$0.794^{\pm0.119}$	$0.891^{\pm0.095}$	$0.762^{\pm0.15}$	$0.859^{\pm0.104}$	$0.891^{\pm0.136}$	$0.924^{\pm0.112}$	$0.801^{\pm0.143}$	$0.875^{\pm0.124}$	$0.889^{\pm0.114}$	$0.873^{\pm0.119}$
CV2	A	$0.935^{\pm0.139}$	$0.969^{\pm0.098}$	$0.872^{\pm0.132}$	$0.976^{\pm0.111}$	$0.969^{\pm0.139}$	$1.001^{\pm0.112}$	$0.958^{\pm0.126}$	$0.998^{\pm0.113}$	$0.981^{\pm0.136}$	$0.999^{\pm0.116}$
	AD	$0.972^{\pm0.089}$	$0.995^{\pm0.056}$	$0.909^{\pm0.09}$	$0.999^{\pm0.061}$	$1.008^{\pm0.118}$	$1.015^{\pm0.094}$	$0.994^{\pm0.125}$	$1.031^{\pm0.087}$	$1.013^{\pm0.093}$	$1.011^{\pm0.096}$
CV3.1	A	$0.872^{\pm0.206}$	$0.961^{\pm0.191}$	$0.793^{\pm0.198}$	$0.882^{\pm0.213}$	$0.876^{\pm0.212}$	$0.95^{\pm0.203}$	$0.858^{\pm0.208}$	$0.919^{\pm0.208}$	$0.955^{\pm0.214}$	$0.893^{\pm0.202}$
	AD	$0.823^{\pm0.202}$	$0.934^{\pm0.195}$	$0.744^{\pm0.248}$	$0.794^{\pm0.155}$	$0.849^{\pm0.205}$	$0.937^{\pm0.201}$	$0.807^{\pm0.254}$	$0.866^{\pm0.188}$	$0.934^{\pm0.207}$	$0.828^{\pm0.192}$
CV3.2	A	$1.01^{\pm0.165}$	$1.07^{\pm0.14}$	$0.933^{\pm0.179}$	$1.031^{\pm0.176}$	$0.995^{\pm0.185}$	$1.052^{\pm0.182}$	$1.05^{\pm0.165}$	$1.121^{\pm0.157}$	$1.062^{\pm0.189}$	$1.051^{\pm0.171}$
	AD	$1.008^{\pm0.115}$	$1.048^{\pm0.09}$	$0.923^{\pm0.168}$	$1.012^{\pm0.09}$	$1.011^{\pm0.16}$	$1.075^{\pm0.179}$	$1.072^{\pm0.199}$	$1.126^{\pm0.128}$	$1.072^{\pm0.137}$	$1.037^{\pm0.132}$

Table 6. Prediction bias for Scenarios 6, 7, and 8.

		Scenario 6		Scenario 8			Scenario 7					
CV	**Model**	**1.PI.LN**	**2.AN.IN**	**1.PI.LN**	**2.AN.LN**	**2.AN.IN**	**1.PI.LN**	**1.PI.IN**	**1.AN.LN**	**1.AN.IN**	**2.PI.LN**	**2.PI.IN**
CV1	A	$0.904^{\pm0.208}$	$0.94^{\pm0.159}$	$0.876^{\pm0.195}$	$0.896^{\pm0.176}$	$0.926^{\pm0.148}$	$0.84^{\pm0.176}$	$0.89^{\pm0.145}$	$0.822^{\pm0.177}$	$0.969^{\pm0.135}$	$0.926^{\pm0.147}$	$0.959^{\pm0.112}$
	AD	$0.823^{\pm0.174}$	$0.897^{\pm0.125}$	$0.802^{\pm0.165}$	$0.848^{\pm0.168}$	$0.877^{\pm0.115}$	$0.762^{\pm0.15}$	$0.871^{\pm0.115}$	$0.692^{\pm0.163}$	$0.877^{\pm0.117}$	$0.844^{\pm0.114}$	$0.907^{\pm0.088}$
CV2	A	$0.923^{\pm0.208}$	$0.98^{\pm0.142}$	$0.902^{\pm0.193}$	$0.933^{\pm0.176}$	$0.963^{\pm0.132}$	$0.881^{\pm0.177}$	$0.923^{\pm0.147}$	$0.819^{\pm0.155}$	$0.976^{\pm0.133}$	$0.965^{\pm0.136}$	$0.983^{\pm0.125}$
	AD	$0.927^{\pm0.181}$	$0.985^{\pm0.125}$	$0.903^{\pm0.158}$	$0.947^{\pm0.151}$	$1.012^{\pm0.104}$	$0.973^{\pm0.127}$	$1.027^{\pm0.097}$	$0.853^{\pm0.109}$	$0.987^{\pm0.083}$	$0.918^{\pm0.09}$	$0.939^{\pm0.082}$
CV3.1	A	$0.844^{\pm0.275}$	$0.881^{\pm0.248}$	$0.818^{\pm0.263}$	$0.819^{\pm0.235}$	$0.875^{\pm0.241}$	$0.795^{\pm0.237}$	$0.889^{\pm0.204}$	$0.757^{\pm0.222}$	$0.883^{\pm0.221}$	$0.858^{\pm0.217}$	$1^{\pm0.199}$
	AD	$0.829^{\pm0.227}$	$0.864^{\pm0.203}$	$0.808^{\pm0.215}$	$0.847^{\pm0.279}$	$0.842^{\pm0.194}$	$0.766^{\pm0.203}$	$0.876^{\pm0.219}$	$0.638^{\pm0.24}$	$0.797^{\pm0.183}$	$0.841^{\pm0.229}$	$0.987^{\pm0.182}$
CV3.2	A	$0.927^{\pm0.271}$	$0.955^{\pm0.208}$	$0.89^{\pm0.26}$	$1.034^{\pm0.228}$	$1.03^{\pm0.242}$	$0.918^{\pm0.201}$	$0.987^{\pm0.185}$	$0.848^{\pm0.205}$	$1^{\pm0.191}$	$0.961^{\pm0.176}$	$1.08^{\pm0.172}$
	AD	$0.957^{\pm0.215}$	$0.968^{\pm0.197}$	$0.903^{\pm0.198}$	$1.071^{\pm0.201}$	$1.053^{\pm0.171}$	$0.99^{\pm0.129}$	$1.066^{\pm0.123}$	$0.849^{\pm0.145}$	$0.997^{\pm0.103}$	$0.904^{\pm0.119}$	$0.986^{\pm0.097}$

Table 7. Prediction bias for Scenario 1

		Scenario 1							
CV	**Model**	**1.PI.LN**	**1.PI.IN**	**1.AN.LN**	**1.AN.IN**	**2.PI.LN**	**2.PI.IN**	**2.AN.LN**	**2.AN.IN**
CV1	A	$0.833^{\pm 0.174}$	$0.879^{\pm 0.144}$	$0.814^{\pm 0.17}$	$0.963^{\pm 0.132}$	$0.923^{\pm 0.145}$	$0.955^{\pm 0.111}$	$0.847^{\pm 0.154}$	$0.89^{\pm 0.139}$
	AD	$0.751^{\pm 0.152}$	$0.864^{\pm 0.121}$	$0.688^{\pm 0.163}$	$0.877^{\pm 0.119}$	$0.834^{\pm 0.113}$	$0.906^{\pm 0.09}$	$0.8^{\pm 0.159}$	$0.835^{\pm 0.107}$
CV2	A	$0.875^{\pm 0.172}$	$0.911^{\pm 0.145}$	$0.816^{\pm 0.149}$	$0.974^{\pm 0.131}$	$0.966^{\pm 0.136}$	$0.981^{\pm 0.121}$	$0.865^{\pm 0.157}$	$0.953^{\pm 0.137}$
	AD	$0.965^{\pm 0.123}$	$1.007^{\pm 0.087}$	$0.858^{\pm 0.105}$	$0.981^{\pm 0.084}$	$0.936^{\pm 0.081}$	$0.946^{\pm 0.082}$	$0.897^{\pm 0.107}$	$0.982^{\pm 0.089}$
CV3.1	A	$0.784^{\pm 0.238}$	$0.877^{\pm 0.206}$	$0.749^{\pm 0.219}$	$0.877^{\pm 0.216}$	$0.852^{\pm 0.216}$	$0.993^{\pm 0.202}$	$0.781^{\pm 0.218}$	$0.84^{\pm 0.231}$
	AD	$0.759^{\pm 0.203}$	$0.871^{\pm 0.219}$	$0.632^{\pm 0.241}$	$0.798^{\pm 0.179}$	$0.84^{\pm 0.232}$	$0.987^{\pm 0.182}$	$0.813^{\pm 0.265}$	$0.797^{\pm 0.184}$
CV3.2	A	$0.886^{\pm 0.203}$	$0.943^{\pm 0.186}$	$0.843^{\pm 0.186}$	$1.003^{\pm 0.19}$	$0.983^{\pm 0.167}$	$1.086^{\pm 0.159}$	$0.929^{\pm 0.18}$	$0.973^{\pm 0.197}$
	AD	$0.969^{\pm 0.131}$	$1.023^{\pm 0.125}$	$0.853^{\pm 0.128}$	$0.997^{\pm 0.103}$	$0.952^{\pm 0.109}$	$1.008^{\pm 0.087}$	$0.934^{\pm 0.164}$	$0.979^{\pm 0.116}$

FIGURES

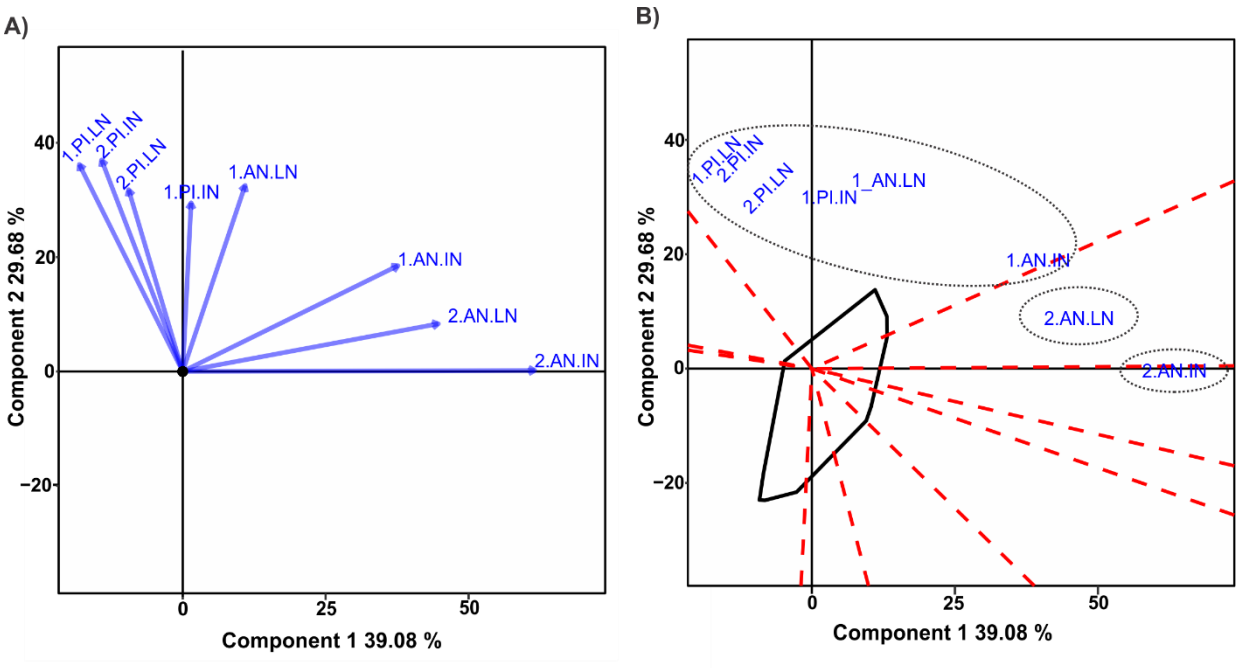

Figure 1. GGEBiplot. A) The relationship among environments; B)Which whon where of hybrids among trials. Dashed circles correspond to the identified "mega-environments."

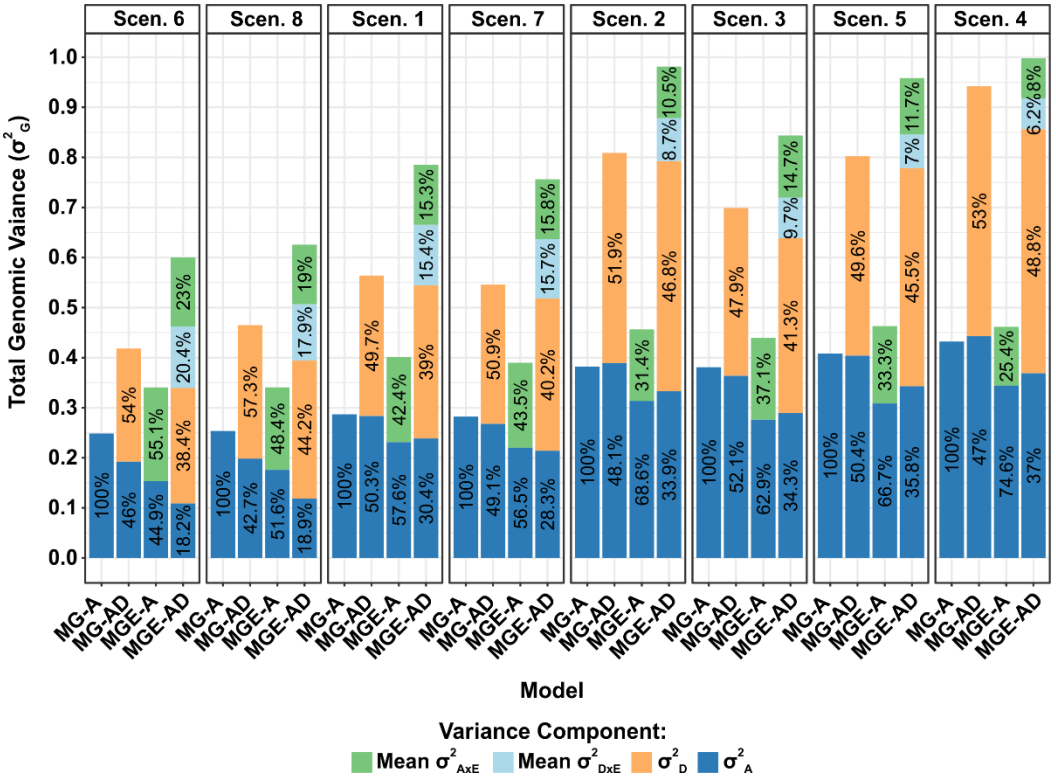

Figure 2. Contribution of main additive and dominance variance, and average additive and dominance by environment variances across environments to the total genomic variance by scenario and model. The categorical x-axis variables are organized according to the magnitude of the mean Spearman correlation of the environments within the scenario, from left to right, lowest to highest.

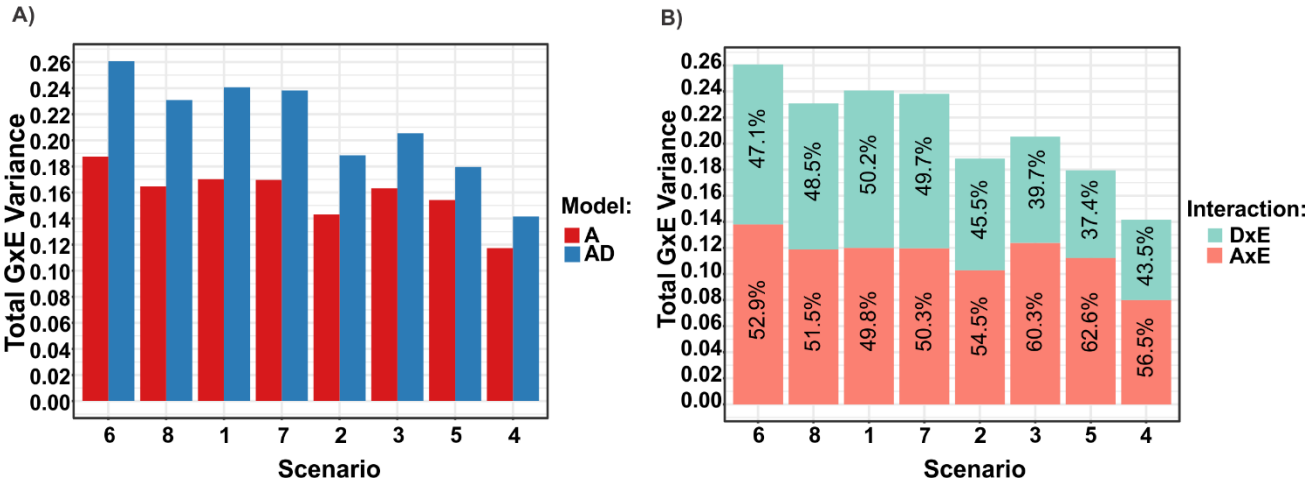

Figure 3. Barplots of $G \times E$ interactions: **A)** Total $G \times E$ interaction recovered by the additive (A) and additive-dominance model (A+D); **B)** Partition of the total $G \times E$, estimated in the additive-dominance model, into additive and dominance by environment interactions ($A \times E$ and $D \times E$, respectively). The x-axis was ordered according to the $G \times E$ magnitude, from lowest to highest average Spearman's correlation estimates.

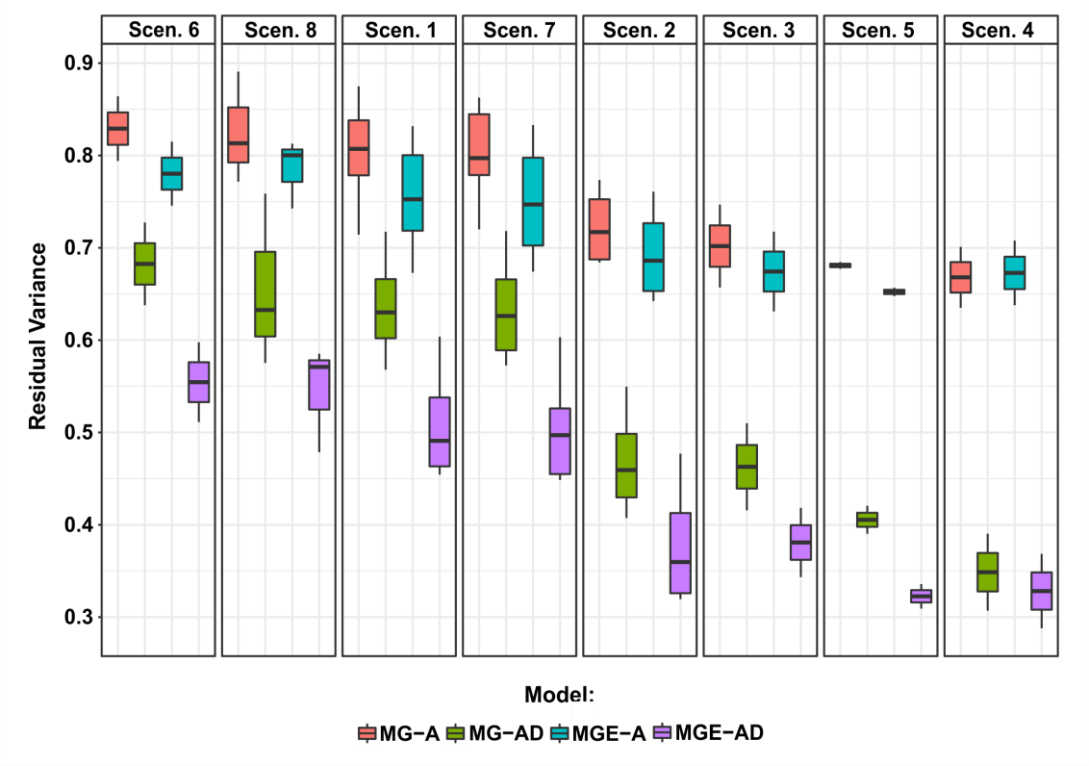

Figure 4. Boxplot of the residual variance posterior means estimated by the environment within scenario by the models (MG-A, MG-AD, MGE-A, and MGE-AD). The categorical x-axis variables are organized according to the magnitude of the mean Spearman correlation of the environments within the scenario, from left to right, lowest to highest.

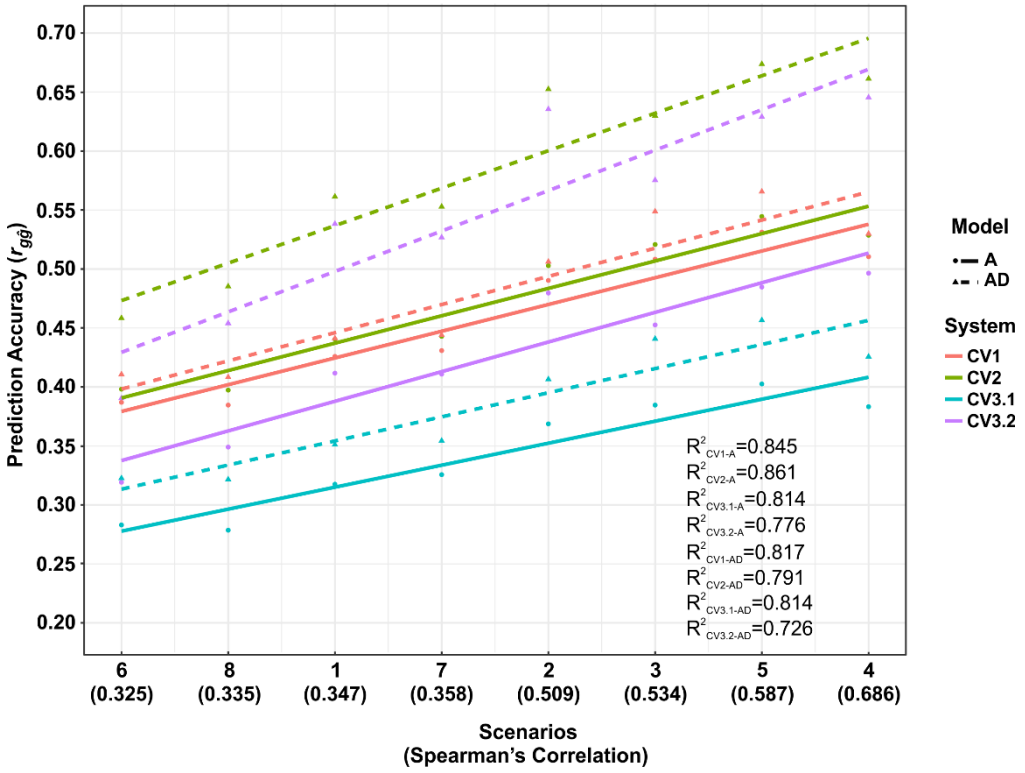

Figure 5. Mean prediction accuracy vs. scenarios for the additive (A) and additive-dominance (AD) prediction models, by validation system (CV1, CV2, CV3.1, and CV3.2) using the MGE model. The categorical x-axis variables are organized according to the magnitude of the mean Spearman correlation of the environments within the scenario, from left to right, lowest to highest.

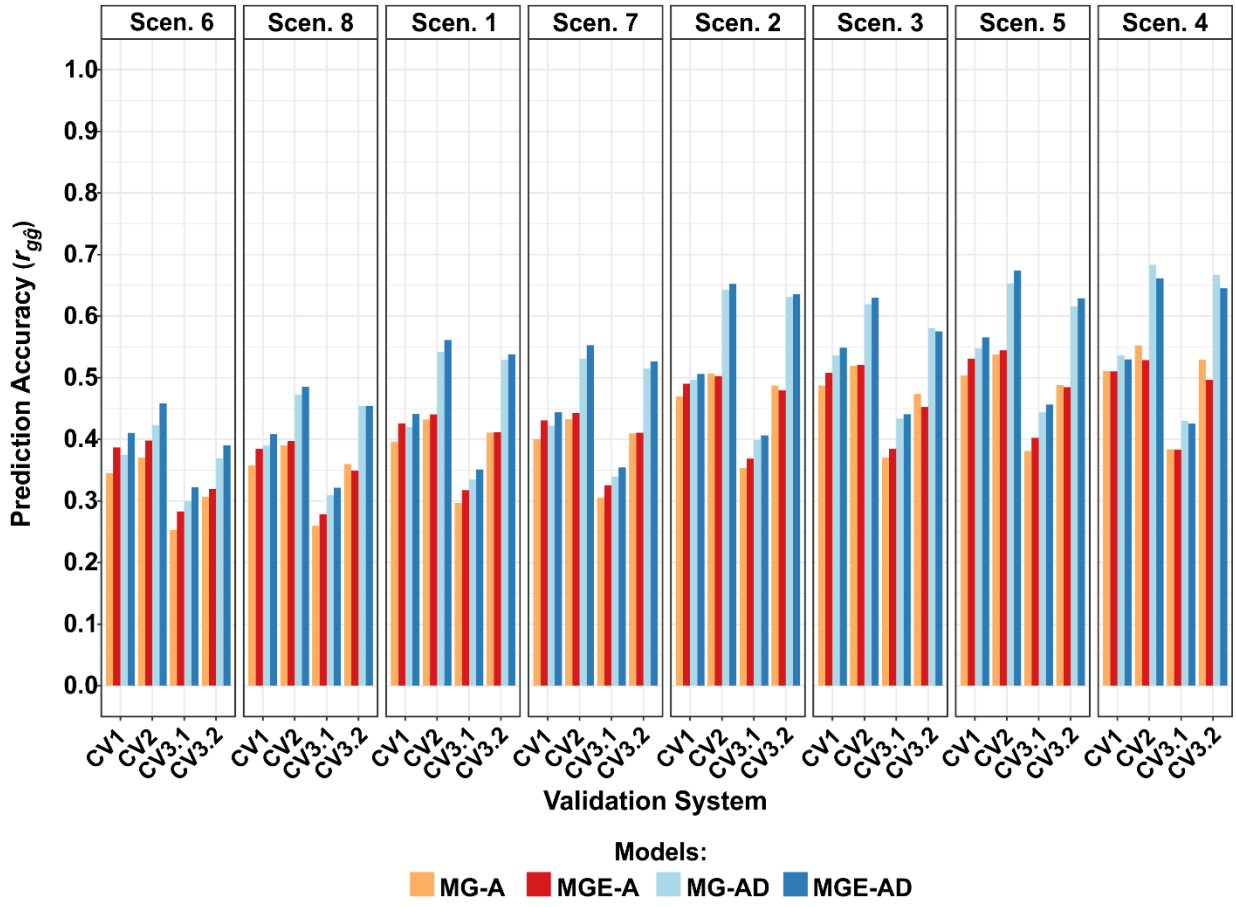

Figure 6. Mean prediction accuracy across environments within scenarios obtained in the MGE, by cross-validation scheme and model (A or A+D). The categorical x-axis variables are organized according to the magnitude of the mean Spearman correlation of the environments within the scenario, from left to right, lowest to highest.

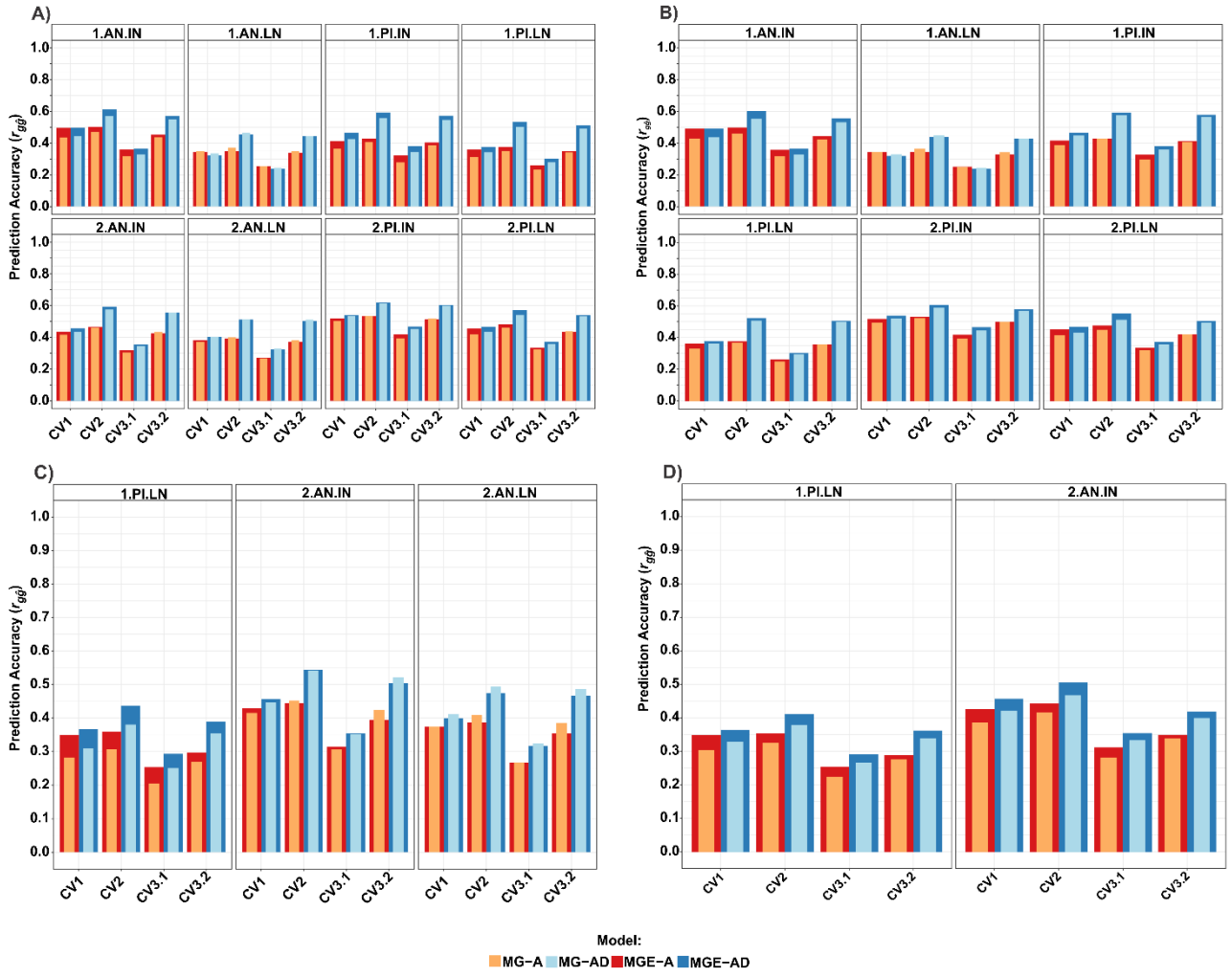

Figure 7. Mean prediction accuracy, by environments, validation system, and genomic model. A - scenario 1; B - scenario 7; C - scenario 8; D - scenario 6.

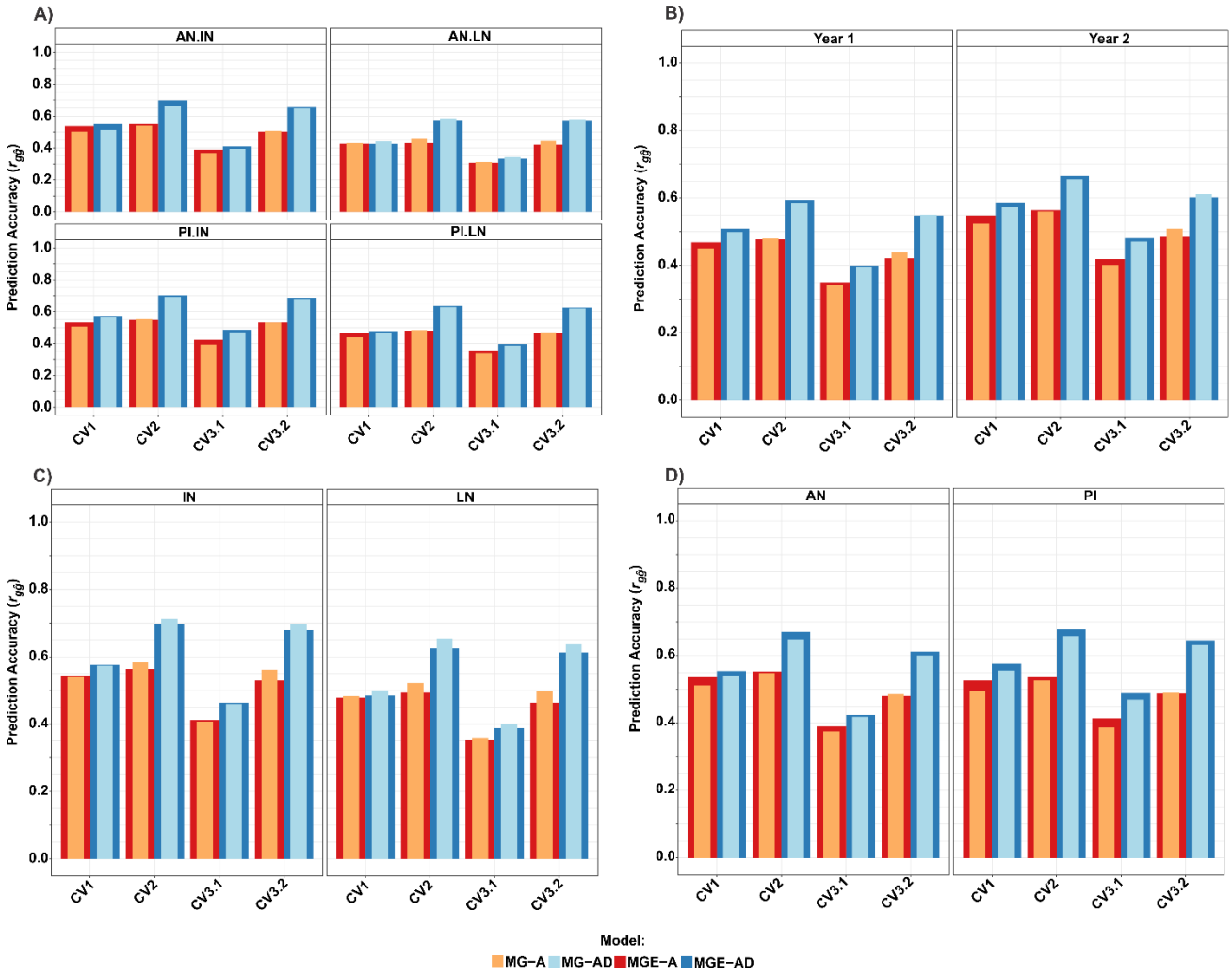

Figure 8. Mean prediction accuracy, by environments, validation system, and genomic model. A - scenario 2; B - scenario 3; C - scenario 4; D - scenario 5.

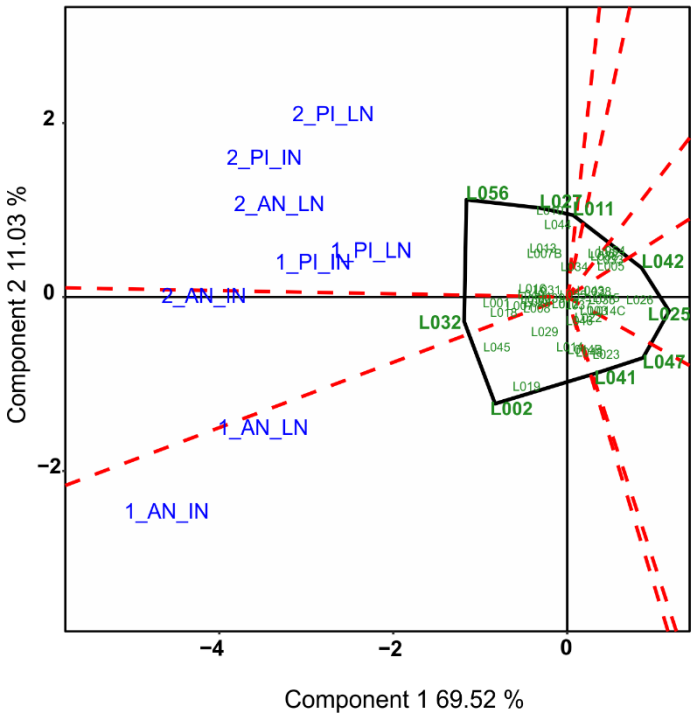

Figure 9. Which won/where of inbred lines yield based on the mean performance of hybrids for eight environments.

SUPPLEMENTARY TABLES

Table S1. Posterior means (± posterior standard deviations) of variance components, broad-sense genomic heritability (H^2), narrow-sense heritability ($\boldsymbol{h^2}$), and proportion of variance explained by the dominance effects ($\boldsymbol{d^2}$) by model (MG and MGE) for Scenario 1

		MG		MGE	
Component		**A**	**AD**	**A**	**AD**
σ^2_A		$0.287^{\pm 0.065}$	$0.284^{\pm 0.081}$	$0.231^{\pm 0.057}$	$0.239^{\pm 0.083}$
σ^2_D		-	$0.28^{\pm 0.028}$	-	$0.306^{\pm 0.03}$
$\sigma^2_{\mathrm{G\times E}}$		-	-	0.17	0.241
$\sigma^2_{\mathrm{A\times E}}$		-	-	$0.17^{\pm 0.048}$	$0.12^{\pm 0.039}$
	$\sigma^2_{\mathrm{A\times 1.PI.LN}}$	-	-	$0.18^{\pm 0.048}$	$0.126^{\pm 0.038}$
	$\sigma^2_{\mathrm{A\times 1.PI.IN}}$	-	-	$0.177^{\pm 0.048}$	$0.122^{\pm 0.038}$
	$\sigma^2_{\mathrm{A\times 1.AN.LN}}$	-	-	$0.144^{\pm 0.038}$	$0.104^{\pm 0.031}$
	$\sigma^2_{\mathrm{A\times 1.AN.IN}}$	-	-	$0.193^{\pm 0.051}$	$0.144^{\pm 0.043}$
	$\sigma^2_{\mathrm{A\times 2.PI.LN}}$	-	-	$0.186^{\pm 0.051}$	$0.131^{\pm 0.043}$
	$\sigma^2_{\mathrm{A\times 2.PI.IN}}$	-	-	$0.159^{\pm 0.041}$	$0.106^{\pm 0.031}$
	$\sigma^2_{\mathrm{A\times 2.AN.LN}}$	-	-	$0.155^{\pm 0.041}$	$0.107^{\pm 0.032}$
	$\sigma^2_{\mathrm{A\times 2.AN.IN}}$	-	-	$0.166^{\pm 0.045}$	$0.118^{\pm 0.036}$
$\sigma^2_{\mathrm{D\times E}}$		-	-	-	$0.121^{\pm 0.037}$
	$\sigma^2_{\mathrm{D\times 1.PI.LN}}$	-	-	-	$0.124^{\pm 0.036}$
	$\sigma^2_{\mathrm{D\times 1.PI.IN}}$	-	-	-	$0.136^{\pm 0.04}$
	$\sigma^2_{\mathrm{D\times 1.AN.LN}}$	-	-	-	$0.129^{\pm 0.039}$
	$\sigma^2_{\mathrm{D\times 1.AN.IN}}$	-	-	-	$0.104^{\pm 0.028}$
	$\sigma^2_{\mathrm{D\times 2.PI.LN}}$	-	-	-	$0.133^{\pm 0.039}$
	$\sigma^2_{\mathrm{D\times 2.PI.IN}}$	-	-	-	$0.106^{\pm 0.029}$
	$\sigma^2_{\mathrm{D\times 2.AN.LN}}$	-	-	-	$0.107^{\pm 0.03}$
	$\sigma^2_{\mathrm{D\times 2.AN.IN}}$	-	-	-	$0.128^{\pm 0.038}$
	$\frac{\sigma^2_D}{\sigma^2_A}$	-	0.985	-	1.28
Error					
	$\sigma^2_{\varepsilon-1.PI.LN}$	$0.772^{\pm 0.045}$	$0.603^{\pm 0.038}$	$0.694^{\pm 0.041}$	$0.454^{\pm 0.034}$
	$\sigma^2_{\varepsilon-1.PI.IN}$	$0.86^{\pm 0.05}$	$0.717^{\pm 0.045}$	$0.832^{\pm 0.049}$	$0.604^{\pm 0.046}$
	$\sigma^2_{\varepsilon-1.AN.LN}$	$0.831^{\pm 0.049}$	$0.615^{\pm 0.039}$	$0.767^{\pm 0.045}$	$0.455^{\pm 0.038}$
	$\sigma^2_{\varepsilon-1.AN.IN}$	$0.875^{\pm 0.051}$	$0.68^{\pm 0.042}$	$0.808^{\pm 0.047}$	$0.527^{\pm 0.04}$
	$\sigma^2_{\varepsilon-2.PI.LN}$	$0.781^{\pm 0.045}$	$0.6^{\pm 0.037}$	$0.738^{\pm 0.044}$	$0.475^{\pm 0.038}$
	$\sigma^2_{\varepsilon-2.PI.IN}$	$0.831^{\pm 0.049}$	$0.662^{\pm 0.04}$	$0.798^{\pm 0.047}$	$0.569^{\pm 0.04}$
	$\sigma^2_{\varepsilon-2.AN.LN}$	$0.714^{\pm 0.042}$	$0.568^{\pm 0.035}$	$0.673^{\pm 0.04}$	$0.466^{\pm 0.034}$
	$\sigma^2_{\varepsilon-2.AN.IN}$	$0.783^{\pm 0.046}$	$0.645^{\pm 0.04}$	$0.727^{\pm 0.043}$	$0.507^{\pm 0.039}$

$H^2_{1.PI.LN}$	$0.269^{\pm 0.045}$	$0.481^{\pm 0.04}$	$0.37^{\pm 0.044}$	$0.634^{\pm 0.034}$
$H^2_{1.PI.IN}$	$0.248^{\pm 0.042}$	$0.438^{\pm 0.039}$	$0.327^{\pm 0.042}$	$0.569^{\pm 0.036}$
$H^2_{1.AN.LN}$	$0.255^{\pm 0.043}$	$0.476^{\pm 0.04}$	$0.327^{\pm 0.042}$	$0.629^{\pm 0.036}$
$H^2_{1.AN.IN}$	$0.245^{\pm 0.042}$	$0.452^{\pm 0.04}$	$0.342^{\pm 0.041}$	$0.599^{\pm 0.035}$
$H^2_{2.PI.LN}$	$0.267^{\pm 0.044}$	$0.482^{\pm 0.04}$	$0.359^{\pm 0.043}$	$0.628^{\pm 0.035}$
$H^2_{2.PI.IN}$	$0.255^{\pm 0.043}$	$0.458^{\pm 0.039}$	$0.327^{\pm 0.041}$	$0.569^{\pm 0.035}$
$H^2_{2.AN.LN}$	$0.284^{\pm 0.046}$	$0.496^{\pm 0.039}$	$0.363^{\pm 0.044}$	$0.618^{\pm 0.035}$
$H^2_{2.AN.IN}$	$0.266^{\pm 0.044}$	$0.464^{\pm 0.039}$	$0.352^{\pm 0.043}$	$0.607^{\pm 0.035}$
$h^2_{1.PI.LN}$	$0.269^{\pm 0.045}$	$0.24^{\pm 0.052}$	$0.37^{\pm 0.044}$	$0.289^{\pm 0.052}$
$h^2_{1.PI.IN}$	$0.248^{\pm 0.042}$	$0.219^{\pm 0.049}$	$0.327^{\pm 0.042}$	$0.254^{\pm 0.048}$
$h^2_{1.AN.LN}$	$0.255^{\pm 0.043}$	$0.238^{\pm 0.052}$	$0.327^{\pm 0.042}$	$0.275^{\pm 0.052}$
$h^2_{1.AN.IN}$	$0.245^{\pm 0.042}$	$0.225^{\pm 0.05}$	$0.342^{\pm 0.041}$	$0.287^{\pm 0.05}$
$h^2_{2.PI.LN}$	$0.267^{\pm 0.044}$	$0.24^{\pm 0.052}$	$0.359^{\pm 0.043}$	$0.285^{\pm 0.052}$
$h^2_{2.PI.IN}$	$0.255^{\pm 0.043}$	$0.229^{\pm 0.05}$	$0.327^{\pm 0.041}$	$0.257^{\pm 0.049}$
$h^2_{2.AN.LN}$	$0.284^{\pm 0.046}$	$0.247^{\pm 0.053}$	$0.363^{\pm 0.044}$	$0.279^{\pm 0.053}$
$h^2_{2.AN.IN}$	$0.266^{\pm 0.044}$	$0.232^{\pm 0.051}$	$0.352^{\pm 0.043}$	$0.272^{\pm 0.051}$
$d^2_{1.PI.LN}$	-	$0.241^{\pm 0.027}$	-	$0.345^{\pm 0.037}$
$d^2_{1.PI.IN}$	-	$0.22^{\pm 0.024}$	-	$0.315^{\pm 0.034}$
$d^2_{1.AN.LN}$	-	$0.239^{\pm 0.026}$	-	$0.354^{\pm 0.038}$
$d^2_{1.AN.IN}$	-	$0.226^{\pm 0.025}$	-	$0.312^{\pm 0.033}$
$d^2_{2.PI.LN}$	-	$0.242^{\pm 0.027}$	-	$0.343^{\pm 0.037}$
$d^2_{2.PI.IN}$	-	$0.23^{\pm 0.025}$	-	$0.312^{\pm 0.032}$
$d^2_{2.AN.LN}$	-	$0.249^{\pm 0.027}$	-	$0.338^{\pm 0.035}$
$d^2_{2.AN.IN}$	-	$0.233^{\pm 0.025}$	-	$0.335^{\pm 0.035}$

Table S2. Posterior means (± posterior standard deviations) of variance components, broad-sense genomic heritability (H^2), narrow-sense heritability ($\boldsymbol{h^2}$), and proportion of variance explained by the dominance effects ($\boldsymbol{d^2}$) by model (MG and MGE) for Scenario 2

	MG		MGE	
Component	**A**	**AD**	**A**	**AD**
σ^2_A	$0.382^{\pm 0.089}$	$0.389^{\pm 0.115}$	$0.313^{\pm 0.08}$	$0.333^{\pm 0.116}$
σ^2_D	-	$0.42^{\pm 0.043}$	-	$0.46^{\pm 0.046}$
$\sigma^2_{\mathrm{G\times E}}$			0.143	0.189
$\sigma^2_{\mathrm{A\times E}}$	-	-	$0.143^{\pm 0.042}$	$0.103^{\pm 0.035}$
$\sigma^2_{\mathrm{A\times PI.LN}}$	-	-	$0.141^{\pm 0.039}$	$0.1^{\pm 0.031}$
$\sigma^2_{\mathrm{A\times PI.IN}}$	-	-	$0.139^{\pm 0.038}$	$0.092^{\pm 0.028}$
$\sigma^2_{\mathrm{A\times AN.LN}}$	-	-	$0.126^{\pm 0.034}$	$0.091^{\pm 0.028}$
$\sigma^2_{\mathrm{A\times AN.IN}}$	-	-	$0.166^{\pm 0.046}$	$0.128^{\pm 0.04}$
$\sigma^2_{\mathrm{D\times E}}$	-	-	-	$0.086^{\pm 0.023}$
$\sigma^2_{\mathrm{D\times PI.LN}}$	-	-	-	$0.088^{\pm 0.024}$
$\sigma^2_{\mathrm{D\times PI.IN}}$	-	-	-	$0.082^{\pm 0.022}$
$\sigma^2_{\mathrm{D\times AN.LN}}$	-	-	-	$0.088^{\pm 0.023}$
$\sigma^2_{\mathrm{D\times AN.IN}}$	-	-	-	$0.085^{\pm 0.022}$
$\frac{\sigma^2_D}{\sigma^2_A}$	-	1.079	-	1.381
Error	-	-	-	-
$\sigma^2_{\varepsilon-PI.LN}$	$0.688^{\pm 0.04}$	$0.437^{\pm 0.03}$	$0.642^{\pm 0.038}$	$0.319^{\pm 0.026}$
$\sigma^2_{\varepsilon-PI.IN}$	$0.774^{\pm 0.045}$	$0.55^{\pm 0.036}$	$0.761^{\pm 0.045}$	$0.477^{\pm 0.035}$
$\sigma^2_{\varepsilon-AN.LN}$	$0.684^{\pm 0.04}$	$0.407^{\pm 0.029}$	$0.657^{\pm 0.038}$	$0.328^{\pm 0.026}$
$\sigma^2_{\varepsilon-AN.IN}$	$0.746^{\pm 0.044}$	$0.481^{\pm 0.032}$	$0.715^{\pm 0.043}$	$0.391^{\pm 0.03}$
$H^2_{PI.LN}$	$0.353^{\pm 0.053}$	$0.646^{\pm 0.037}$	$0.411^{\pm 0.048}$	$0.752^{\pm 0.029}$
$H^2_{PI.IN}$	$0.327^{\pm 0.051}$	$0.593^{\pm 0.038}$	$0.37^{\pm 0.046}$	$0.668^{\pm 0.033}$
$H^2_{AN.LN}$	$0.355^{\pm 0.052}$	$0.662^{\pm 0.036}$	$0.398^{\pm 0.048}$	$0.745^{\pm 0.029}$
$H^2_{AN.IN}$	$0.335^{\pm 0.051}$	$0.624^{\pm 0.038}$	$0.399^{\pm 0.046}$	$0.718^{\pm 0.03}$
$h^2_{PI.LN}$	$0.353^{\pm 0.053}$	$0.307^{\pm 0.062}$	$0.411^{\pm 0.048}$	$0.328^{\pm 0.061}$
$h^2_{PI.IN}$	$0.327^{\pm 0.051}$	$0.282^{\pm 0.059}$	$0.37^{\pm 0.046}$	$0.291^{\pm 0.058}$
$h^2_{AN.LN}$	$0.355^{\pm 0.052}$	$0.315^{\pm 0.063}$	$0.398^{\pm 0.048}$	$0.322^{\pm 0.061}$
$h^2_{AN.IN}$	$0.335^{\pm 0.051}$	$0.297^{\pm 0.061}$	$0.399^{\pm 0.046}$	$0.326^{\pm 0.058}$
$d^2_{PI.LN}$	-	$0.339^{\pm 0.04}$	-	$0.424^{\pm 0.046}$
$d^2_{PI.IN}$	-	$0.311^{\pm 0.035}$	-	$0.377^{\pm 0.039}$
$d^2_{AN.LN}$	-	$0.347^{\pm 0.041}$	-	$0.424^{\pm 0.046}$
$d^2_{AN.IN}$	-	$0.327^{\pm 0.038}$	-	$0.392^{\pm 0.042}$

Table S3. Posterior means (± posterior standard deviations) of variance components, broad-sense genomic heritability (H^2), narrow-sense heritability ($\boldsymbol{h^2}$), and proportion of variance explained by the dominance effects ($\boldsymbol{d^2}$) by model (MG and MGE) for Scenario 3

	MG		**MGE**	
Component	**A**	**AD**	**A**	**AD**
σ_A^2	$0.381^{\pm 0.09}$	$0.364^{\pm 0.108}$	$0.276^{\pm 0.085}$	$0.289^{\pm 0.113}$
σ_D^2	-	$0.335^{\pm 0.046}$	-	$0.349^{\pm 0.049}$
$\sigma^2_{\mathrm{G\times E}}$			0.163	0.205
$\sigma^2_{\mathrm{A\times E}}$	-	-	$0.163^{\pm 0.054}$	$0.124^{\pm 0.047}$
$\sigma^2_{\mathrm{A\times 1}}$	-	-	$0.153^{\pm 0.05}$	$0.123^{\pm 0.046}$
$\sigma^2_{\mathrm{A\times 2}}$	-	-	$0.174^{\pm 0.057}$	$0.125^{\pm 0.047}$
$\sigma^2_{\mathrm{D\times E}}$	-	-	-	$0.081^{\pm 0.024}$
$\sigma^2_{\mathrm{D\times 1}}$	-	-	-	$0.083^{\pm 0.025}$
$\sigma^2_{\mathrm{D\times 2}}$	-	-	-	$0.08^{\pm 0.023}$
$\frac{\sigma_D^2}{\sigma_A^2}$	-	0.92	-	1.207
Error	-	-	-	-
$\sigma^2_{\varepsilon-1}$	$0.747^{\pm 0.044}$	$0.51^{\pm 0.038}$	$0.717^{\pm 0.042}$	$0.418^{\pm 0.035}$
$\sigma^2_{\varepsilon-2}$	$0.657^{\pm 0.039}$	$0.416^{\pm 0.033}$	$0.631^{\pm 0.037}$	$0.343^{\pm 0.029}$
H_1^2	$0.334^{\pm 0.052}$	$0.575^{\pm 0.045}$	$0.371^{\pm 0.051}$	$0.666^{\pm 0.041}$
H_2^2	$0.363^{\pm 0.055}$	$0.624^{\pm 0.044}$	$0.413^{\pm 0.051}$	$0.708^{\pm 0.038}$
h_1^2	$0.334^{\pm 0.052}$	$0.296^{\pm 0.062}$	$0.371^{\pm 0.051}$	$0.322^{\pm 0.062}$
h_2^2	$0.363^{\pm 0.055}$	$0.321^{\pm 0.065}$	$0.413^{\pm 0.051}$	$0.344^{\pm 0.064}$
d_1^2	-	$0.279^{\pm 0.04}$	-	$0.344^{\pm 0.044}$
d_2^2	-	$0.302^{\pm 0.043}$	-	$0.364^{\pm 0.047}$

Table S4. Posterior means (± posterior standard deviations) of variance components, broad-sense genomic heritability (H^2), narrow-sense heritability ($\boldsymbol{h^2}$), and proportion of variance explained by the dominance effects ($\boldsymbol{d^2}$) by model (MG and MGE) for Scenario 4

	MG		**MGE**	
Component	**A**	**AD**	**A**	**AD**
σ_A^2	$0.432^{\pm 0.103}$	$0.443^{\pm 0.139}$	$0.344^{\pm 0.095}$	$0.369^{\pm 0.135}$
σ_D^2	-	$0.499^{\pm 0.056}$	-	$0.487^{\pm 0.057}$
$\sigma^2_{\mathrm{G\times E}}$	-	-	0.117	0.142
$\sigma^2_{\mathrm{A\times E}}$	-	-	$0.117^{\pm 0.036}$	$0.08^{\pm 0.026}$
$\sigma^2_{\mathrm{A\times LN}}$	-	-	$0.111^{\pm 0.033}$	$0.077^{\pm 0.025}$
$\sigma^2_{\mathrm{A\times IN}}$	-	-	$0.123^{\pm 0.038}$	$0.083^{\pm 0.027}$
$\sigma^2_{\mathrm{D\times E}}$	-	-	-	$0.062^{\pm 0.016}$
$\sigma^2_{\mathrm{D\times LN}}$	-	-	-	$0.062^{\pm 0.016}$
$\sigma^2_{\mathrm{D\times IN}}$	-	-	-	$0.061^{\pm 0.016}$
$\frac{\sigma_D^2}{\sigma_A^2}$	-	1.126	-	1.319
Error	-	-	-	-
$\sigma^2_{\varepsilon-LN}$	$0.635^{\pm 0.037}$	$0.307^{\pm 0.025}$	$0.638^{\pm 0.038}$	$0.288^{\pm 0.025}$
$\sigma^2_{\varepsilon-IN}$	$0.701^{\pm 0.041}$	$0.39^{\pm 0.03}$	$0.708^{\pm 0.042}$	$0.369^{\pm 0.03}$
H^2_{LN}	$0.4^{\pm 0.057}$	$0.751^{\pm 0.034}$	$0.413^{\pm 0.053}$	$0.773^{\pm 0.03}$
H^2_{IN}	$0.377^{\pm 0.056}$	$0.704^{\pm 0.037}$	$0.394^{\pm 0.051}$	$0.728^{\pm 0.034}$
h^2_{LN}	$0.4^{\pm 0.057}$	$0.348^{\pm 0.07}$	$0.413^{\pm 0.053}$	$0.341^{\pm 0.069}$
h^2_{IN}	$0.377^{\pm 0.056}$	$0.326^{\pm 0.068}$	$0.394^{\pm 0.051}$	$0.325^{\pm 0.066}$
d^2_{LN}	-	$0.403^{\pm 0.052}$	-	$0.432^{\pm 0.054}$
d^2_{IN}	-	$0.377^{\pm 0.047}$	-	$0.404^{\pm 0.049}$

Table S5. Posterior means (± posterior standard deviations) of variance components, broad-sense genomic heritability (H^2), narrow-sense heritability ($\boldsymbol{h^2}$), and proportion of variance explained by the dominance effects ($\boldsymbol{d^2}$) by model (MG and MGE) for Scenario 5

	MG		**MGE**	
Component	**A**	**AD**	**A**	**AD**
σ_A^2	$0.408^{\pm 0.096}$	$0.404^{\pm 0.122}$	$0.309^{\pm 0.091}$	$0.343^{\pm 0.125}$
σ_D^2	-	$0.398^{\pm 0.049}$	-	$0.436^{\pm 0.053}$
$\sigma^2_{\mathrm{G\times E}}$	-	-	0.154	0.179
$\sigma^2_{\mathrm{A\times E}}$	-	-	$0.154^{\pm 0.05}$	$0.112^{\pm 0.04}$
$\sigma^2_{\mathrm{A\times PI}}$	-	-	$0.151^{\pm 0.048}$	$0.106^{\pm 0.037}$
$\sigma^2_{\mathrm{A\times AN}}$	-	-	$0.158^{\pm 0.051}$	$0.119^{\pm 0.043}$
$\sigma^2_{\mathrm{D\times E}}$	-	-	-	$0.067^{\pm 0.018}$
$\sigma^2_{\mathrm{D\times PI}}$	-	-	-	$0.071^{\pm 0.019}$
$\sigma^2_{\mathrm{D\times AN}}$	-	-	-	$0.064^{\pm 0.017}$
$\frac{\sigma_D^2}{\sigma_A^2}$	-	1.015	-	1.271
Error	-	-	-	-
$\sigma^2_{\varepsilon-PI}$	$0.677^{\pm 0.041}$	$0.421^{\pm 0.033}$	$0.648^{\pm 0.038}$	$0.336^{\pm 0.028}$
$\sigma^2_{\varepsilon-AN}$	$0.685^{\pm 0.041}$	$0.39^{\pm 0.031}$	$0.657^{\pm 0.039}$	$0.309^{\pm 0.026}$
H^2_{PI}	$0.372^{\pm 0.055}$	$0.653^{\pm 0.042}$	$0.411^{\pm 0.052}$	$0.737^{\pm 0.033}$
H^2_{AN}	$0.369^{\pm 0.055}$	$0.669^{\pm 0.041}$	$0.412^{\pm 0.052}$	$0.754^{\pm 0.032}$
h^2_{PI}	$0.372^{\pm 0.055}$	$0.325^{\pm 0.066}$	$0.411^{\pm 0.052}$	$0.342^{\pm 0.065}$
h^2_{AN}	$0.369^{\pm 0.055}$	$0.333^{\pm 0.067}$	$0.412^{\pm 0.052}$	$0.358^{\pm 0.064}$
d^2_{PI}	-	$0.328^{\pm 0.043}$	-	$0.395^{\pm 0.048}$
d^2_{AN}	-	$0.336^{\pm 0.045}$	-	$0.396^{\pm 0.049}$

Table S6. Posterior means (± posterior standard deviations) of variance components, broad-sense genomic heritability (H^2), narrow-sense heritability ($\boldsymbol{h^2}$), and proportion of variance explained by the dominance effects ($\boldsymbol{d^2}$) by model (MG and MGE) for Scenario 6

	MG		MGE	
Component	**A**	**AD**	**A**	**AD**
σ^2_A	$0.249^{\pm 0.063}$	$0.192^{\pm 0.063}$	$0.153^{\pm 0.054}$	$0.109^{\pm 0.051}$
σ^2_D	-	$0.226^{\pm 0.045}$	-	$0.23^{\pm 0.052}$
$\sigma^2_{\mathrm{G\times E}}$	-	-	0.188	0.261
$\sigma^2_{\mathrm{A\times E}}$	-	-	$0.188^{\pm 0.063}$	$0.138^{\pm 0.054}$
$\sigma^2_{\mathrm{A\times 1.PI.LN}}$	-	-	$0.169^{\pm 0.054}$	$0.126^{\pm 0.047}$
$\sigma^2_{\mathrm{A\times 2.AN.IN}}$	-	-	$0.206^{\pm 0.066}$	$0.15^{\pm 0.058}$
$\sigma^2_{\mathrm{D\times E}}$	-	-	-	$0.123^{\pm 0.043}$
$\sigma^2_{\mathrm{D\times 1.PI.LN}}$	-	-	-	$0.118^{\pm 0.041}$
$\sigma^2_{\mathrm{D\times 2.AN.IN}}$	-	-	-	$0.128^{\pm 0.044}$
$\frac{\sigma^2_D}{\sigma^2_A}$	-	1.177	-	2.11
Error	-	-	-	-
$\sigma^2_{\varepsilon-\mathrm{1.PI.LN}}$	$0.864^{\pm 0.052}$	$0.727^{\pm 0.051}$	$0.815^{\pm 0.048}$	$0.598^{\pm 0.049}$
$\sigma^2_{\varepsilon-\mathrm{2.AN.IN}}$	$0.794^{\pm 0.047}$	$0.638^{\pm 0.048}$	$0.746^{\pm 0.044}$	$0.511^{\pm 0.045}$
$H^2_{\mathrm{1.PI.LN}}$	$0.222^{\pm 0.044}$	$0.363^{\pm 0.045}$	$0.281^{\pm 0.047}$	$0.492^{\pm 0.049}$
$H^2_{\mathrm{2.AN.IN}}$	$0.236^{\pm 0.046}$	$0.394^{\pm 0.048}$	$0.322^{\pm 0.048}$	$0.545^{\pm 0.049}$
$h^2_{\mathrm{1.PI.LN}}$	$0.222^{\pm 0.044}$	$0.166^{\pm 0.045}$	$0.281^{\pm 0.047}$	$0.197^{\pm 0.046}$
$h^2_{\mathrm{2.AN.IN}}$	$0.236^{\pm 0.046}$	$0.18^{\pm 0.049}$	$0.322^{\pm 0.048}$	$0.228^{\pm 0.05}$
$d^2_{\mathrm{1.PI.LN}}$	-	$0.197^{\pm 0.037}$	-	$0.295^{\pm 0.047}$
$d^2_{\mathrm{2.AN.IN}}$	-	$0.214^{\pm 0.04}$	-	$0.317^{\pm 0.05}$

Table S7. Posterior means (± posterior standard deviations) of variance components, broad-sense genomic heritability (H^2), narrow-sense heritability ($\boldsymbol{h^2}$), and proportion of variance explained by the dominance effects ($\boldsymbol{d^2}$) by model (MG and MGE) for Scenario 7

	MG		MGE	
Component	**A**	**AD**	**A**	**AD**
σ^2_A	$0.282^{\pm 0.063}$	$0.268^{\pm 0.077}$	$0.22^{\pm 0.058}$	$0.214^{\pm 0.078}$
σ^2_D	-	$0.278^{\pm 0.031}$	-	$0.304^{\pm 0.034}$
$\sigma^2_{\mathrm{G\times E}}$	-	-	0.17	0.238
$\sigma^2_{\mathrm{A\times E}}$	-	-	$0.17^{\pm 0.051}$	$0.12^{\pm 0.042}$
$\sigma^2_{\mathrm{A\times 1.PI.LN}}$	-	-	$0.162^{\pm 0.044}$	$0.113^{\pm 0.035}$
$\sigma^2_{\mathrm{A\times 1.PI.IN}}$	-	-	$0.155^{\pm 0.041}$	$0.104^{\pm 0.032}$
$\sigma^2_{\mathrm{A\times 1.AN.LN}}$	-	-	$0.142^{\pm 0.038}$	$0.104^{\pm 0.031}$
$\sigma^2_{\mathrm{A\times 1.AN.IN}}$	-	-	$0.195^{\pm 0.052}$	$0.145^{\pm 0.045}$
$\sigma^2_{\mathrm{A\times 2.PI.LN}}$	-	-	$0.197^{\pm 0.056}$	$0.142^{\pm 0.048}$
$\sigma^2_{\mathrm{A\times 2.PI.IN}}$	-	-	$0.167^{\pm 0.044}$	$0.112^{\pm 0.034}$
$\sigma^2_{\mathrm{D\times E}}$	-	-	-	$0.118^{\pm 0.036}$
$\sigma^2_{\mathrm{D\times 1.PI.LN}}$	-	-	-	$0.114^{\pm 0.033}$
$\sigma^2_{\mathrm{D\times 1.PI.IN}}$	-	-	-	$0.122^{\pm 0.034}$
$\sigma^2_{\mathrm{D\times 1.AN.LN}}$	-	-	-	$0.124^{\pm 0.039}$
$\sigma^2_{\mathrm{D\times 1.AN.IN}}$	-	-	-	$0.102^{\pm 0.028}$
$\sigma^2_{\mathrm{D\times 2.PI.LN}}$	-	-	-	$0.136^{\pm 0.04}$
$\sigma^2_{\mathrm{D\times 2.PI.IN}}$	-	-	-	$0.112^{\pm 0.031}$
$\frac{\sigma^2_D}{\sigma^2_A}$	-	1.037	-	1.42
Error	-	-	-	-
$\sigma^2_{\varepsilon-1.PI.LN}$	$0.775^{\pm 0.046}$	$0.601^{\pm 0.039}$	$0.694^{\pm 0.041}$	$0.45^{\pm 0.034}$
$\sigma^2_{\varepsilon-1.PI.IN}$	$0.863^{\pm 0.051}$	$0.718^{\pm 0.045}$	$0.833^{\pm 0.049}$	$0.603^{\pm 0.046}$
$\sigma^2_{\varepsilon-1.AN.LN}$	$0.806^{\pm 0.047}$	$0.573^{\pm 0.037}$	$0.765^{\pm 0.045}$	$0.449^{\pm 0.036}$
$\sigma^2_{\varepsilon-1.AN.IN}$	$0.858^{\pm 0.05}$	$0.651^{\pm 0.042}$	$0.808^{\pm 0.048}$	$0.527^{\pm 0.04}$
$\sigma^2_{\varepsilon-2.PI.LN}$	$0.72^{\pm 0.043}$	$0.585^{\pm 0.038}$	$0.674^{\pm 0.04}$	$0.471^{\pm 0.036}$
$\sigma^2_{\varepsilon-2.PI.IN}$	$0.789^{\pm 0.046}$	$0.671^{\pm 0.043}$	$0.729^{\pm 0.044}$	$0.523^{\pm 0.041}$
$H^2_{1.PI.LN}$	$0.265^{\pm 0.044}$	$0.474^{\pm 0.041}$	$0.353^{\pm 0.044}$	$0.622^{\pm 0.035}$
$H^2_{1.PI.IN}$	$0.245^{\pm 0.042}$	$0.43^{\pm 0.039}$	$0.309^{\pm 0.041}$	$0.551^{\pm 0.037}$
$H^2_{1.AN.LN}$	$0.257^{\pm 0.043}$	$0.486^{\pm 0.041}$	$0.319^{\pm 0.042}$	$0.623^{\pm 0.037}$
$H^2_{1.AN.IN}$	$0.246^{\pm 0.042}$	$0.454^{\pm 0.04}$	$0.337^{\pm 0.042}$	$0.591^{\pm 0.036}$
$H^2_{2.PI.LN}$	$0.279^{\pm 0.045}$	$0.481^{\pm 0.04}$	$0.38^{\pm 0.046}$	$0.626^{\pm 0.035}$
$H^2_{2.PI.IN}$	$0.261^{\pm 0.043}$	$0.447^{\pm 0.039}$	$0.345^{\pm 0.043}$	$0.585^{\pm 0.036}$
$h^2_{1.PI.LN}$	$0.265^{\pm 0.044}$	$0.231^{\pm 0.051}$	$0.353^{\pm 0.044}$	$0.271^{\pm 0.052}$
$h^2_{1.PI.IN}$	$0.245^{\pm 0.042}$	$0.21^{\pm 0.047}$	$0.309^{\pm 0.041}$	$0.234^{\pm 0.047}$

$h^2_{1.AN.LN}$	$0.257^{\pm 0.043}$	$0.237^{\pm 0.051}$	$0.319^{\pm 0.042}$	$0.263^{\pm 0.052}$
$h^2_{1.AN.IN}$	$0.246^{\pm 0.042}$	$0.221^{\pm 0.049}$	$0.337^{\pm 0.042}$	$0.275^{\pm 0.05}$
$h^2_{2.PI.LN}$	$0.279^{\pm 0.045}$	$0.234^{\pm 0.051}$	$0.38^{\pm 0.046}$	$0.278^{\pm 0.052}$
$h^2_{2.PI.IN}$	$0.261^{\pm 0.043}$	$0.218^{\pm 0.049}$	$0.345^{\pm 0.043}$	$0.255^{\pm 0.05}$
$d^2_{1.PI.LN}$	-	$0.243^{\pm 0.028}$	-	$0.351^{\pm 0.037}$
$d^2_{1.PI.IN}$	-	$0.22^{\pm 0.025}$	-	$0.317^{\pm 0.033}$
$d^2_{1.AN.LN}$	-	$0.249^{\pm 0.029}$	-	$0.359^{\pm 0.039}$
$d^2_{1.AN.IN}$	-	$0.233^{\pm 0.027}$	-	$0.316^{\pm 0.034}$
$d^2_{2.PI.LN}$	-	$0.247^{\pm 0.028}$	-	$0.348^{\pm 0.038}$
$d^2_{2.PI.IN}$	-	$0.229^{\pm 0.026}$	-	$0.33^{\pm 0.035}$

Table S8. Posterior means (± posterior standard deviations) of variance components, broad-sense genomic heritability (H^2), narrow-sense heritability ($\boldsymbol{h^2}$), and proportion of variance explained by the dominance effects ($\boldsymbol{d^2}$) by model (MG and MGE) for Scenario 8

	MG		MGE	
Component	**A**	**AD**	**A**	**AD**
σ_A^2	$0.254^{\pm 0.06}$	$0.199^{\pm 0.065}$	$0.176^{\pm 0.055}$	$0.119^{\pm 0.056}$
σ_D^2	-	$0.266^{\pm 0.039}$	-	$0.276^{\pm 0.041}$
$\sigma^2_{\mathrm{G\times E}}$	-	-	0.165	0.231
$\sigma^2_{\mathrm{A\times E}}$	-	-	$0.165^{\pm 0.053}$	$0.119^{\pm 0.045}$
$\sigma^2_{\mathrm{A\times 1.PI.LN}}$	-	-	$0.185^{\pm 0.055}$	$0.14^{\pm 0.049}$
$\sigma^2_{\mathrm{A\times 2.AN.LN}}$	-	-	$0.142^{\pm 0.042}$	$0.097^{\pm 0.032}$
$\sigma^2_{\mathrm{A\times 2.AN.IN}}$	-	-	$0.168^{\pm 0.051}$	$0.119^{\pm 0.042}$
$\sigma^2_{\mathrm{D\times E}}$	-	-	-	$0.112^{\pm 0.038}$
$\sigma^2_{\mathrm{D\times 1.PI.LN}}$	-	-	-	$0.122^{\pm 0.041}$
$\sigma^2_{\mathrm{D\times 2.AN.LN}}$	-	-	-	$0.096^{\pm 0.028}$
$\sigma^2_{\mathrm{D\times 2.AN.IN}}$	-	-	-	$0.118^{\pm 0.038}$
$\frac{\sigma_D^2}{\sigma_A^2}$	-	1.336	-	2.319
Error	-	-	-	-
$\sigma^2_{\varepsilon-1.PI.LN}$	$0.891^{\pm 0.053}$	$0.759^{\pm 0.05}$	$0.813^{\pm 0.048}$	$0.585^{\pm 0.046}$
$\sigma^2_{\varepsilon-2.AN.LN}$	$0.772^{\pm 0.046}$	$0.575^{\pm 0.04}$	$0.743^{\pm 0.044}$	$0.479^{\pm 0.04}$
$\sigma^2_{\varepsilon-2.AN.IN}$	$0.813^{\pm 0.048}$	$0.633^{\pm 0.043}$	$0.8^{\pm 0.047}$	$0.571^{\pm 0.043}$
$H^2_{1.PI.LN}$	$0.22^{\pm 0.041}$	$0.378^{\pm 0.04}$	$0.281^{\pm 0.047}$	$0.492^{\pm 0.049}$
$H^2_{2.AN.LN}$	$0.245^{\pm 0.045}$	$0.445^{\pm 0.044}$	$0.322^{\pm 0.048}$	$0.545^{\pm 0.049}$
$H^2_{2.AN.IN}$	$0.236^{\pm 0.043}$	$0.422^{\pm 0.043}$	$0.281^{\pm 0.047}$	$0.197^{\pm 0.046}$
$h^2_{1.PI.LN}$	$0.22^{\pm 0.041}$	$0.16^{\pm 0.044}$	$0.322^{\pm 0.048}$	$0.228^{\pm 0.05}$
$h^2_{2.AN.LN}$	$0.245^{\pm 0.045}$	$0.188^{\pm 0.05}$	$0.281^{\pm 0.047}$	$0.295^{\pm 0.047}$
$h^2_{2.AN.IN}$	$0.236^{\pm 0.043}$	$0.179^{\pm 0.048}$	$0.322^{\pm 0.048}$	$0.317^{\pm 0.05}$
$d^2_{1.PI.LN}$	-	$0.218^{\pm 0.03}$	-	$0.492^{\pm 0.049}$
$d^2_{2.AN.LN}$	-	$0.257^{\pm 0.036}$	-	$0.545^{\pm 0.049}$
$d^2_{2.AN.IN}$	-	$0.243^{\pm 0.034}$	-	$0.197^{\pm 0.046}$

Table S9. Genomic correlations in Scenarios 2, 3, 4 and 5.

Correlations of genetic values estimated from the additive and additive-dominance models among environments (upper and low diagonal, respectively)

Scenario 2					Scenario 3			Scenario 4			Scenario 5		
	PI.LN	PI.IN	AN.LN	AN.IN		Year 1	Year 2		LN	IN		PI	AN
PI.LN	-	0.69	0.70	0.67	Year 1	-	0.62	LN	-	0.74	PI	-	0.66
PI.IN	0.81	-	0.70	0.67	Year 2	0.75	-	IN	0.86	-	AN	0.81	-
AN.LN	0.81	0.82	-	0.68									
AN.IN	0.80	0.80	0.80	-									

Correlations of additive and dominance effects among environments (upper and low diagonal, respectively)

Scenario 2					Scenario 3			Scenario 4			Scenario 5		
	PI.LN	PI.IN	AN.LN	AN.IN		Year 1	Year 2		LN	IN		PI	AN
PI.LN	-	0.76	0.76	0.73	Year 1	-	0.68	LN	-	0.81	PI	-	0.74
PI.IN	0.84	-	0.77	0.74	Year 2	0.81	-	IN	0.89	-	AN	0.87	-
AN.LN	0.84	0.85	-	0.74									
AN.IN	0.84	0.85	0.84	-									

Table S10. Genomic correlations in Scenarios 6, 8, and 7.

Correlations of genetic values estimated from the additive and additive-dominance models among environments (upper and low diagonal, respectively)

Scenario 6			Scenario 8				Scenario 7						
	1.PI.LN	2.AN.IN		1.PI.LN	2.AN.LN	2.AN.IN		1.PI.LN	1.PI.IN	1.AN.LN	1.AN.IN	2.PI.LN	2.PI.IN
1.PI.LN	-	0.45	1.PI.LN	-	0.52	0.50	1.PI.LN	-	0.58	0.59	0.55	0.55	0.57
2.AN.IN	0.57	-	2.AN.LN	0.63	-	0.53	1.PI.IN	0.69	-	0.59	0.55	0.55	0.57
			2.AN.IN	0.61	0.65	-	1.AN.LN	0.69	0.69	-	0.56	0.56	0.58
							1.AN.IN	0.68	0.69	0.68	-	0.53	0.55
							2.PI.LN	0.67	0.67	0.67	0.66	-	0.55
							2.PI.IN	0.70	0.70	0.70	0.69	0.67	-

Correlations of additive and dominance effects among environments (upper and low diagonal, respectively)

Scenario 6			Scenario 8				Scenario 7						
	1.PI.LN	2.AN.IN		1.PI.LN	2.AN.LN	2.AN.IN		1.PI.LN	1.PI.IN	1.AN.LN	1.AN.IN	2.PI.LN	2.PI.IN
1.PI.LN	-	0.43	1.PI.LN	-	0.49	0.46	1.PI.LN	-	0.65	0.65	0.61	0.62	0.64
2.AN.IN	0.65	-	2.AN.LN	0.72	-	0.51	1.PI.IN	0.72	-	0.66	0.62	0.62	0.65
			2.AN.IN	0.72	0.74	-	1.AN.LN	0.72	0.72	-	0.62	0.62	0.65
							1.AN.IN	0.72	0.72	0.71	-	0.59	0.61
							2.PI.LN	0.72	0.72	0.71	0.73	-	0.62
							2.PI.IN	0.72	0.72	0.71	0.73	0.70	-

Table S11. Genomic correlations in Scenario 1.

Correlations of genetic values estimated from the additive and additive-dominance models among environments (upper and low diagonal, respectively)								
	1.PI.LN	1.PI.IN	1.AN.LN	1.AN.IN	2.PI.LN	2.PI.IN	2.AN.LN	2.AN.IN
1.PI.LN	-	0.56	0.59	0.55	0.56	0.57	0.58	0.57
1.PI.IN	0.68	-	0.59	0.55	0.56	0.58	0.58	0.57
1.AN.LN	0.69	0.69	-	0.58	0.58	0.60	0.60	0.60
1.AN.IN	0.68	0.68	0.69	-	0.55	0.57	0.57	0.56
2.PI.LN	0.68	0.67	0.69	0.68	-	0.57	0.57	0.57
2.PI.IN	0.70	0.70	0.71	0.70	0.69	-	0.59	0.58
2.AN.LN	0.70	0.70	0.71	0.70	0.69	0.72	-	0.59
2.AN.IN	0.69	0.68	0.69	0.69	0.68	0.70	0.70	-
Correlations of additive and dominance effects among environments (upper and low diagonal, respectively)								
	1.PI.LN	1.PI.IN	1.AN.LN	1.AN.IN	2.PI.LN	2.PI.IN	2.AN.LN	2.AN.IN
1.PI.LN	-	0.65	0.66	0.63	0.64	0.66	0.66	0.65
1.PI.IN	0.70	-	0.67	0.63	0.64	0.66	0.66	0.65
1.AN.LN	0.70	0.70	-	0.65	0.66	0.68	0.68	0.67
1.AN.IN	0.70	0.70	0.70	-	0.62	0.65	0.64	0.63
2.PI.LN	0.70	0.70	0.70	0.72	-	0.66	0.66	0.65
2.PI.IN	0.70	0.70	0.70	0.72	0.70	-	0.68	0.67
2.AN.LN	0.70	0.70	0.70	0.72	0.70	0.72	-	0.67
2.AN.IN	0.70	0.70	0.70	0.72	0.70	0.72	0.72	-

SUPPLEMENTARY FIGURES

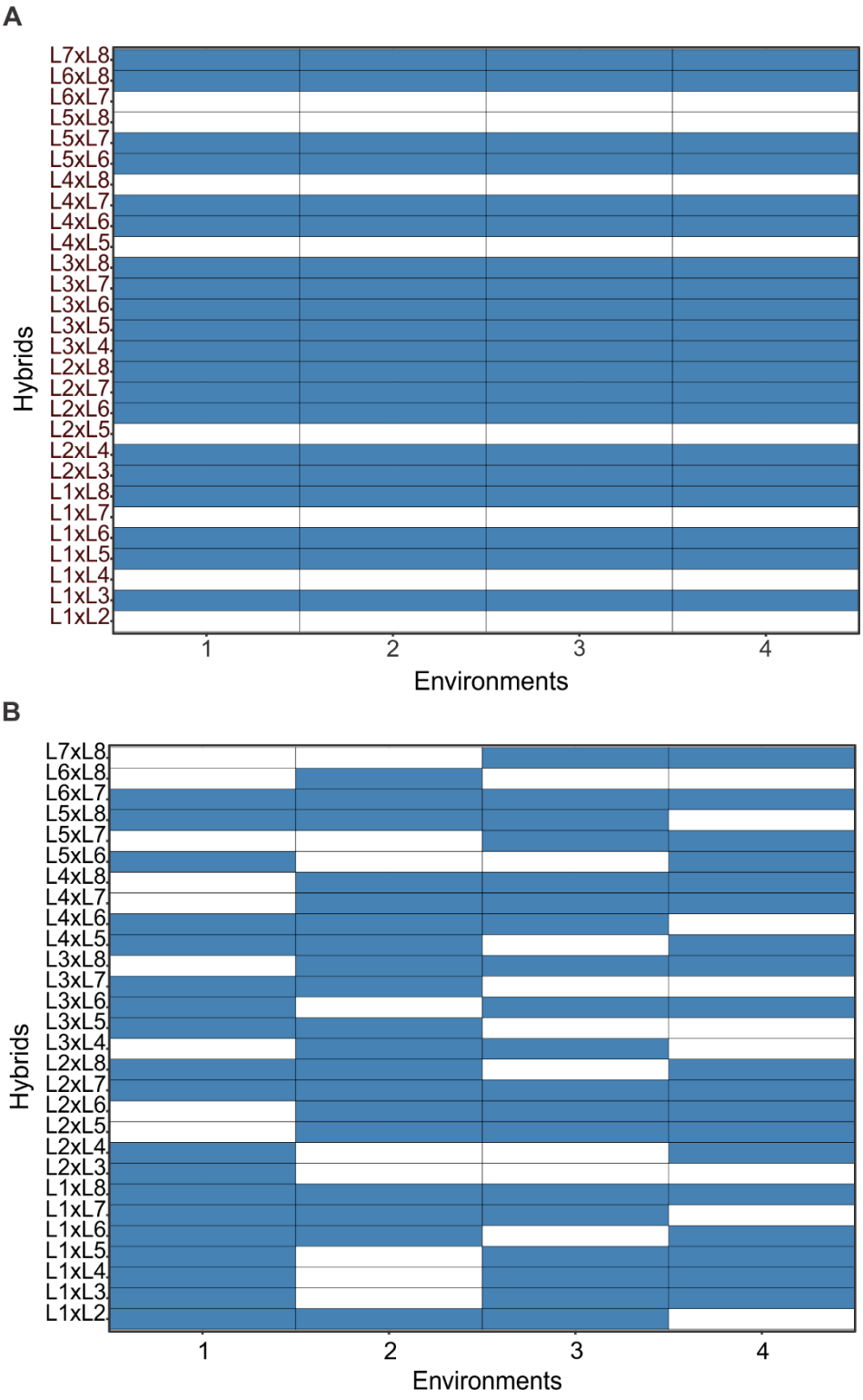

Figure S1. Supplementary Figure 1: Validation systems based on the sampling of hybrids. A) CV1; B) CV2. White blocks represent the testing set (TST), blue blocks correspond to training set (TRN). Axis-x corresponds to environments whereas each line of axis-y represents one hybrid

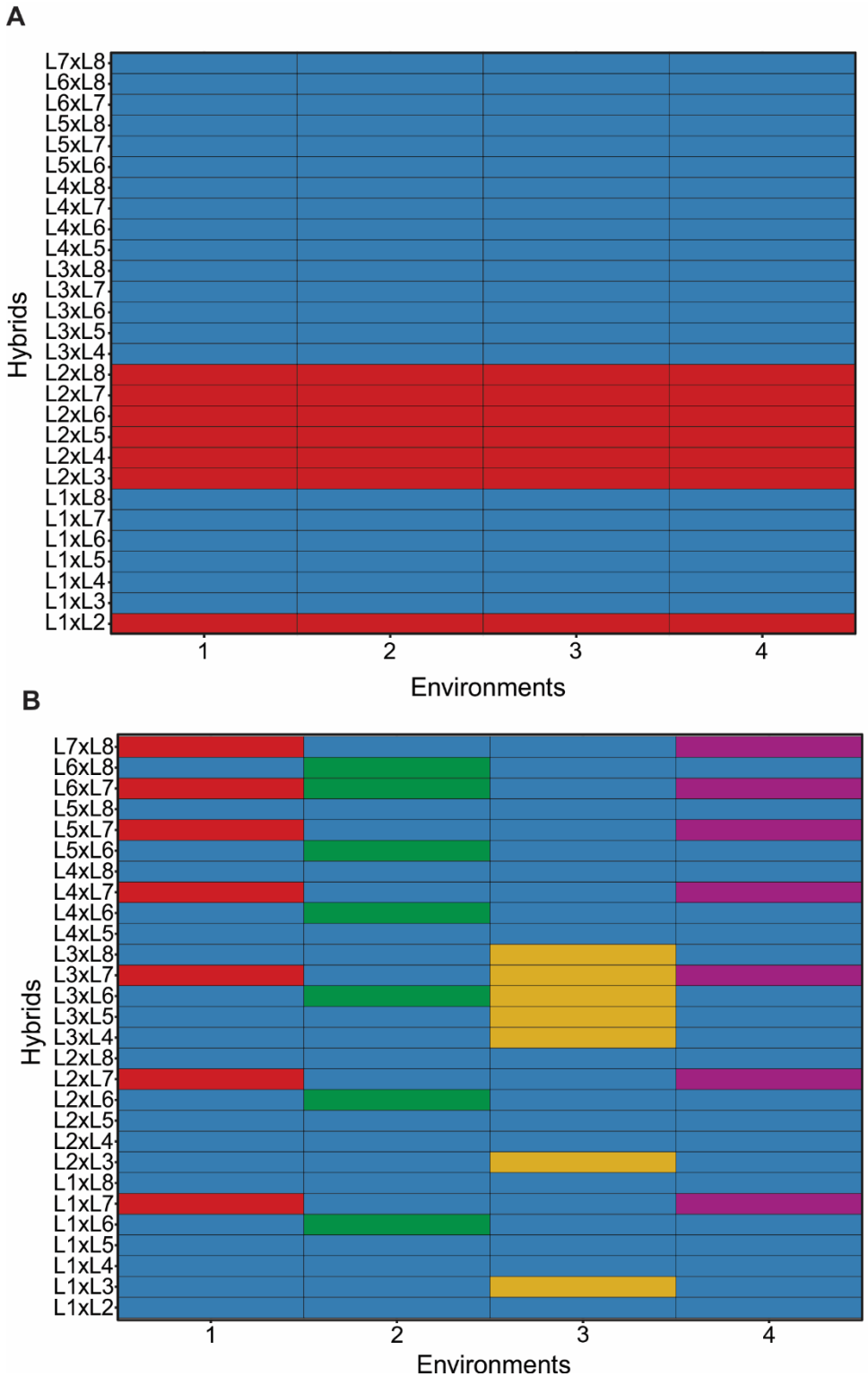

Figure S2. Validation systems based on the sampling of parental lines. **A)** CV3.1; **B)** CV3.2. Blue blocks correspond to training set (TRN) and other colors represent the hybrids originated from a sampled inbred line composing the testing set (TST). Axis-x corresponds to environments whereas each line of axis-y represents one hybrid.

4. GENERAL CONCLUSIONS

Modelling additive and non-additive effects for hybrid prediction is advantageous for both single and multi-environment trials. Non-additive effects are more important in stressed conditions.

The $G \times E$ complexity linearly affects the prediction accuracy of multi-environments trials. Is possible to take advantage of the genotype by environment interaction for prediction of non-tested half-sib families, by the targeting of families in specific environments. The inclusion of data of external environments increases the prediction accuracy of lowly correlated environments.